Modeling and mathematical analysis of the dynamics of soil organic carbon

Alaaeddine Hammoudi

Collège Doctoral du Languedoc-Roussillon

THÈSE

Pour obtenir le grade de

Docteur

Délivré par **Université de MONTPELLIER**

Préparée au sein de l'école doctorale I2S
Et l'Institut Montpelliérain Alexander Grothendieck

Spécialité : **Mathématiques Appliquées.**

Présentée par **Alaaeddine HAMMOUDI**

UNIVERSITÉ DE MONTPELLIER

Modélisation et analyse mathématique de la dynamique du carbone organique dans le sol.

Mme Oana IOSIFESCU, MCF, HDR Université de Montpellier	Directeur de thèse
M. Martial BERNOUX, DR IRD, UMR Eco&Sol, Montpellier	Co-directeur de thèse
M. Michel PIERRE, PR ENS Cachan Antenne de Bretagne	Rapporteur
M. Philippe SOUPLET, PR Université Paris 13	Rapporteur
M. M. Jérôme BALESDENT, DR INRA (GSE), Aix en Provence	Rapporteur - Ecologie
M. Alain RAPAPORT, DR UMR MISTEA - INRA Montpellier	Examinateur
M. Stéphane CORDIER, PR Université d'Orléans	Examinateur

Collège Doctoral du Languedoc-Roussillon

THÈSE

Pour obtenir le grade de

Docteur

Délivré par **Université de MONTPELLIER**

Préparée au sein de l'école doctorale I2S
Et l'Institut Montpelliérain Alexander Grothendieck

Spécialité : **Mathématiques Appliquées.**

Présentée par **Alaaeddine HAMMOUDI**

UNIVERSITÉ DE MONTPELLIER

Modélisation et analyse mathématique de la dynamique du carbone organique dans le sol.

Mme Oana IOSIFESCU, MCF, HDR Université de Montpellier	Directeur de thèse
M. Martial BERNOUX, DR IRD, UMR Eco&Sol, Montpellier	Co-directeur de thèse
M. Michel PIERRE, PR ENS Cachan Antenne de Bretagne	Rapporteur
M. Philippe SOUPLET, PR Université Paris 13	Rapporteur
M. M. Jérôme BALESDENT, DR INRA (GSE), Aix en Provence	Rapporteur - Ecologie
M. Alain RAPAPORT, DR UMR MISTEA - INRA Montpellier	Examinateur
M. Stéphane CORDIER, PR Université d'Orléans	Examinateur

Remerciements

Je tiens à remercier avant tout mes Directeurs de thèse Madame Oana IOSIFESCU et Monsieur Martial BERNOUX, pour leur soutien indéfectible et leur bienveillance durant mes travaux de recherches. Je les remercie pour la confiance qu'ils m'ont accordée en acceptant d'encadrer ce travail doctoral et pour tout ce que j'ai pu apprendre pendant nos innombrables échanges. J'ai été extrêmement sensible à leurs qualités humaines d'écoute et de compréhension.

Je suis particulièrement reconnaissant à Messieurs Michel PIERRE, Philippe SOUPLET et Jérôme BALESDENT de l'intérêt qu'ils ont manifesté à l'égard de cette recherche en s'engageant à être rapporteurs.

Je remercie Messieurs Stéphane CORDIER et Alain RAPAPORT pour m'avoir fait l'honneur d'être membres du Jury.

Je remercie Monsieur Pascal AZERAD pour ses précieux conseils et ses encouragements.

Je remercie également Madame Bernadette LACAN pour sa patience et son aide précieuse dans l'élaboration des documents administratifs.

Mes remerciements s'adressent à tous les membres de l'équipe Eco&Sol de l'IRD qui m'ont accueilli pendant mes travaux de thèse ainsi que mon stage de Master. Je remercie l'équipe dynamique de l'UMR MISTEA, un incubateur d'idées et un catalyseur d'échanges très intéressants.

Je pense aussi à Monsieur Marc PANSU pour le temps qu'il m'a consacré, j'ai tiré grand profit de nos nombreuses discussions.

Mes pensées vont également à Hatem, Alexandre, Pierre, Myriam, Francesco, Yousri, Christophe, Arnaud, Pierre, Etienne, Julien et Julien pour leur convivialité et leur soutien.

Ma reconnaissance va aussi aux écoles doctorales I2S et SIBAGHE ainsi qu'aux LabEx NUMEV et CeMEB pour le financement de mes travaux.

Ma gratitude va enfin à mes parents, mes sœurs et toute ma famille. Ils ont su m'entourer de leur affection et m'accompagner tout au long de mes recherches.

Je dédie cette thèse à mon fils Kaïs que j'ai vu grandir au cours de ce projet et à ma femme qui a supporté mon humeur et mon humour.

Table des matières

Chapitre 1

Introduction Générale

La matière organique du sol (MOS) est considérée comme l'indicateur principal de la qualité des sols. Le carbone organique, qui constitue plus de 50% de la MOS, est devenu un enjeu mondial non seulement à cause de sa relation avec la qualité des terrains agricoles mais aussi par sa grande influence sur d'autres phénomènes écologiques majeurs tels que la désertification, les gaz à effets de serre ou encore la biodiversité.

En effet, la MOS contribue à la durabilité de l'agriculture en maintenant des sols de meilleure qualité :faible érodabilité, meilleure rétention de l'eau et amélioration du stockage des nutriments par le sol au service des plantes (voir Rawls et al 2003[1]). Le carbone organique est ainsi primordial pour la sécurité alimentaire des sociétés. Par ailleurs, le carbone organique du sol joue un rôle principal dans la libération des gaz et donc dans le réchauffement climatique. Le sol est de surcroît, le plus grand réservoir de carbone en interaction avec l'atmosphère .

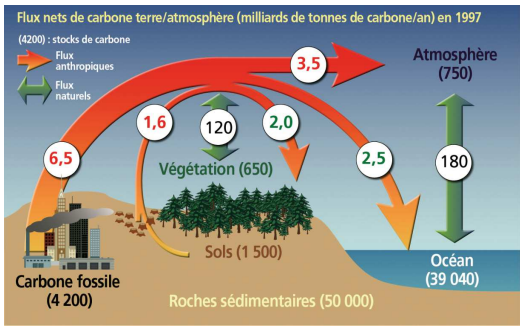

Figure 1.1: Le cycle du carbone. Image : METSTORE.

La couche superficielle du sol (allant jusqu'à 1m de profondeur) contient selon certaines estimations 3 fois plus de carbone que l'atmosphère et 4 fois plus que les plantes. Ce stock impressionnant n'est pas inerte, mais soumis à une dynamique. Il est connu que les écosystèmes forestiers et agricoles contribuent, grâce à la photosynthèse, à la baisse de la concentration du carbone dans l'atmosphère, nous parlons dans ce cas de **séquestration de carbone** : le carbone atmosphérique est piégé sous forme de matière organique du sol et de biomasses.
Cependant, ce flux n'est pas unidirectionnel. Les chercheurs ont établi que la modification d'usage des terres (déforestation, brulis, pâturage ...) conduisait à une libération du carbone du sol vers l'atmosphère (Post et Kwon [2], Guo et Gifford 2002 [3]). Des analyses et des expérimentations plus fines ont permis d'identifier plusieurs facteurs déterminants de la variation du stock du carbone organique du sol dont le type de végétation, les propriétés physico-chimiques du sol, l'usage agricole ou encore les facteurs climatiques dont l'humidité et la température. (Guo et Gifford 2002 [3], Del Grosso et al 2005 [4], Battle-Aguilar et al 2011 [5] and Hamdi et al 2011 and 2013 [6] [7]).

Cet ensemble de connaissances et d'observations a permis de développer des modèles décrivant ainsi ce cycle biogéochimique de manière plus ou moins complexe, et plus ou moins détaillée. Plusieurs méthodologies ont été adoptées suivant les objectifs et obéissant à plusieurs contraintes comme les données récoltées. Manzoni et al [8] ont répertorié plus de 200 modèles différents au niveau de l'approche ou de la conceptualisation. Nous distinguons ainsi les modèles informatiques dits multi-agents dont l'importance réside d'abord dans la simplicité de son implémentation informatique (Masse et al 2007 [9] Cambier et al [10]). Puis, ces modèles ont été utilisés pour si-

muler des scénarios ou pour mesurer la plausibilité de certaines hypothèses, un premier pas vers la simulation par virtualisation du monde biologique. Cependant, mêmes les modèles multi-agents les plus simples sont assez complexes du point de vue mathématique, ce qui rend difficile toute étude rigoureuse préalable des résultats qu'ils fournissent. Néanmoins, ils peuvent prendre en compte plusieurs paramètres, et considérer des modifications lourdes comme la spatialisation.

Le lien établi entre le carbone organique du sol et le réchauffement climatique et la demande croissante de production agricole sont deux facteurs qui mettent les sociétés modernes devant un dilemme très important. Comment optimiser l'usage des sols agricoles ou forestiers sans catalyser le réchauffement climatique, sans nuire à la biodiversité ? Les efforts fournis pour la modélisation de la matière organique dans le sol essayent d'apporter des éléments de réponse à cette question.

1.1 Aperçu sur la modélisation mathématique du cycle la MOS

L'idée de la modélisation du cycle de la MOS a vu le jour dans les années 30 avec les travaux de Nikiforoff [11]. Il s'intéressait aux différents facteurs et paramètres qui contrôlent la dégradation de la MOS. Hénin et Dupuis [12] ont proposé en 1945 un modèle simple à deux compartiments : un compartiment pour la matière organique stable, et un autre pour la matière organique fraîche. En 1977, Schlesinger [13] a adopté la même approche pour modéliser le phénomène et estimer le stock mondial de débris végétaux. Inspirée de la littérature des domaines écologiques ainsi que des modèles utilisés en Médecine et en Chimie, il a utilisé un modèle compartimental simple . Le concept de ces modèles est basé sur le principe de conservation de la masse :
- Identifier les différents (du moins les principaux) acteurs régissant les phénomènes, ces derniers sont présentés par des compartiments et ont donc des masses.
- Entre les différents compartiments, ils se passent des échanges de matière qui font varier la masse dans chaque compartiment et qui sont commandés par des processus physico-chimiques et biologiques. Ces relations entre compartiments sont appelées les flux : i.e la différence entre la quantité de matière qui sort et celle qui rentre dans un compartiment précis.

Schlesinger a insisté sur l'idée de flux et de compartiments ainsi que sur

l'idée du stockage à long terme du carbone dans le sol. Les modèles de dynamique du carbone organique du sol fractionnent la matière organique en plusieurs compartiments homogènes et différenciés par des coefficients de dégradation : stable (faible coefficient de dégradation : difficile à dégrader) et labile (fort coefficient de dégradation : facile à dégrader) ou par un aspect fonctionnel : la mortalité, l'assimilabilité, la respiration.
Avant d'être utilisé, chaque modèle passe par la phase de calibration, qui consiste à chercher, en comparant les résultats du modèle et les données, les valeurs les plus probables des différents paramètres et coefficients du modèle. Finalement, nous obtenons la phase de validation où la capacité du modèle, cette fois-ci calibré, est testée à reproduire des résultats proches des données réelles récoltées sur différents sites d'expérience.
Mathématiquement, ces modèles se traduisent par des systèmes d'équations différentielles, généralement linéaires.

Les modèles basés sur des systèmes d'équations différentielles sont largement utilisés par les chercheurs car ils sont faciles à calibrer et moins couteux en données ainsi qu'en temps de calcul que d'autres modèles plus complexes. Il est à noter que les systèmes compartimentaux sont largement utilisés plus généralement en biologie, en médecine et en chimie. Ils soulèvent des questions diverses parmi lesquelles des questions d'existence et de positivité des solutions, la contrôlabilité (un système de contrôle est dit contrôlable si il peut être amené, en temps fini, d'un état initial arbitraire vers un état final prescrit) et l'observabilité (i.e, la connaissance de la trajectoire observée détermine de manière univoque l'état initial) (voir Jacquez 1974 [14]). L'utilisation intensive de ce type de modèles et de méthodologie a certainement inspiré son introduction dans l'étude du cycle du carbone organique dans le sol.

L'amélioration de ces modèles est toujours d'actualité. En même temps, d'autres modèles plus évolués ont été développés pour diverses raisons. Par exemple, le fractionnement de la MOS en nombre discret de compartiments selon la qualité et les propriétés chimiques simplifie grandement le phénomène biologique mais pose aussi une question fondamentale : à quel degré notre modèle est fidèle à la réalité du phénomène modélisé ? Bosatta et Agren [15](1996) ont mis en place des modèles à qualité continue et surtout physiquement mesurable (la qualité sera donc la taille ou l'âge des particules au lieu de considérer des coefficients issus des expériences). Ces modèles peuvent être considérés comme des modèles à infinité de compartiments. Ainsi, ils ont remplacé le nombre discret des coefficients expérimentaux d'as-

similation microbienne par une fonction continue. Les objets mathématiques qui en découlent sont des systèmes d'équations intégro-différentielles ou des systèmes d'équations EDO-EDP.

Finalement, au vue de la structure complexe du sol et la tendance des modèles à négliger l'effet de l'espace sur le cycle de la matière organique ainsi que les phénomènes multi-physiques et biologiques liés (diffusion de la température, diffusion de la matière, variabilité spatiale et topographique, multi-échelles, chemotaxis), certains chercheurs ont commencé à préparer une nouvelle génération de modèles dont l'espace est explicitement considéré, non seulement par des opérateurs de diffusion et de transport, mais aussi par la variabilité spatiale des différents paramètres. Dans ce cadre, nous pouvons citer les travaux de Elzein et Blaesdent en 1995 [16], Goudjo et al 2001 [17], Braakhekke et al 2013 [18] et Masse et al 2007 [9]. Les approches utilisées sont purement informatiques (Masse), ou basée sur des équations à dérivés partielles (Blasdent, Goudjo, Braakhekke). Avec les nouvelles techniques d'imagerie et les performances des nouveaux calculateurs, ces modèles permettront la réévaluation des modèles, à l'échelle macroscopique des parcelles et à l'échelle microscopique des molécules.

1.2 Le choix du modèle MOMOS

Les modèles les plus populaires utilisés dans l'étude du cycle du carbone organique dans le sol sont les modèles compartimentaux. Ils se basent sur le principe de conservation de la masse (Manzoni et al 2009 [8]). La majorité des modèles adopte en plus le principe de fractionnement de la matière organique du sol selon leurs vitesses de dégradation. Cette idée directrice a fait l'objet d'une validation expérimentale (voir Thuries et al 2001 [19]). Les différents flux existants entre ces fractions, modélisées par les compartiments, se justifient par des relations et réactions chimiques ou biologiques dont les facteurs cinétiques sont normalisés par des fonctions de température et d'humidité, ou des paramètres physico-chimiques du sol comme le taux d'argile ou le pH. Les modèles les plus connus et les plus utilisés se traduisent par des systèmes d'équations différentielles dont les variables d'état modélisent la quantité de la matière des différents compartiments. Les entrées de ces modèles sont les nouveaux apports donnés au sol, par exemple sous formes de résidus ou compost de végétaux : la sortie correspond aux pertes de masse sous forme de CO_2, par respiration microbienne : ce phénomène s'appelle la minéralisation du carbone organique.

Les modèles les plus connus et les plus utilisés par les instances mondiales tels que l'Organisation des Nations Unies pour l'Alimentation et l'Agriculture (FAO) ou la Banque Mondiale (BM) sont RothC (Jenkinson et al 1977 [20]) et Century (Parton et al. 1987 [21]).

Face à la panoplie de modèles proposés dans la littérature, nous avons choisi un modèle récent et très prometteur développé par Marc Pansu ([22] [23] [24])à l'UMR Eco&Sol-IRD de Montpellier. : MOMOS, qui se traduit par un système différentiel non linéaire assez proche des modèles cités plus haut. Nous prsentons son diagramme des flux :

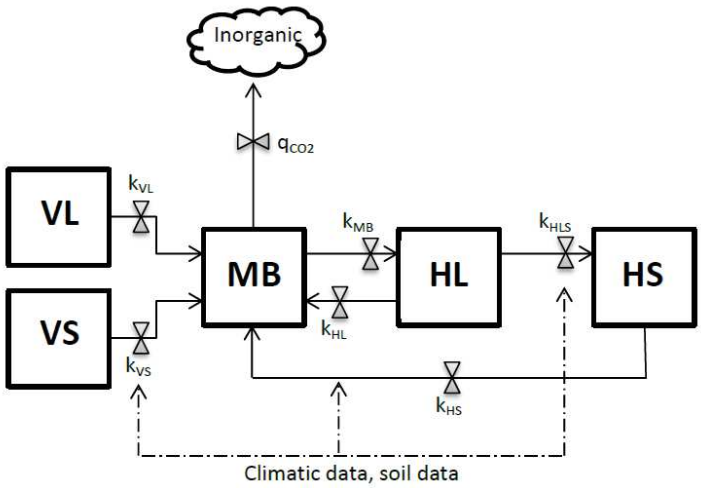

Figure 1.2: Diagramme des flux du modèle MOMOS.

MOMOS apporte une nouveauté au niveau de la structure. Il distingue 5 compartiments de carbone organique : un compartiment de carbone microbien (MB) deux compartiments de résidus végétaux : un labile (VL) et l'autre stable (VS), et de la même façon deux compartiments d'humus, un labile (HL) et l'autre stable (HS).

Le cycle du carbone organique dans MOMOS peut être décrit comme suit : les compartiments des végétaux ainsi que ceux de l'humus se dégradent selon différentes vitesses pour alimenter le compartiment du carbone micro-

bien : ceux sont les flux des compartiments VL,VS, HL et HS vers le compartiment de la biomasse microbienne MB. Par mortalité, la biomasse microbienne se transforme en humus labile HL, dont une partie se transforme à son tour en humus stable HS. La perte de carbone par minéralisation s'opère seulement au niveau du compartiment microbien : c'est la respiration microbienne (dans les autres modèles connus de la dynamique de la MOS, la perte se fait au niveau de chaque compartiment). Cette perte agit comme un frein à la croissance du carbone microbien dans le système. MOMOS peut être donc traduit par ce système d'équations différentielles :

$$\dot{\mathbf{v}} = F\left(T,\theta\right)\begin{pmatrix} -k_{VL}v_1 + f_1(t) \\ -k_{VS}v_2 + f_2(t) \\ k_{VL}v_1 + k_{VS}v_2 - k_{MB}v_3 - qv_3^2 + k_{HL}v_4 + k_{HS}v_5 \\ -\left(k_{HLS} + k_{HL}\right)v_4 + k_{MB}v_3 \\ -k_{HS}v_5 + k_{HLS}v_4 \end{pmatrix}, \quad (1.2.1)$$

qui peut être simplifié en éliminant les deux premières équations simples sous la forme suivante :

$$\dot{\mathbf{u}} = F\left(T,\theta\right)\begin{pmatrix} -k_1u_1 - qu_1^2 + k_2u_2 + k_3u_3 \\ k_1u_1 - (k_2 + k_4)u_2 \\ k_4u_2 - k_3u_3 \end{pmatrix} + \begin{pmatrix} f(t) \\ 0 \\ 0 \end{pmatrix} = G(t,u), \quad (1.2.2)$$

où u_1 représente le carbone microbien, u_2 représente l'humus labile, et u_3 représente l'humus stable. Les différents coefficients positifs k_i sont les différentes vitesses de décomposition ou de mortalité. Ils sont normalisés par une fonction de température et d'humidité $F\left(T,\theta\right)$. Le terme quadratique représente la perte de matière par respiration microbienne.

Ce choix fut motivé par plusieurs raisons. Tout d'abord, MOMOS apporte une nouveauté conceptuelle.
En effet, le modèle donne un poids considérable à la communauté microbienne dans le cycle de la matière organique du sol. Le compartiment microbien est très actif et se situe au cœur de tout processus de transformation : de l'assimilation par dégradation à la perte par minéralisation. Il était donc logique de le retrouver à l'origine de 6 flux sur les 7 existants entre les différents compartiments du modèle. Cette nouveauté est réconfortante pour les chercheurs qui considèrent la biomasse microbienne comme la clé des processus dans sol (voir par exemple Powlson et al 2001 [25]).

Le choix de MOMOS fut également motivé par la finesse des étapes de son développement et sa souplesse vis-à-vis des objectifs de modélisation

diverses. Il est capital de noter que le modèle est passé par cinq transformations majeures afin de produire des simulations performantes à différentes échelles temporelles (contrairement à Century), et fiables indépendamment du climat et des sites étudiés (contrairement à RothC adapté à un certain type de climat). Pansu n'a pas hésité à modifier et améliorer la conceptualisation de son modèle au fur et à mesure des recherches et à la lumière des nouveaux résultats.

MOMOS est aussi modulable, dans le sens où il est possible de le modifier pour tenir compte d'autres phénomènes biologiques comme par exemple le priming effect (voir Fontaine et al 2004 [26], Perveen et al 2014 [27]) sans que cela n'affecte sa robustesse mathématique. Par ailleurs, MOMOS est en pleine extension, puisque, en plus du carbone, il existe d'autres versions : MOMOS-N et MOMOS-P pour les cycles de l'azote et du phosphore, éléments essentiels à la croissance des plantes et à la production de la biomasse végétale.
En effet, l'atmosphère contient 79% de diazote, un gaz très peu biodisponible pour les plantes (i.e les plantes sont incapables d'extraire en grande quantité d'azote de l'air contrairement au CO_2). Quelques bactéries du sol ont la capacité de casser la triple liaison N-N pour produire du nitrate, une forme d'azote assimilable par les plantes. En contrepartie, les plantes fournissent des glucides pour les bactéries.

Dans ce contexte, MOMOS (Carbon) a été couplé avec succès avec MOMOS-N pour modéliser le cycle de l'azote (Pansu et al [24]). Une autre version MOMOS-P est en cours de validation, afin de modéliser le cycle du phosphore qui est un élément essentiel à la fabrication par les plantes d'acides nucléiques et de molécules énergétiques.

Finalement, une comparaison entre MOMOS et les autres modèles du carbone organique du sol conduit à la conclusion que MOMOS peut être vu comme le premier modèle prenant en compte l'effet de la présence des microbes sur les caractéristiques et la structure du sol. En effet, dans RothC ou Century, la perte de carbone dans le sol par minéralisation se traduit par un terme linéaire : $-k_{resp}u_i$ où k_{resp} est un coefficient qui dépend des propriétés physico-chimiques du sol et u_i modélise le contenu d'un compartiment quelconque du modèle.

Dans MOMOS, la non-linéarité au niveau du terme de la respiration microbienne $-qu_1^2$, dans l'équation (1.2.2) de la variation de la biomasse

microbienne du modèle, peut être vue comme une équation linéaire augmentée par un certain couplage entre le sol et les microbes. Le terme k_{resp} de MOMOS est de la forme : qu_1, ou q comme précédemment, dépend des propriétés physico-chimiques du sol. Cette forme peut donc être vue comme l'effet de la présence des microbes sur les propriétés du sol. C'est ce que nous appelons **interaction entre microbe et structure du sol**. Dans MOMOS, la présence des microbes affecte les propriétés du sol d'une manière à favoriser la minéralisation de la matière organique. Cette interaction est complètement absente dans les autres modèles purement linéaires.

Nous pourrions aussi adopter le point de vue de la dynamique des populations pour remarquer que cette non-linéarité permet également à MOMOS d'avoir une structure proche de celle des modèles de chémostats avec une loi logistique de Verhulst utilisée dans l'étude des bioréacteurs. La non-linéarité introduit un terme équivalent à une capacité d'accueil dépendante des facteurs pédologiques et climatiques.

Malgré les bonnes propriétés citées ci-dessus, la nature du phénomène ainsi que les objectifs originels pour lesquels le modèle a été élaboré présentent des carences au niveau structural, et donc une nécessité d'amélioration. MOMOS dans son état actuel, ne peut servir à modéliser le cycle du carbone à très grande échelle de temps.
En effet, le modèle (généralement utilisé) RothC considère l'existence d'une partie inerte de la matière organique. En l'absence d'entrée de matière organique, c'est cette partie de la MOS, protégée de la dégradation, qui permet au modèle RothC de retourner des valeurs non nulles pour le stock total en matière organique.

D'un autre côté, MOMOS ne considère pas de matière inerte ou protégée. En faisant la somme des différentes équations du système (2) nous remarquons que le fait d'avoir des entrées de matière organiques nulles ($f(\cdot) \equiv 0$) implique un presque vidage du système après un temps fini.

De plus, comme la majorité des autres modèles du sol basés sur des systèmes d'équations différentielles, MOMOS ne prend pas en compte de façon mesurable l'effet de l'hétérogénéité du sol. Le nouveau flux de données provenant des nouvelles techniques de l'imagerie et de la télédétection (cartes topographique, carte du taux d'argile, ...) n'est pas exploité. Ces techniques peuvent donner une meilleure compréhension du phénomène, notamment à grande échelle spatiale. Les simulations actuelles se basent sur des données et

des mesures dont nous savons qu'elles souffrent de grandes variabilités spatiales. Le fait de spatialiser le modèle et d'incorporer des données physico-chimiques (topographie, taux d'argile...) spatialisées, mesurées grâces aux satellites, peut améliorer et certainement modifier les modèles.
Nous pouvons aussi penser au rôle de l'oxygène dans le cycle du carbone. L'oxygène influence fortement le comportement des microorganismes et puisqu'il devient rare en profondeur, prendre en compte une dimension de l'espace permettra de considérer l'effet de cette limitation sur le phénomène.

Le sujet de cette thèse se situe ainsi à la frontière des sciences des sols, de l'écologie et des mathématiques. Nous nous sommes particulièrement intéressés à l'étude du modèle MOMOS modélisant le cycle du carbone organique dans le sol.

1.3 Organisation de la thèse

Dans le chapitre 2, nous nous sommes intéressé à la validation mathématique du système différentiel (1.2.1). Nous avons utilisé la méthode classique des sous et sur-solutions de la théorie des systèmes monotones de Smith [28]. Comme dans Martin et al [29], nous avons étudié l'existence des solutions périodiques dans le cas où les données climatiques et les entrées en matière organique sont périodiques. Si Martin utilisait les séries de Fourier, le terme non-linéaire dans notre système nous empêchait d'utiliser la même méthode. L'idée était de démontrer à l'aide de suites et des bonnes propriétés de monotonie, que l'application de Poincaré

$$\begin{cases} U_0 = x_0 \in \mathbb{R}^5_+ \\ U_{n+1} = x(nT, U_0) \end{cases}$$

admettait un point fixe. Nous avons surtout exploité le caractère coopératif du système (1.2.1) pour pouvoir mener à bien les calculs. Ainsi, la méthode pourrait être appliquée à certains systèmes différentiels monotones, de forme assez proche du système différentiel MOMOS. Ces résultats font l'objet d'une publication parue dans *Differential Equations and Dynamical Systems.*

Dans les chapitres suivants nous nous sommes intéressés à proposer plusieurs prototypes de modèles, basés sur MOMOS, où nous avons utilisé la théorie des équations à dérivés partielles dans différents contextes et pour des objectifs divers.

Dans le chapitre 3, nous avons spatialisé le modèle MOMOS. Ainsi, nous sommes en présence d'un système d'équations à dérivés partielles d'advection-diffusion-réaction faiblement couplées.

$$\begin{cases} \partial_t u_i - \operatorname{div}(\mathbf{A}_i(t,x)\nabla u_i) + \mathbf{B}_i(t,x)\nabla u_i = G_i(t,x,\mathbf{u}),\ (t,x) \in \Omega_T \\ \gamma\left(\mathbf{A}_i(t,x)\nabla u_i\right)\cdot\nu + \beta_i(t,x)u_i = 0, (t,x) \in \Sigma_T \\ u_i(0) = u_{i,0} \quad \text{in } \Omega, \end{cases} \tag{1.3.1}$$

où $\mathbf{A}_i$ et la matrice de diffusion et $\mathbf{B}_i$ est un vecteur de transport, pour $i = 1, 2, 3$. Les conditions au bord sont, soit de type Dirichlet si ($\gamma = 0,\ \beta_i \equiv 1$), soit de type Neumann-Robin si ($\gamma = 1,\ \beta_i(t,x) \geq 0$). Le terme de reaction G est définie comme dans (1.2.2). Le système est considéré sur un domaine ouvert et borné en dimension 3 et suffisamment régulier pour pouvoir utiliser les injections de Sobolev. Le mouvement aléatoire des micro-organismes ainsi que la diffusion molaire entrainent la dispersion et le mélange de la matière organique dans le sol. Ceci justifie physiquement et biologiquement le terme de flux.

La partie advective du flux $\mathbf{B}_i(t,x)\nabla u_i$ se justifie par le phénomène de transport de la matière organique emportée par l'eau dans la matrice du sol pendant les intempéries. Cette modification du modèle permet de prendre en compte l'effet de la nature hétérogène du sol en tant que bioréacteur sur le cycle du carbone organique : les différents coefficients de (1.3.1) dépendent non seulement du temps mais aussi de l'espace. Dans un premier temps, nous montrons que le problème est bien posé.

Nous avons utilisé ici la méthode Faedo Galerkin, qui consiste à construire d'abord des solutions discrétisées. Puis, nous sommes passés à la limite grâce à des arguments de compacité.

Dans un second temps, et grâce aux techniques de sous et sur-solutions, nous avons pu montrer l'existence d'une unique solution périodique faible dans le cas où les différents paramètres sont périodiques. Sous certaines hypothèses, nous montrons l'attractivité de cette solution et nous exhibons un bassin d'attraction.
Les résultats de ce chapitre font l'objet d'une publication soumise.

Dans le chapitre 4 nous présentons un résultat d'homogénéisation. Nous avons voulu répondre à la question suivante : Peut-on simplifier le modéle spatial (1.3.1) en un système plus simple ou l'hétérogénéité spatiale a un moindre effet ?

Pour cela nous avons étudié le problème d'homogénéisation sous-jacent. Nous avons considéré que le domaine est de dimension 2 et est pavé par une structure périodique de cellule microscopique unitaire Y. Nous avons utilisé des arguments de compacité ainsi que des résultats d'homogénisation de Bensoussan [30], Tartar [31] and Cioranescu [32].
Le comportement macroscopique suit un systeme homogène dont on explicitera les paramètres.

Dans le chapitre 5, nous avons utilisé le cadre des équations paraboliques pour dériver un nouveau prototype qui s'affranchie de la fragmentation de la matière organique suivant la méthodologie de Bossatta et Agren. Il ne sera plus question de plusieurs compartiments discrets pour la matière organique mais d'un seul compartiment, $v(t,x)$ ou x ne désigne plus l'espace physique mais l'espace des qualités à une dimension. La dynamique du compartiment de la biomasse microbienne u est décrite par l'équation différentielle ordinaire non linéaire, couplée faiblement à une équation à dérivés partielles :

$$\begin{cases} \dot{u} = -k_1(t)u - q|u|u + \int_\Omega k(t,x)v(t,x)dx, \quad t > 0, \\ \frac{\partial v}{\partial t} = \frac{\partial}{\partial x}(a\frac{\partial}{\partial x}v - \alpha(t,x)v) - k(t,x)v + k_1(t)ug(x) + f(t,x), \quad (t,x) \in \Omega_T, \\ u(0) = u_0 \geq 0, \\ v(0,x) = v_0 \geq 0. \end{cases}$$

Ce système est couplé avec les conditions au bord suivantes

$$a\frac{\partial}{\partial x}v(t,0) - \alpha(t,0)v(t,0) = 0, \ t \in (0,T)$$

et

$$a\frac{\partial}{\partial x}v(t,1) - \alpha(t,1)v(t,1) = 0, \ t \in (0,T)$$

et où g est une fonction positive de répartition i.e telle que $\int_\Omega g\,(x)\,dx = 1$, $k(.,x)$ est la fonction de dégradation selon la qualité, inspirée grandement des coefficients de dégradation du modèle MOMOS, alors que la fonction positive $\alpha\,(.,x)$ modélisera l'effet de l'âge sur la qualité de la matière organique.

En utilisant la méthode de Faedo Galerkin ainsi que les résultats classiques de compacité, nous avons montré l'existence et l'unicité des solutions positives, puis nous avons procédé à des simulations pour calibrer et valider le modèle contre des données de sites différents. Les différentes simulations ont été faites grâce à un couplage de deux logiciels : Matlab et Comsol.

Cette partie est inspirée des travaux de Bruun et al [33], Agreen et Bosatta [15] et fera l'objet d'un article futur pour une revue d'écologie.

Dans les chapitres 6 et 7, afin de répondre à une demande de modélisation, nous avons obtenu deux derniers modèles avec un terme de chemotaxis qui permettent de reproduire des structures spatiales (Patterns au sens de Turing [34]). Cette organisation spatiale peut émerger dans les modèles de réaction-diffusion (Murray [35][36], Gringrod [37]).
L'obtention d'une organisation spatiale des micro-organismes, grâce â une modification du modèle MOMOS, permettra de réconcilier les modèles utilisés à l'échelle macroscopique de la parcelle, avec des observations expérimentales microscopiques (voir Vogel et al 2014 [38]).

Nous avons proposé deux modèles simples de deux équations, une équation pour la biomasse microbienne et une seconde pour la matière organique. Dans un domaine Ω de frontière suffisamment régulière :

$$\begin{cases} \frac{\partial u}{\partial t} = d_1 \Delta u - \beta \nabla.(h(u)\nabla v) - k_1 u - q u^2 + k_2 v, \quad (t,x) \in \Omega_T \\ \frac{\partial v}{\partial t} = d_2 \Delta v - k_2 v + k_1 u + f, \quad (t,x) \in \Omega_T. \end{cases}$$

Le système est couplé avec des conditions de Neumann homogènes sur le bord

$$\nabla u.\eta = \nabla v.\eta = 0 \ sur \ \partial\Sigma_T$$

Lorsque la fonction h est non identiquement nulle, le modèle prend en compte le phénomène de la chemotaxis, qui est la capacité de certains organismes à orienter leur mouvement selon certaines espèces chimiques présentes dans l'environnement. Le flux de matière est composé de deux parties : un flux molaire classique ($J_{mol} = a\nabla u$) et un autre chimiotactique ($J_{chem} = \beta h(u)\nabla v$).

Nous avons par ailleurs démontré l'existence des solutions pour deux différentes fonctions de sensibilité chimiotactique h, ainsi que l'existence d'attracteur exponentiel.
La théorie utilisée ici est basée sur les idées de Lions [39] et a été utlisée par Osaki [40](voir aussi [41]), basée sur la méthode de Faedo-Galerkin, ainsi que les résultats de Temam [42] [43] et de Ryu [44].
Des simulations numériques ont été réalisées dans le but d'illustrer la capacité de ces modèles à produire les structures spatiales.

Les travaux concernant ce type de système ont été initiés par le papier de Turing, puis Keller et Segel [45] et Murray. D'autres auteurs se sont

intéressés à ce type de systèmes dans plusieurs contextes : Bendahmane [46], Cieslak[47] Wrozesk[48], Hillen et Painter[49] ...
Le chapitre 6 fera l'objet d'un prochain article, alors que le chapitre 7 a été soumis à une revue d'écologie.

Chapitre 2

Mathematical validation of MOMOS.

Abstract

MOMOS model (Modelling Organic changes by Micro-Organisms of Soil), is a nonlinear differential ordinary system of equations, which models the dynamics of carbon in soil. This "compartmental" model emphasizes the role of the microbial biomass which is responsible for the model nonlinearity. We show here that, for any initial condition, there exists a global unique solution. Moreover if we assume periodicity of model entries we prove existence and uniqueness of a periodic solution which is also a global attractor for any other solution of this periodic system.

2.1 Introduction

The global carbon cycle is of major concern due to its relationship with the greenhouse effect and climate change [50]. Terrestrial ecosystems play a major role in regulating atmospheric CO_2 concentrations. The net balance of photosynthesis and respiration corresponds to a current terrestrial sink of about 1-3 Pg C [51]. Top soils (0-30 cm) contain more carbon than all vegetation, and as much as the atmosphere [52]. Moreover, soil organic carbon (SOC) pools and turnover play key roles in building and sustaining soil fertility, a food security component [53]. Therefore understanding and modelling of soil organic carbon dynamics are especially critical regarding climate change and food security issues.

The soil organic carbon content results of the equilibrium between inputs and outputs into the soil system. Major inputs correspond to the accumulation of organic matter (OM) from plants both as litter (plant residues)

and as rhizodeposition. This OM originates from the photosynthetic carbon fixation by plants. Outputs result from the heterotrophic respiration processes when soil organic carbon is used as energy source by soil organisms and returned back to the atmosphere in form of CO_2 [5]. Most soil heterotrophic respiration is the result of organic compound degradation by enzyme functions [6]. As a result of the large diversity of the organic compounds themselves and of the soil biodiversity, the soil organic carbon represents a large variety of forms. In order to simplify this heterogeneity, soil scientists have tried to summarize this continuum into few discrete pools [8]). The different compartments (or pools) are supposed to correspond to different chemical characteristics with more or less degradability.
Compartmental analysis was often used in biology, medicine and ecology. Based on local mass balance, this approach leads to ordinary differential systems that Jacquez and Simon [14] extensively investigated. (see also Sandberg [54]). For the carbon dynamics in soil, Manzoni and Porporato [8] summarized the historic evolution of model complexity. The authors list more than 200 compartmental models, which simplify the biochemical process and where the soil is divided into homogeneous pools. Most models adopted a discrete representation of soil organic matter into few pools, generally from 2 to 5, characterized by different chemical characteristics or degradability. The decomposition rates, applied to each pool, are governed by kinetic and stoichiometric laws and are mainly controlled by the environmental conditions (e.g., soil moisture level, aeration, soil temperature). In the past four decades, soil scientists have identified key processes and feedbacks for accurately modeling the soil organic carbon decomposition and the CO_2 fluxes [7]. But, as highlighted by Manzoni and Porporato [8] most traditional models (e.g. the Roth-C and Century models, see [55]) neglect direct influence of microbial-mediated processes that transform and stabilize soil C inputs [56]. The huge variety of models depends on the current understanding of soil carbon cycle and the simplifications made on such complex system.
For this purpose, a number of parameters need to be calibrated in order to get results close to land data. Kinetic parameters are linked to geological and environmental influence, while flow fraction parameters (efficiency factors) are independent of soil moisture or temperature. Generally, models are over parametrized and not sensitive to climate change. These parameters also affect the type of the differential system. Mainly, two types of systems have been elaborated. The first type is linear, since the rate of decrease of organic matter in every pool is proportional to its content. Such systems are relatively easy to calibrate and to study since the analytical expression of the solutions can be reached. The second type is nonlinear and models, in a

better way, complex phenomena. But these models are also more intricate and less satisfactory since we generally have only qualitative informations about solutions.
MOMOS (Modelling Organic changes by Micro-Organisms of Soil) is one of the recent nonlinear models. It is used to simulate and predict the carbon cycle. Introduced by Pansu et al. [23] , MOMOS contains five compartments : Microbial Biomass (MB), Labile and Stable fractions of necromass materials (VL and VS) and finally Labile and Stable fractions of humus (HL,HS). MOMOS is in fact, a mixture of nonlinear and linear models. It is centred on the microbial biomass activity and was initially built and validated from a comparative study using isotopic tracers in two sites (Pansu et al., [22]). Thereafter, MOMOS was validated on another labelling experiment in other contrasted sites along a large altitudinal gradient ([23]). Six different approaches have been tested [22], in connection with the behaviour of the microbial biomass activity. Empirically the best model corresponds to a nonlinear approach, linked to the respiratory function of microbial biomass.
This model has been since widely used, ([22],[57],[23], [24]) but a rigorous analysis of its mathematical properties was lacking.
The organization of this paper is as follows. In Section 2 we formulate the mathematical model. In section 3, we prove first that the vector solution components are positive, which is expected, since we deal with carbon concentrations in different compartments. Second we state the existence of a global solution, which is important as we predict, through this model, how concentrations will evolve over time. Finally we focus on the nature of the solution dependence on both constant parameters and initial condition, as it is necessary to justify the calibration step while building the model. In section 4, under periodicity assumption of carbon inputs, temperature and soil moisture, we prove that the model has a unique periodic solution which is globally attractive.

2.2 Description of MOMOS model.

The general MOMOS equation is :

$$\dot{\mathbf{x}} = f_1(T) f_2(\theta) \mathbf{A_c}\, \mathbf{x} + \mathbf{B}(t) \tag{2.2.1}$$

where

$$\mathbf{x} = \begin{pmatrix} x_{VL} \\ x_{VS} \\ x_{MB} \\ x_{HL} \\ x_{HS} \end{pmatrix}$$

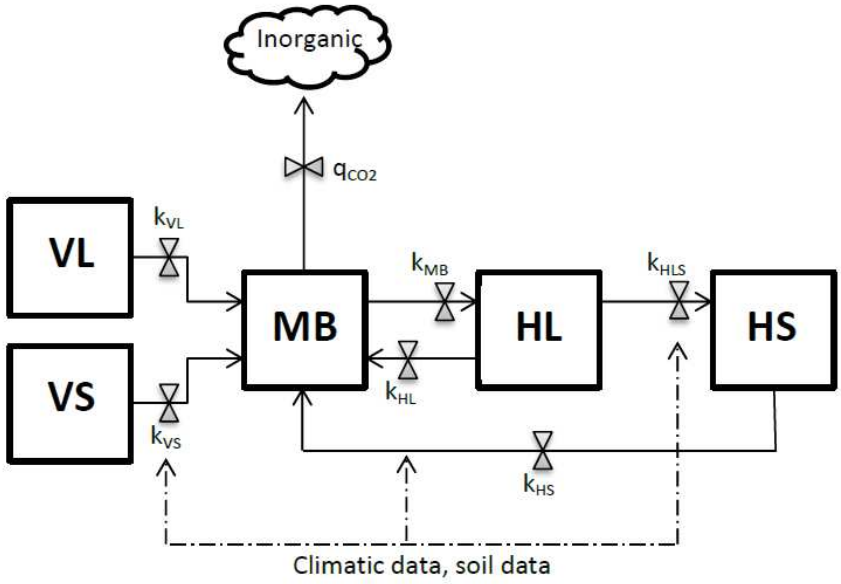

Figure 2.1: The flow Diagram of the MOMOS model.

is the vector of the state variables, $\mathbf{A_c}$ is the parameter matrix dependent on $\mathbf{x}$, $\mathbf{B}$ is a vector function regulating the external inputs. Function $f_1(T)$ is the response to temperature correction [23] :

$$f_1(T) = {Q_{10}}^{(T-T_{op})/10},$$

where T is the actual daily soil temperature equal to air temperature, Q_{10} is a constant representing the sensitivity of soil respiration to an increase of temperature by 10°C, ([7]) and T_{op}, set to 28°C, is the optimal decomposition temperature. Constant Q_{10} is defined as the ratio of respiration occuring at $T + 10$ to that at T, when T is a temperature. In most soil studies, Q_{10}

values range between 2 and 3 (see [7]).
Function $f_2(\theta)$ is the response function to soil moisture :

$$f_2(\theta) = \text{MIN}(1, \frac{\theta}{\text{WHC}}).$$

This last functions varies from 0 to 1. As in theory the water holding capacity WHC is always greater than θ , we set here :

$$f_2(\theta) = \frac{\theta}{\text{WHC}}$$

The soil moisture θ and soil temperature T are considered smooth and time-dependent since they represent a continuous real phenomenon. We can simplify then the equation (2.2.1) by writting :

$$\dot{\mathbf{x}} = g(t)\mathbf{A_c}\,\mathbf{x} + \mathbf{B}(t) = \mathbf{h}(t, \mathbf{x}) \tag{2.2.2}$$

where $g(t) = f_1(T)f_2(\theta)$ is a strictly positive time-dependent scalar function which represents the effect of the temperature and the humidity on the solution. Vector function $\mathbf{B}(\cdot)$ models the external feed of organic material. Only its two first coordinates are not equal to zero. Later in this article, we will consider as periodic the two time-dependent terms $\mathbf{B}(t)$ and $g(t)$.
For the carbon cycle, the model sets a particular parameter matrix. Parameters are strictly positive.

$$\mathbf{A_c} = \begin{pmatrix} -k_{VL} & 0 & 0 & 0 & 0 \\ 0 & -k_{VS} & 0 & 0 & 0 \\ k_{VL} & k_{VS} & -(q_{CO_2} + k_{MB}) & k_{HL} & k_{HS} \\ 0 & 0 & k_{MB} & -(k_{HL} + k_{HLS}) & 0 \\ 0 & 0 & 0 & k_{HLS} & -k_{HS} \end{pmatrix} \tag{2.2.3}$$

The q_{CO_2}-term is the metabolic quotient of the microbial biomass, used in (2.2.3) is defined by :

$$q_{CO_2} = q\, x_{MB} = \frac{k_{resp}}{C^0_{MB}}\, x_{MB}$$

Due to the metabolic quotient term, we then obtain a nonlinear differential system. Since the second member of (2.2.2) depends explicitly on time, the system is also non-autonomous.

2.3 Existence and stability of MOMOS solution.

2.3.1 Existence and positivity of the solution.

Definition 2.1. *: Cooperative system.*
Let us consider a differential system in $\mathbb{R}^n$

$$\dot{\mathbf{x}} = \mathbf{f}(\mathbf{x}, t),$$

where f *is* C^1 *with respect to* $\mathbf{x}$ *and measurable with respect to* t*.*
The system is called cooperative if, for $i \neq j$*, it verifies :*

$$\frac{\partial \mathbf{f}_i}{\partial x_j} \geq 0 \tag{2.3.1}$$

This class of system has interesting property of monotonicity but let us first define an order relation on $\mathbb{R}^n$.

Definition 2.2. *Semi-order on* $\mathbb{R}^n$*.*
Let $\mathbf{x}$ *and* $\mathbf{y}$ *be in* $\mathbb{R}^n$*. We write* $\mathbf{x} \geq \mathbf{y}$ *if* $x_i \geq y_i$*, for all* i *such that* $1 \leq i \leq n$*.*

Any relation of order between two vectors in this paper will be taken in this sense. A key result for our model is the following :

Proposition 2.1. *: Monotonicity of the solutions ([28] proposition 1.1)*
Let $\mathbf{M} \subset \mathbb{R}^n$*. Let* $\mathbf{f}$ *and* $\mathbf{g} : \mathbb{R}_+ \times \mathbf{M} \to \mathbb{R}^n$ *be both* C^1 *with respect to* $\mathbf{x}$ *and measurable with respect to* t *and such that :*

i) $\forall \mathbf{z} \in \mathbf{M}$*,* $\forall t \geq t_0$*,* $\mathbf{f}(t, \mathbf{z}) \leq \mathbf{g}(t, \mathbf{z})$*,*

ii) The system $\dot{\mathbf{x}} = \mathbf{f}(t, \mathbf{x})$ *is cooperative.*

Let $\mathbf{x}_0, \mathbf{y}_0 \in \mathbb{R}^n$ *such that* $\mathbf{x}_0 \leq \mathbf{y}_0$*. If* $\mathbf{x}(\cdot)$ *and* $\mathbf{y}(\cdot)$ *are solutions of :*

$$\begin{cases} \dot{\mathbf{x}} = \mathbf{f}(t, \mathbf{x}); & \mathbf{x}(t_0) = \mathbf{x}_0 \\ \dot{\mathbf{y}} = \mathbf{g}(t, \mathbf{y}); & \mathbf{y}(t_0) = \mathbf{y}_0 \end{cases}$$

then

$$\mathbf{x}(t) \leq \mathbf{y}(t), \ \forall t \geq t_0.$$

Theorem 2.1. *For each positive initial condition, the MOMOS differential system* (2.2.2) *admits a positive global solution.*

Proof. *The proof is divided in three steps.*
Step1 : Local existence. The vectorial function $\mathbf{h}$ *defined in* (2.2.2) *is supposed here at least continuous with respect to* t *and* C^1 *with respect to* $\mathbf{x}$. *By Cauchy's theorem we obtain the local existence and the uniqueness of the solution* (2.2.2) *that verifies* $\mathbf{x}(t_0) = \mathbf{x}_0$ *with* $\mathbf{x}_0 \in \mathbf{P^5}$.

Step 2 : Positivity. Let us prove that the solution of (2.2.2) *is in* $\mathbf{P^5}$ *for any time and any initial condition in* $\mathbf{P^5}$. *Let us consider a new differential system :*

$$\dot{\mathbf{x}} = g(t)\mathbf{A}_c\,\mathbf{x} = \mathbf{f}(t, \mathbf{x}) \tag{2.3.2}$$

The trivial vector $\mathbf{0}$ *is a solution of* (2.3.2) *and the vector functions* $\mathbf{f}$ *and* $\mathbf{h}$ *defined in* (2.2.2) *verify the conditions of proposition* 2.1. *We conclude that a solution* $\mathbf{x}$ *of MOMOS system* (2.2.2) *such that* $\mathbf{x}(t_0) \in \mathbf{P^5}$ *remains positive for* $t \geq t_0$.

Step 3 : Global existence. For the seek of simplicity we note respectively the state vector $\mathbf{x}$ *in* (2.2.2) *as :*

$$\mathbf{x} = \begin{pmatrix} x_1 \\ x_2 \\ x_3 \\ x_4 \\ x_5 \end{pmatrix}$$

and the matrix $\mathbf{A_c}$ *in* (2.2.2) *as :*

$$\mathbf{A_c} = \begin{pmatrix} -k_1 & 0 & 0 & 0 & 0 \\ 0 & -k_2 & 0 & 0 & 0 \\ k_1 & k_2 & -(qx_3 + k_3) & k_4 & k_5 \\ 0 & 0 & k_3 & -(k_4 + k_6) & 0 \\ 0 & 0 & 0 & k_6 & -k_5 \end{pmatrix} \tag{2.3.3}$$

Let us consider the linear differential system defined by :

$$\dot{\mathbf{x}} = g(t)\mathbf{A}\,\mathbf{x} + \mathbf{B}(t) = \mathbf{L}(t, \mathbf{x}) \tag{2.3.4}$$

where the matrix $\mathbf{A}$ *is :*

$$\mathbf{A} = \begin{pmatrix} -k_1 & 0 & 0 & 0 & 0 \\ 0 & -k_2 & 0 & 0 & 0 \\ k_1 & k_2 & -k_3 & k_4 & k_5 \\ 0 & 0 & k_3 & -(k_4 + k_6) & 0 \\ 0 & 0 & 0 & k_6 & -k_5 \end{pmatrix}$$

First, for any initial condition $\mathbf{x}(t_0)$ *in* $\mathbb{R}^5$*, the continuous affine system* (2.3.4) *admits a unique solution defined for all* $t \geq t_0$ *(see [58] theorem 11.1). It is also obvious that for all* $\mathbf{z} \in \mathbb{R}^5$ *and for all* $t \geq t_0$*, we have* $\mathbf{h}(t, \mathbf{z}) \leq \mathbf{L}(t, \mathbf{z})$*, with* $\mathbf{h}$ *the right term of a cooperative system (*(2.2.2)*). Let* $\mathbf{x}(.)$ *respectively* $\mathbf{y}(.)$ *be the unique solutions of* (2.2.2)*, respectively* (2.3.4)*, for the same initial condition. Then, by proposition* 2.1*, we obtain that the MOMOS solution verify the inequality :*

$$\mathbf{x}(t) \leq \mathbf{y}(t), \quad \forall t \geq t_0,$$

and thus $\mathbf{x}(t)$ *exists for all* $t \geq t_0$*.*

2.3.2 Stability on initial condition and parameters.

Let us first recall some results :

Proposition 2.2. *: Dependence on initial condition ([58] theorem 14.3) Let* $\dot{\mathbf{x}} = \mathbf{f}(t, \mathbf{x})$ *be a differential system. Suppose that the partial derivative of* $\mathbf{f}$ *with respect to the second variable* $\mathbf{x}$ *exists and is continuous. The application* $\Phi : \nu \mapsto x(\cdot)$*, which associates to a vector* $\nu \in \mathbb{R}^n$ *the vector function* $\mathbf{x}(\cdot)$ *such that*

$$\dot{\mathbf{x}} = \mathbf{f}(t, \mathbf{x}), \quad \mathbf{x}(t_0) = \nu,$$

is $C^1(\mathbb{R}^n)$*.*

Stability notions are essential for our problem. When we model real phenomena by using dynamical systems, it is common to have only approximate knowledge of parameters and initial conditions. We prove here that, MOMOS solution (2.2.2) is continuously dependent on the initial condition as well as on different parameters. The first assertion is obvious thanks to proposition 2.2. This means that if we have an approximation $\mathbf{y}_0$ of the initial condition $\mathbf{x}_0$, then the calculated solution $\mathbf{y}(\cdot)$ is an approximation of $\mathbf{x}(\cdot)$. For the error estimation, we need to suppose that $g(\cdot)$ is at least C^1 with a bounded derivative thus, it is uniformly continuous. In this case, theorem 2.8 of [59] provides that :

$$\|\mathbf{x}(t) - \mathbf{y}(t)\| \leq \|\mathbf{x}_0 - \mathbf{y}_0\| e^{L(t-t_0)}$$

where

$$L = \sup_{(t,\mathbf{x}) \neq (t,\mathbf{y}) \in \mathbf{V}} \frac{\|\mathbf{h}(t, \mathbf{x}) - \mathbf{h}(t, \mathbf{y})\|}{\|\mathbf{x} - \mathbf{y}\|}$$

and $\mathbf{V} \subset \mathbf{U}$ a set containing the graphs of $\mathbf{x}(\cdot)$ and $\mathbf{y}(\cdot)$
In fact, we do not have better result for error approximation even for simple differential equations. This can be a problem especially for the case of large time simulation. Nevertheless the continuous dependence result justifies the calibration step (varying a chosen parameter while fixing the others). One can extend the result of proposition 2.2 to the stability on parameters. If $\mathbf{f}$ depends on a parameter vector $\mathbf{k} \in \mathbb{R}^p$, let $\mathbf{x}(\cdot, \mathbf{k})$ be the solution of $\dot{\mathbf{x}} = \mathbf{f}(t, \mathbf{x})$ corresponding to an initial condition $\mathbf{x}_0$. By setting a new variable :

$$\tilde{\mathbf{x}} = \begin{pmatrix} \mathbf{x} \\ \mathbf{k} \end{pmatrix}$$

we obtain that $\tilde{\mathbf{x}}$ verifies

$$\dot{\tilde{\mathbf{x}}} = \tilde{\mathbf{f}}(t, \mathbf{x}) = \begin{pmatrix} \mathbf{f}(t, \mathbf{x}) \\ \mathbf{0} \end{pmatrix}, \quad \tilde{\mathbf{x}}_0 = \begin{pmatrix} \mathbf{x}_0 \\ \mathbf{k} \end{pmatrix},$$

with $\tilde{\mathbf{f}}$ satisfying the hypothesis of proposition 2.2, and we conclude.

2.4 Periodic solutions.

When modelling the bio-geochemical transformations of soil organics matters, MOMOS take into account the effect of temperature, soil moisture and external feeds in carbonic material. To compute the long-term behaviour of this model, assuming periodic different time-dependent parameters (seasonal variations) is necessary in many applications. The purpose of this is to provide answers to critical theoretical scenarios.
We prove here that in the cyclic-variation case ($\mathbf{B}(\cdot)$ and $g(\cdot)$ are periodic in time with period T) the equation (2.2.2) has exactly one periodic solution with period T. More, this solution is an attractor for any other solution of (2.2.2), when time goes to infinity.
A result comparable with this one is stated in Sandberg [54], for a large class of compartmental models. The arguments of [54] depend critically of a set of eight hypothesis that must be satisfied. But in our case three of them (H2, H5, H8) failed and Sandberg's theory is useless.

One can deal with the two first equations of MOMOS system separately. Since $k_i > 0$, for all i in $\{1, 2\}$ and $g(\cdot)$ is positive and not identically zero then, for each i in $\{1, 2\}$, there exists a unique positive T-periodic solution. This solution has the initial condition in t_0 :

$$x_{p,i}(t_0) = (-1+e^{k_i \int_{t_0}^{T+t_0} g(s)\,\mathrm{ds}})^{-1} \int_{t_0}^{T+t_0} e^{(k_i \int_{t_0}^{s} g(\tau)\,\mathrm{d}\tau)} B_i(s)\,\mathrm{ds}, \quad \forall i \in \{1, 2\}.$$

We notice that these two periodic solutions are strictly positive. More, if $x_{p,i}(t_0) > 0$, there exists $m_i > 0$ such that $x_{p,i}(t) \geq m_i$, for all $t \geq t_0$ and i in $\{1, 2\}$.
Any other solution of the first two equations tends respectively to these periodic solution, when time goes to infinity. Indeed, another solution has obviously the form :

$$x_i(\cdot) = x_{0,i}(\cdot) + x_{p,i}(\cdot), \quad \text{with } i \in \{1, 2\},$$

and $x_{0,i}(t)$, a solution of the correspondent homogeneous linear differential equation, which goes to 0 when t goes to infinity.

The last three equations of the system will be investigated by using the properties of cooperative systems as we cannot get analytical expression of this solution. Thus, we introduce the "reduced" MOMOS system :

$$\dot{\mathbf{x}} = g(t)\mathbf{A}_r\,\mathbf{x} + g(t)\begin{pmatrix} -qx_1^2 \\ 0 \\ 0 \end{pmatrix} + \begin{pmatrix} b(t) \\ 0 \\ 0 \end{pmatrix} = \mathbf{h}_r(t, \mathbf{x}) \tag{2.4.1}$$

where

$$\mathbf{A}_r = \begin{pmatrix} -k_3 & k_4 & k_5 \\ k_3 & -(k_4 + k_6) & 0 \\ 0 & k_6 & -k_5 \end{pmatrix} \tag{2.4.2}$$

and $b(t) = g(t)(k_1 x_{p,1}(t) + k_2 x_{p,2}(t))$. For all $t \geq t_0$, $b(t)$ is strictly positive and T-periodic and we note $m = \inf_{t \geq t_0} b(t)$. The state vector becomes in this section :

$$\mathbf{x} = \begin{pmatrix} x_1 \\ x_2 \\ x_3 \end{pmatrix}$$

The "reduced" MOMOS system is obviously cooperative.

Proposition 2.3. *Let $\alpha > 0$ real. The eigenvalues of the following matrix*

$$\mathbf{A}_{r,\alpha} = \begin{pmatrix} -k_3 - \alpha & k_4 & k_5 \\ k_3 & -(k_4 + k_6) & 0 \\ 0 & k_6 & -k_5 \end{pmatrix} \tag{2.4.3}$$

has strictly negative real parts.

Proof. *Gerschgorin's theorem [60] provides for this matrix that eigenvalues are zero or have strictly negative real parts. Because zero can not be an eigenvalue for this problem we conclude.*

Proposition 2.4. *If* $\mathbf{x}(\cdot)$ *is the solution of the "reduced" MOMOS* (2.4.1) *corresponding to the initial condition* $\mathbf{x}_0 = \mathbf{x}(t_0)$ *in* $\mathbf{P^3} = \mathbb{R}^3_+$ *and if there exists* $\varepsilon > 0$ *such that* $x_1(t_0) \geq \varepsilon$, *then* $x_1(t) \geq \varepsilon$, *for all* $t \geq t_0$.

Proof. *Let* $\mathbf{x}_0$ *and* $\mathbf{x}(\cdot)$ *define as previous. Let be the new variable*

$$\mathbf{y}(\cdot) = \mathbf{x}(\cdot) - \begin{pmatrix} \varepsilon \\ 0 \\ 0 \end{pmatrix}$$

We see that $\mathbf{y}(\cdot)$ *verifies :*

$$\dot{\mathbf{y}} = g(t)\mathbf{A}_r\mathbf{y} + g(t)\begin{pmatrix} -qy_1^2 \\ 0 \\ 0 \end{pmatrix} + \begin{pmatrix} b(t) \\ 0 \\ 0 \end{pmatrix} + g(t)\begin{pmatrix} -k_3\varepsilon - 2q\varepsilon y_1 - q\varepsilon^2 \\ k_3\varepsilon \\ 0 \end{pmatrix}$$

This can be written as :

$$\dot{\mathbf{y}} = g(t)\mathbf{A}_{r,2\varepsilon q}\mathbf{y} + g(t)\begin{pmatrix} -qy_1^2 \\ 0 \\ 0 \end{pmatrix} + \begin{pmatrix} b(t) \\ 0 \\ 0 \end{pmatrix} + g(t)\begin{pmatrix} -k_3\varepsilon - q\varepsilon^2 \\ k_3\varepsilon \\ 0 \end{pmatrix} = \mathbf{h}_{r,2\varepsilon q}(t, \mathbf{y})$$

Since $m = \inf_{t \geq t_0} b(t)$ *is strictly positive then, for* $0 \leq \varepsilon \leq \gamma$, *with* $\gamma = \frac{-k_3 + \sqrt{k_3^2 + 4qm}}{2q}$, *we have* $b(t) - k_3\varepsilon - q\varepsilon^2 \geq 0$, *for all* t. *This leads to the following inequality :*

$$\forall t,\ \forall \mathbf{y}, \quad \mathbf{h}_r^0(t, \mathbf{y}) \leq \mathbf{h}_{r,2\varepsilon q}(t, \mathbf{y}),$$

with

$$\mathbf{h}_r^0(t, \mathbf{y}) = g(t)\mathbf{A}_{r,2\varepsilon q}\,\mathbf{y} + g(t)\begin{pmatrix} -qy_1^2 \\ 0 \\ 0 \end{pmatrix}$$

Using the proposition 2.1 *and the fact that* $\mathbf{0}$ *is a solution of* $\dot{\mathbf{y}} = \mathbf{h}_r^0(t, \mathbf{y})$ *we obtain that* $\mathbf{y}(t) \geq 0$, *for all* $t \geq t_0$.

Proposition 2.5. *Let $\varepsilon > 0$ be fixed. The following system*

$$\dot{\mathbf{y}} = g(t)\mathbf{A}_r\,\mathbf{y} + \begin{pmatrix} b(t) \\ 0 \\ 0 \end{pmatrix} + g(t) \begin{pmatrix} -q\varepsilon y_1 \\ 0\varepsilon \\ 0 \end{pmatrix} = \mathbf{h}_{r,lin}(t, \mathbf{y}, \varepsilon) \quad (2.4.4)$$

has a unique T-periodical solution. Any solution of this differential system is bounded.

Proof. *The system (2.4.4) can be written as :*

$$\dot{\mathbf{y}} = g(t)\mathbf{A}_{r,q\varepsilon}\,\mathbf{y} + \begin{pmatrix} b(t) \\ 0 \\ 0 \end{pmatrix}$$

By proposition 2.3*, the matrix $A_{r,q\varepsilon}$ has three different complex eigenvalues with strictly negative real parts. Like in the case of one linear differential equation we can prove that the linear differential system* (2.4.4) *admits a unique T-periodic solution $\mathbf{y}_p(t)$, for a given initial condition $\mathbf{y}_{p\,0}$. More, any other solution $\mathbf{y}(\cdot)$ of* (2.4.4) *verifies :*

$$\|\mathbf{y}(t) - \mathbf{y}_p(t)\| \to 0 \text{ when } t \to \infty.$$

Then $\mathbf{y}(\cdot)$ is bounded.

Proposition 2.6. *Any positive solution of the "reduced" MOMOS* (2.4.1) *is bounded.*

Proof. *Let $\mathbf{x}(\cdot)$ be a positive solution of* (2.4.1)*. It exists t_0 and ε such that $0 < \varepsilon \leq \gamma$ and $x_1(t_0) \geq \varepsilon$. We notice that :*

$$\mathbf{h}_r(t, \mathbf{x}) \leq \mathbf{h}_{r,lin}(t, \mathbf{x}, \varepsilon),\ \forall t, \forall \mathbf{x} \text{ with } x_1 \geq \varepsilon.$$

By the previous proposition and by proposition 2.1 *we conclude.*

Theorem 2.2. *There is a unique positive periodic solution of the MOMOS differential system. This solution is globally attractive.*

Proof. *The proof is divided in three steps. First, we prove the existence of a periodic solution of* (2.4.1)*. Second, we show that such a positive periodic solution is unique. Finally, we show that any other positive solution of the periodic MOMOS system* (2.2.2) *tends to its unique periodic solution when t tends to infinity.*

Step 1. Let us prove the existence of a periodic solution for the "reduced" MOMOS system (2.4.1).
We define a vector sequence $(\mathbf{U}_n)_{n\geq 0}$ *in* $(\mathbf{P}^3)$ *by :*

$$\left\{ \begin{array}{ll} \mathbf{U}_0 & = \mathbf{0} \\ \mathbf{U}_{n+1} & = \mathbf{x}(T, \mathbf{U}_n) \end{array} \right.$$

where $\mathbf{x}(\cdot, \mathbf{x}_0)$ *is the the solution of the "reduced" MOMOS differential system corresponding to an initial condition* $\mathbf{x}_0$*. We notice that, thanks to the periodicity of the system,* $\mathbf{U}_{n+1} = \mathbf{x}((n+1)T, \mathbf{U}_0)$*. By the previous proposition, the sequence* $(\mathbf{U}_n)_{n\geq 0}$ *is bounded. Since the system* (2.4.1) *is cooperative, we have, due to proposition* 2.1*, that* $\mathbf{U}_{n+1} \geq \mathbf{U}_n$*, for all* n *. As a monotone, bounded sequence,* $(\mathbf{U}_n)_{n\geq 0}$ *converges to* $\mathbf{Y}_0$ *in* $\mathbf{P}^3$ *which verifies* $\mathbf{Y}_0 = \mathbf{x}(T, \mathbf{Y}_0)$*. Then* $\mathbf{y}_p(\cdot) = \mathbf{x}((\cdot, \mathbf{Y}_0)$ *is a periodic solution of the "reduced" MOMOS system.*

Step 2. We suppose the existence of another periodic and positive solution $\tilde{\mathbf{y}}_p$ *of* (2.4.1)*. We define the variable* $\mathbf{z} = \mathbf{y}_p - \tilde{\mathbf{y}}_p$*. There verifies :*

$$\dot{\mathbf{z}} = g(t)\mathbf{A}_r\,\mathbf{z} + g(t)\begin{pmatrix} -qz_1^2 \\ 0 \\ 0 \end{pmatrix} + g(t)\begin{pmatrix} -2qz_1\tilde{y}_{p,1} \\ 0 \\ 0 \end{pmatrix} = \mathbf{h}_{r,p}(t, \mathbf{z}) \quad (2.4.5)$$

We notice that function $s(\cdot) := \sum_{i=1}^{3} z_i(\cdot)$ *is periodic and satisfies*

$$\dot{s}(t) = -g(t)qz_1(y_{p,1} + \tilde{y}_{p,1}).$$

If $z_1(\cdot)$ *has the same sign on the interval of one period, then* $s(\cdot)$ *is monotone on this interval. Thus* $z_1(t) = 0$ *for all* $t \geq t_0$*, thanks to its periodicity. Then* $\mathbf{z}(t) = \mathbf{0}$*, for all* $t \geq t_0$ *.*
If $z_1(\cdot)$ *changes sign, there exists* t_0 *such that* $z_1(t_0) = 0$*. More,* $z_2(t_0)$ *and* $z_3(t_0)$ *have different sign. Indeed, if* $z_2(t_0)$ *and* $z_3(t_0)$ *have same sign, the cooperativity of system* (2.4.5)*, implies that* $\mathbf{z}(t)$ *has the sign of* $\mathbf{z}(t_0)$ *on* $[t_0, t_0 + T]$*. Then we obtain a contradiction with the fact that* $z_1(\cdot)$ *change sign on the same interval. Without loss of generality we suppose that* $t_0 = 0$*. Suppose for example, that* $z_2(0) > 0$ *and* $z_3(0) < 0$*. Let* $\mathbf{z}^+(\cdot)$ *be the solution of* (2.4.5) *corresponding to the initial condition* $\mathbf{z}_0^+ = \begin{pmatrix} 0 \\ z_2(0) \\ 0 \end{pmatrix}$*.*
By proposition 2.1*, we have* $\mathbf{z}(t) \leq \mathbf{z}^+(t)$*, for all* $t \geq 0$*. Let* $\sigma = \inf_{t\geq 0} \tilde{\mathbf{y}}_{p,1}(t)$*.*

We define a new differential system

$$\dot{\mathbf{z}} = g(t)\mathbf{A}_r\,\mathbf{z} + g(t)\begin{pmatrix} -2qz_1\sigma \\ 0 \\ 0 \end{pmatrix} = \mathbf{h}_{r,p,\sigma}(t,\mathbf{z}) \tag{2.4.6}$$

We have then

$$\mathbf{h}_{r,p}(t,\mathbf{z}) \leq \mathbf{h}_{r,p,\sigma}(t,\mathbf{z}),\ \forall t,\ \forall \mathbf{z} \in \mathbf{P}^3 \tag{2.4.7}$$

Let $\mathbf{z}_\sigma^+(\cdot)$ *be the solution of* (2.4.6) *corresponding to the initial condition* $\mathbf{z}_0^+$. *Again, proposition* (2.1) *implies that* $\mathbf{z}(t) \leq \mathbf{z}_\sigma^+(t)$ *for all* $t \geq 0$. *Regarding to the proposition* (2.3), $\mathbf{z}_\sigma^+(t) \to \mathbf{0}$ *when* $t \to \infty$. *Because the periodicity of* $\mathbf{z}(\cdot)$ *we have that* $\mathbf{z}(t) \leq \mathbf{0}$, *for all* $t \geq 0$. *By contradiction with the previous assertion we deduce that the "reduced" MOMOS system has a unique periodic solution. Thus the MOMOS differential system* (2.2.2) *has a unique periodic solution.*

Step 3. We show that if $\mathbf{x}(\cdot)$ *is the solution of the periodic MOMOS differential system* (2.2.2), *with the initial condition* $\mathbf{x}(t_0) = \mathbf{x}_0 \geq \mathbf{0}$, *and if* $\mathbf{y}_p(\cdot)$ *is the unique positive periodic solution, we have :*

$$\mathbf{x}(t) \to \mathbf{y}_p(t)\ when\, t \to \infty$$

In the case where $\mathbf{x}_0 \leq \mathbf{y}_p(t_0)$, *we write the equation satisfied by* $\mathbf{y}_p - \mathbf{x}$. *Like in the previous step,* $\mathbf{y}_p - \mathbf{x}$ *is smaller that the solution, with initial condition* $\mathbf{y}_p(t_0) - \mathbf{x}_0$, *of an homogeneous, linear, differential system. This new system has five eigenvalues with strictly negative real part, and* $\mathbf{0}$ *is an attractive solution for any solution of the system. Thus the conclusion is obvious in this case. The case* $\mathbf{x}_0 \geq \mathbf{y}_p(t_0)$ *is similar. If we have no order relation between* $\mathbf{x}_0$ *and* $\mathbf{y}_p(t_0)$ *we construct two initial conditions in* t_0, $\mathbf{x}_0^+$ *and* $\mathbf{x}_0^-$, *such that* $\mathbf{x}_0^- \leq \mathbf{y}_p(t_0)$, $\mathbf{x}_0 \leq \mathbf{x}_0^+$ *and we consider two solutions* $\mathbf{x}^+(\cdot)$, *respectively* $\mathbf{x}^-(\cdot)$ *of* (2.2.2), *starting in* $\mathbf{x}_0^+$, *respectively* $\mathbf{x}_0^-$. *Then we have :*

$$\mathbf{x}^-(t) \leq \mathbf{y}_p(t), \mathbf{x}(t) \leq \mathbf{x}^+(t), \quad \text{for all } t.$$

Since $\mathbf{x}^-(t)$ *and* $\mathbf{x}^+(t)$ *goes to* $\mathbf{y}_p(t)$ *when* t *goes to infinity, we conclude.*

2.5 Numerical simulations.

To illustrate the theoretical results exposed previously, numerical simulations were done based on real data. Field data already published by Pansu

et al. in [23] were selected. Briefly, data are from an Andean pàramo site (alpine-like vegetation) of Gavidia. This site is located in a glacial valley at 3400 m, near the upper limit of agriculture. The mean temperature is 8.9° with large daily fluctuations. More detailed information is available in [23]. The different parameters to run the model were set using [23] and updated values published recently in Pansu et al. [24]. The first simulation considerer no organic carbon input as indicated in [23].

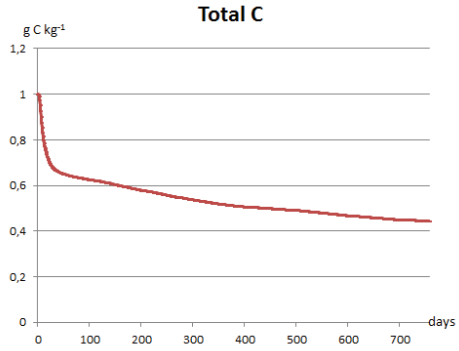

Figure 2.2: Total soil organic carbon dynamic simulated without any organic input.

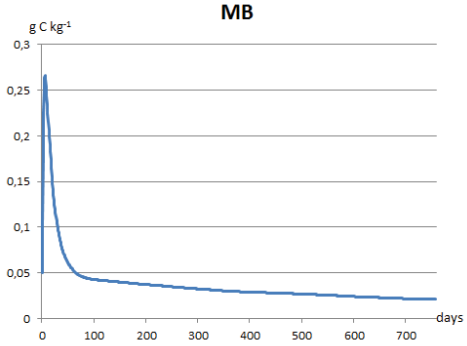

Figure 2.3: Dynamic of soil microbial biomass, when inputs are set to zero.

As expected, since there is no organic input, a loss in the total amount of soil organic matter due to respiration is simulated (Fig.2.2). Microbial biomass increases in first days, this rapid increase will be restrained by substrate

availability, mostly in the more labile pools (Fig.2.3). These numerical results were experimentally validated, more details can be found in [23].

In a second step a theoretical simulation were conducted concidering a scenario using the previous set of parameters and climate data, but with a constant carbon influx of 345 g C m^{-2} $year^{-1}$. The initial conditions in all pools are set to zero except for VL, VS and MB pools. Since we considered initial condition away from "equilibrium", we see that the total organic matter continues to increase (Fig.2.4) while microbial biomass reaches rapidly a ceiling amount (Fig.2.5).

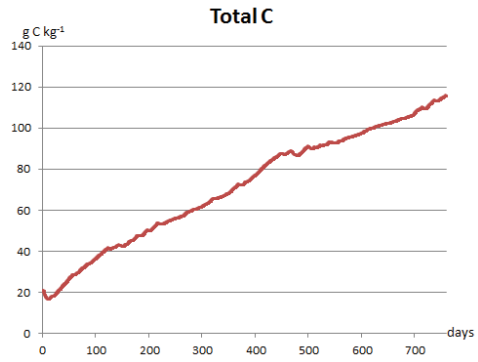

Figure 2.4: Total soil organic carbon dynamic simulated with a constant carbon influx of 345 g C m^{-2} $year^{-1}$.

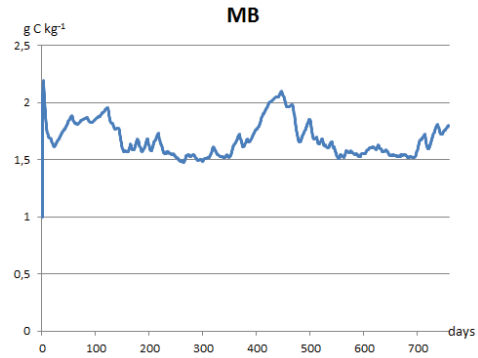

Figure 2.5: Dynamic of soil microbial biomass, with a constant carbon influx of 345 g C m^{-2} $year^{-1}$.

2.6 Conclusion.

We proved in this paper that MOMOS model is mathematically valid. We showed that for any positive initial condition, the solution remains positive, and that its domain of existence is not bounded. We also notice that it has a strong property of monotonicity which means that if we start at t_0 from two different initial values $\mathbf{y}_0$ and $\mathbf{x}_0$ such that $\mathbf{y}_0 \leq \mathbf{x}_0$ then $\mathbf{y}(t) \leq \mathbf{x}(t)$, $\forall t \geq t_0$. This property allowed us to show that if we assume parameters periodic, the system admits a unique periodic positive solution. A similar result was proved for the Rothamsted carbon model (RothC) [29], which is a linear model. This assumption of periodicity is very consistent. The geo-climatic conditions and the agricultural use of a land are not far to be periodic (with a period of several years). We proved then that this periodic solution is globally attractive for any other positive solution of the periodic MOMOS system.

Chapitre 3

Analysis of a spatially distributed model.

Abstract

The goal of this paper is to study the mathematical properties of a new model of soil carbonic dynamics which is a reaction-diffusion-advection system with a quadratic reaction term. This is a spatial version of Modelling Organic changes by Micro-Organisms of Soil model, recently introduced by M. Pansu and his group. We show here that for any nonnegative initial condition, there exists a unique nonnegative weak solution. Moreover, if we assume time periodicity of model entries, taking into account seasonal effects, we prove existence of a minimal and a maximal periodic weak solution. In a particular case these two solutions coincide and they become a global attractor of any bounded solution of the periodic system.

3.1 Introduction

The CO_2 emissions are considered to be the most important factor influencing the Earth's carbon cycle and consequently the greenhouse effect. Human activity emits CO_2 not only by the combustion of fossil fuels, but also by agricultural activities and Land-use changes.

Terrestrial ecosystems play a major role in regulating atmospheric greenhouse gas (CO_2, CH_4 and N_2O) concentrations [50]. Soils are one of the largest organic carbon (OC) compartments, topsoils (0-30 cm) alone contain more carbon than the total vegetation living biomass and as much as the atmosphere [50]. Soil organic carbon (SOC) pools and turnover play key roles in building and sustaining soil fertility, which is a major food security component [53]. Therefore understanding and modelling of SOC dynamics

are especially critical regarding climate change and food security issues.

The SOC is considered to be the result of the equilibrium between inputs into, and outputs out, of the soil system. Major inputs correspond to the accumulation of organic matter (OM) from plants both as litter (plant residues) and as rhizodeposition. This OM originates from the photosynthetic carbon fixation by plants. Outputs result from the heterotrophic respiration processes when soil organic carbon is used as energy source by soil organisms and returned back to the atmosphere in form of CO_2 [5]. Most soil heterotrophic respiration is the result of organic compound degradation by enzyme processes [6]. As a result of the large diversity of the organic compounds themselves and of the soil biodiversity, the SOC may take a large variety of forms. In order to simplify this heterogeneity, soil scientists have tried to summarize this continuum into a few discrete pools [8]). The different compartments (or pools) are often assumed to correspond to different chemical characteristics with different degrees of degradability.

Compartmental analysis is standard in biology, medicine and ecology. Based on local mass balance, this approach leads to ordinary differential systems that Jacquez and Simon [14] extensively investigated. (see also Sandberg [54]). For the carbon dynamics in soil, Manzoni and Porporato [8] summarized the historic evolution of model complexity. The authors list more than 200 compartmental models, which simplify the biochemical process and where the soil is divided into homogeneous pools. Most models adopted a discrete representation of soil organic matter into few pools, generally from two to five, characterized by different chemical characteristics or degradability. The decomposition rates, applied to each pool, are governed by kinetic and stoichiometric laws and are mainly controlled by the environmental conditions (e.g., soil moisture level, aeration, soil temperature). In the past four decades, soil scientists have identified key processes and feedbacks for accurately modeling the SOC decomposition and the CO_2 fluxes [7]. But, as highlighted by Manzoni and Porporato [8], most traditional models (e.g. the Roth-C and Century models ; see [55]) are linear and neglect direct influence of microbial-mediated processes that transform and stabilize soil carbon inputs [56]. A huge variety of models depends on the current understanding of soil carbon cycle and on the simplifications made on such complex system.

The compartmental MOMOS model (Modelling Organic changes by Micro-Organisms of Soil ; see [23], [24]) was selected because it focuses on the role of soil microbial biomass. It is written like a nonlinear ordinary differential system and has been proved to be mathematically valid and providing a unique solution ([61]). Moreover, if the carbon inputs are periodic, there is

a unique periodic solution, which is also a global attractor for any other solution of this periodic model.

In this paper, we improve the initial model, which was not spatially distributed, by adding diffusion and advection terms while keeping the reaction term unchanged. Our goal here is to analyse this new model from a mathematical point of view. First we prove that this model, a reaction-diffusion-advection system, has a unique weak solution. We are looking for weak solutions, because initial inputs are in effect not regular enough to give rise to more "regular" solutions. Second, if we assume periodicity of the data, we prove that there exists a maximal and a minimal periodic solution of this system. In a very particular case, the minimal and the maximal periodic solutions coincide and become a global attractor for any bounded solution of the periodic system.

3.2 Mathematical preliminaries and notations.

Let Ω be a bounded open subset of $\mathbb{R}^N, 1 \leq N \leq 3$, with smooth boundary $\partial\Omega$. Let ν denote the outward unit normal vector along $\partial\Omega$. Let $T > 0$ and $\Omega_T := (0,T) \times \Omega$. If $p > 0$, we let :

$$L^p_+(\Omega_T) := \{u \in L^p(\Omega_T), u \geq 0 \text{ a.e in } \Omega_T\},$$

$$H^1(\Omega) := \{u \in L^2(\Omega), \nabla u \in L^2(\Omega; \mathbb{R}^N))\},$$

$$H^1_0(\Omega) := \{u \in H^1(\Omega),\ u = 0 \text{ on } \partial\Omega \text{ a.e.}\},$$

If X is a Banach space,

$$L^p(0,T,X) := \{u : (0,T) \to X \text{ mesurable}, \|u(t,.)\|_X \in L^p(0,T)\},$$

and $C([0,T],X)$ denotes the space of continuous functions $u : [0,T] \to X$. Next we recall some useful results (for a proof see for example [43]) :

Lemma 3.1. *Let X be a Banach space with X' its dual space and let H be a Hilbert space such that X continously embedded in H identified with its dual space. If $u \in L^p(0,T,X)$ and $\partial_t u \in L^{p'}(0,T,X')$ with $\frac{1}{p} + \frac{1}{p'} = 1$, then $u \in C([0,T],H)$.*

Lemma 3.2. *(Aubin-Lions) Let X_0, X, X_1 be three Banach spaces such that $X_0 \subset X \subset X_1$. Suppose that X_0 is compactly embedded in X and X is continuously embedded in X_1 and that X_0 and X_1 are reflexive spaces. For*

$1 < p, q < \infty$ *let :*

$$W := \{u \in L^p(0,T,X_0), \partial_t u \in L^q(0,T,X_1)\}.$$

Then the embedding of W *in* $L^p(0,T,X)$ *is compact.*

The first MOMOS model (Modelling Organic changes by Micro-Organisms of Soil) is a nonlinear differential ordinary system of equations, which models the dynamics of carbon in soil. It can be written as :

$$\dot{\mathbf{u}} = \mathbf{g}(t, \mathbf{u})$$

where $\mathbf{u} = (u_1, u_2, u_3)$ and

$$\mathbf{g}(t,\mathbf{u}) = g(t) \begin{pmatrix} -k_1 - qu_1 & k_2 & k_3 \\ k_1 & -(k_2+k_4) & 0 \\ 0 & k_4 & -k_3 \end{pmatrix} \mathbf{u} + \begin{pmatrix} f(t) \\ 0 \\ 0 \end{pmatrix}, \quad (3.2.1)$$

where $k_1, \ldots, k_4$ and q are positive constants, $f(t)$ represents the external input at time t of organic matter and $g(t)$ a positive time dependent scalar function which models the effect of temperature and moisture on the solution. As a matter of fact, the vector function $\mathbf{g}$ depends not only on time but also on space thanks to the coefficients variability in soil clay content and soil texture. The phenomena described by this model can also be subjected to the influence of transport and sedimentation through advection and diffusion. Then we introduce the following reaction-diffusion-advection initial problem :

$$\begin{cases} \frac{\partial u_i}{\partial t} - \operatorname{div}(\mathbf{A}_i(t,x)\nabla u_i) + \mathbf{B}_i(t,x)\nabla u_i = g_i^+(t,x,\mathbf{u}), (t,x) \in \Omega_T \\ \gamma\left(\mathbf{A}_i(t,x)\nabla u_i\right)\cdot\nu + \beta_i(t,x)u_i = 0, (t,x) \in \Sigma_T := (0,T)\times\partial\Omega \\ u_i(0) = u_{i,0} \text{ in } \Omega \end{cases} \quad (3.2.2)$$

where $\mathbf{A}_i$ is a diffusion matrix and $\mathbf{B}_i$ a transport vector, for each $i = 1, 2, 3$. The boundary conditions are of either Dirichlet type ($\gamma = 0,\ \beta_i \equiv 1$) or of Neumann-Robin type ($\gamma = 1,\ \beta_i(t,x) \geq 0$). The right hand side term of (3.2.2) is :

$$\mathbf{g}^+(t,x,\mathbf{u}) := \begin{pmatrix} -k_1(t,x)u_1 - q(t,x)|u_1|u_1 + k_2(t,x)u_2 + k_3(t,x)u_3 + f(t,x) \\ k_1(t,x)u_1 - (k_2(t,x)+k_4(t,x))u_2 \\ k_4(t,x)u_2 - k_3(t,x)u_3 \end{pmatrix}$$

where we replaced the term $q(t,x)u_1^2$ with $q(t,x)|u_1|u_1$ for more accuracy,

since $q(t,x)u_1$ corresponds to a kinetic coefficient that cannot be negative. We assume that, for $i = 1, 2, 3$, the diffusion matrix $\mathbf{A}_i$ are bounded, symmetric and coercive :

$$\mathbf{A}_i \in L^\infty(\Omega_T)^{N\times N}, \tag{3.2.3}$$

$$\mathbf{A}_i(t,x)\zeta\cdot\zeta \geq c|\zeta|^2, \quad \forall \zeta \in \mathbb{R}^N, \text{ a.e in } \Omega_T, \text{ with } c>0 \tag{3.2.4}$$

and the transport vectors $\mathbf{B}_i$ are bounded on Ω_T :

$$\mathbf{B}_i \in L^\infty(\Omega_T)^N, \quad |(\mathbf{B}_i(t,x))_j| \leq c_{\max} \text{ a.e in } \Omega_T, \quad \text{for all } j = 1,\dots,N. \tag{3.2.5}$$

The functions k_j, β_i and q are assumed to be nonnegative-valued and bounded for all $j = 1, 2, 3, 4$ and $i = 1, 2, 3$:

$$k_j,\, q \in L^\infty(\Omega_T), \quad 0 \leq k_j(t,x), q(t,x) \leq C_{\max} \text{ a.e } \textit{ on } \Omega_T \tag{3.2.6}$$

$$\beta_i \in L^\infty(\Sigma_T), \quad 0 \leq \beta_i(t,x) \leq C_{\max} \text{ a.e } \textit{ on } \Sigma_T, \tag{3.2.7}$$

for some constant $C_{\max} > 0$. Finally we assume that the initial data and input are nonnegative and bounded :

$$u_{i,0} \in L^2_+(\Omega), \quad f \in L^2_+(\Omega_T), \quad f(t,x) \leq C_{\max} \text{ a.e } \textit{ on } \Omega_T. \tag{3.2.8}$$

It is understood once and for all that, save when otherwise specified, Latin indices take the values 1,2,3.

3.3 Existence result.

Hereafter the space X will be equal to $H^1(\Omega)$ if the boundary conditions are of Neumann-Robin type ($\gamma = 1$) and to $H^1_0(\Omega)$ if the boundary conditions are of Dirichlet type ($\gamma = 0$). We define the vector valued space :

$$\mathbf{W} := \{\mathbf{u} = (u_1,u_2,u_3)/\ \mathbf{u} \in (L^2(0,T,X)^3,\ \partial_t\mathbf{u} \in (L^2(0,T,X'))^3\}.$$

Definition 3.1. *A weak solution of (3.2.2) is a vector field* $\mathbf{u}$ *in* $\mathbf{W}$*, that satisfies :*

$$\begin{cases} \int_0^T < \partial_t u_i, \varphi_i >_{X,X'} dt \\ + \int_0^T \int_\Omega (\mathbf{A}_i(t,x)\nabla u_i \nabla\varphi_i + \mathbf{B}_i(t,x)\nabla u_i\, \varphi_i) dxdt \\ +\gamma \int_0^T \int_{\partial\Omega} \beta_i(t,x) u_i\, \varphi_i d\sigma dt = \int_0^T \int_\Omega g_i^+(t,x,\mathbf{u})\varphi_i dxdt, \\ u_i(0) = u_{i,0} \quad \textit{ in } \Omega \end{cases} \tag{3.3.1}$$

for all $\varphi_i \in L^2(0,T,X)$.

Remark 3.1. *Lemma 3.1 shows that the initial condition makes sense.*

Theorem 3.1. *Assume that (3.2.3)-(3.2.8) hold. Then, for every f in $L^2(0,T,X')$, the initial value problem (3.2.2) has a unique weak solution, which is nonnegative.*

The proof is organised as follows : we first prove the existence of a weak solution by the Faedo-Galerkin method, second we show its positivity and finally we prove its uniqueness.

Construction of an approximate solution.

Since the space X is a separable Hilbert space, it contains a countable dense subset $\{w_1, \ldots, w_n, \ldots\} \subset X$ of linearly independent elements. We assume that they are orthonormal in $L^2(\Omega)$.
We look now for finite dimensional approximate solution to the initial problem (3.3.1) as sequences $\{\mathbf{u}^n\}_{n\geq 1} = \{\,(u_i^n)\,\}_{n\geq 1}$, of the form :

$$u_i^n(t,x) = \sum_{j=1}^{n} \alpha_{ij}^n(t) w_j(x), \qquad (x,t) \in \bar{\Omega} \times (0,T). \tag{3.3.2}$$

Our purpose here is to determine the functions $\{\alpha_{ij}^n(t)\}_{i=1\ldots 3,\ j=1\ldots n}$. For each i, $\{\alpha_{ij}^n(t)\}_{j=1\ldots n}$ is the solution of the following systems of ODE's :

$$\begin{aligned} &< \partial_t u_i^n, w_k >_{X,X'} \\ &+ \int_\Omega \big(\mathbf{A}_i(t,x)\nabla u_i^n \nabla w_k + \mathbf{B}_i(t,x)\nabla u_i^n w_k\big)dx + \gamma \int_{\partial\Omega} \beta_i(t,x) u_i^n w_k d\sigma dt \\ &\qquad = \int_\Omega g_i^+(t,x,\mathbf{u}^n) w_k dx, \quad t>0, \quad k = 1...n, \end{aligned} \tag{3.3.3}$$

with the initial conditions :

$$\alpha_{ij}^n(0) = (u_{i,0}, w_j)_{L^2(\Omega)} \tag{3.3.4}$$

Thus the matrix field $\boldsymbol{\alpha}^n(t) = (\alpha_{ij}^n(t))_{i=1\ldots 3,\ j=1\ldots n},\ t>0$ solves a system of differential equations :

$$\begin{cases} \partial_t \alpha_{ij}^n(t) = F_{ij}(t, \boldsymbol{\alpha}^n(t)), \quad i = 1\ldots 3,\ j = 1\ldots n \\ \alpha_{ij}^n(0) = (u_{i,0}, w_j)_{L^2(\Omega)}. \end{cases} \tag{3.3.5}$$

Since the right-hand side of equation (3.3.3) is nonlinear in $\mathbf{u}$, the right-hand side of equation (3.3.4) is nonlinear in $\boldsymbol{\alpha}$. The existence of a solution

of (3.3.5) on an interval $[0, \rho^n)$, with $\rho^n > 0$, follows by classical results (see for example [62]). We prove that the right-hand side of (3.3.5) is locally lipschitz in the second variable and we apply the Cauchy-Lipschitz theorem. To prove global existence in $(0, T)$, we need a priori estimates of this solution.

Lemma 3.3. *Assume assumptions (3.2.3)-(3.2.8) hold. Then there exists a constant $C > 0$, not depending on n, such that for all $i = 1, 2, 3$:*

$$\begin{cases} \|u_i^n\|_{L^\infty(0,t,L^2(\Omega))} \leq C \\ \|\nabla u_i^n\|_{L^2(Q_t)} \leq C \\ \|\partial_t u_i^n\|_{L^2(0,t,(H^1(\Omega))')} \leq C \end{cases}$$

Proof. From (3.3.3), the approximate solution verify the following weak equations :

$$\begin{aligned} &< \partial_t u_1^n, \varphi_1^n >_{X,X'} + \int_\Omega (\mathbf{A}_1(t,x)\nabla u_1^n \nabla \varphi_1^n + \mathbf{B}_1(t,x)\nabla u_1^n \varphi_1^n)dx \\ &+ \gamma \int_{\partial\Omega} \beta_1(t,x) u_1^n \varphi_1^n d\sigma + \int_\Omega (k_1(t,x)u_1^n + q(t,x)|u_1^n|u_1^n)\varphi_1^n dx \\ &\qquad = \int_\Omega (k_2(t,x)u_2^n + k_3(t,x)u_3^n)\varphi_1^n dx + \int_\Omega f(t,x)\varphi_1^n dx \quad (3.3.6) \end{aligned}$$

$$\begin{aligned} &< \partial_t u_2^n, \varphi_2^n >_{X,X'} + \int_\Omega (\mathbf{A}_2(t,x)\nabla u_2^n \nabla \varphi_2^n + \mathbf{B}_2(t,x)\nabla u_2^n \varphi_2^n)dx \\ &+ \gamma \int_{\partial\Omega} \beta_2(t,x) u_2^n \varphi_2^n d\sigma + \int_\Omega (k_2(t,x) + k_4(t,x))u_2^n \varphi_2^n dx \\ &\qquad = \int_\Omega k_1(t,x)u_1^n \varphi_2^n dx \quad (3.3.7) \end{aligned}$$

$$\begin{aligned} &< \partial_t u_3^n, \varphi_3^n >_{X,X'} + \int_\Omega (\mathbf{A}_3(t,x)\nabla u_3^n \nabla \varphi_3^n + \mathbf{B}_3(t,x)\nabla u_3^n \varphi_3^n)dx \\ &+ \gamma \int_{\partial\Omega} \beta_3(t,x) u_3^n \varphi_3^n d\sigma + \int_\Omega k_3(t,x)u_3^n \varphi_3^n dx \\ &\qquad = \int_\Omega k_4(t,x)u_2^n \varphi_3^n dx \quad (3.3.8) \end{aligned}$$

where $\varphi_i^n(t,x) = \sum_{k=1}^n \theta_{ik}^n(t) w_k(x)$ and $(\theta_{ik}^n)_{i=1\ldots3,\ k=1\ldots n}$ are absolutely continuous functions.

Letting $\varphi_i^n = u_i^n$ in (3.3.6)-(3.3.8) and using Hölder's and Young's inequalities, we obtain :

$$\frac{1}{2}\frac{d}{dt}\|u_1^n(t)\|_{L^2}^2 + c\|\nabla u_1^n(t)\|_{L^2}^2 - c_{\max}(\frac{1}{2\varepsilon}\|u_1^n(t)\|_{L^2}^2 + \frac{\varepsilon}{2}\|\nabla u_1^n(t)\|_{L^2}^2) \leq \frac{1}{2}C_{max}(\|u_2^n\|_{L^2}^2 + 2\|u_1^n\|_{L^2}^2 + \|u_3^n\|_{L^2}^2) + \frac{1}{2\varepsilon'}\|f(t)\|_{L^2(\Omega)}^2 + \frac{\varepsilon'}{2}\|u_1^n(t)\|_{H^1(\Omega)}^2, \quad (3.3.9)$$

$$\frac{1}{2}\frac{d}{dt}\|u_2^n(t)\|_{L^2}^2 + c\|\nabla u_2^n(t)\|_{L^2}^2 - c_{\max}(\frac{1}{2\varepsilon}\|u_2^n(t)\|_{L^2}^2 + \frac{\varepsilon}{2}\|\nabla u_2^n(t)\|_{L^2}^2) \leq \frac{1}{2}C_{max}(\|u_2^n\|_{L^2}^2 + \|u_1^n\|_{L^2}^2), \quad (3.3.10)$$

$$\frac{1}{2}\frac{d}{dt}\|u_3^n(t)\|_{L^2}^2 + c\|\nabla u_3^n(t)\|_{L^2}^2 - c_{\max}(\frac{1}{2\varepsilon}\|u_3^n(t)\|_{L^2}^2 + \frac{\varepsilon}{2}\|\nabla u_3^n(t)\|_{L^2}^2) \leq \frac{1}{2}C_{max}(\|u_2^n\|_{L^2}^2 + \|u_3^n\|_{L^2}^2). \quad (3.3.11)$$

Summing inequalities (3.3.9)-(3.3.11) with appropriate values of ε and ε' we obtain the existence of positive constants C', C'', C''', independent of n, such that :

$$\frac{1}{2}\frac{d}{dt}(\|u_1^n(t)\|_{L^2}^2 + \|u_2^n(t)\|_{L^2}^2 + \|u_3^n(t)\|_{L^2}^2) + C'(\|\nabla u_1^n(t)\|_{L^2}^2 + \|\nabla u_2^n(t)\|_{L^2}^2 + \|\nabla u_3^n(t)\|_{L^2}^2 \leq C''(\|u_1^n(t)\|_{L^2}^2 + \|u_2^n(t)\|_{L^2}^2 + \|u_3^n(t)\|_{L^2}^2) + C'''. \quad (3.3.12)$$

Using Gronwall's lemma, we conclude that there exists a positive constant C_1 independent of n such that :

$$\|u_1^n(t)\|_{L^2}^2 + \|u_2^n(t)\|_{L^2}^2 + \|u_3^n(t)\|_{L^2}^2 \leq C_1, \quad (3.3.13)$$

and consequently there exists a positive constant C_2 independent of n such that :

$$\int_0^t (\|\nabla u_1^n(\sigma)\|_{L^2}^2 + \|\nabla u_2^n(\sigma)\|_{L^2}^2 + \|\nabla u_3^n(\sigma)\|_{L^2})d\sigma \leq C_2$$

So we already proved that :

$$u_i^n,\ 1 \leq i \leq 3,\ \text{are bounded in } L^\infty(0,t,L^2(\Omega)) \cap L^2(0,t,H^1(\Omega)) \quad (3.3.14)$$

It remains to prove that there exists a constant $C_3 > 0$ independent of n such that :

$$\|\partial_t u_i^n\|_{L^2(0,t,(H^1(\Omega))')} \leq C_3.$$

Each sequence $(u_i^n)_{n\geq 1}$ is bounded in $L^4(0,t,L^3(\Omega))$. Indeed, since Ω is regular enough we have $H^1(\Omega) \hookrightarrow L^6(\Omega)$ and using the interpolation technique we obtain :

$$\|u_i^n\|_{L^4(0,t,L^3(\Omega))} \leq \|u_i^n(t)\|^{\frac{1}{2}}_{L^\infty(0,t,L^2(\Omega))} \|u_i^n\|^{\frac{1}{2}}_{L^2(0,t,L^6(\Omega))}, \quad (3.3.15)$$

which allows us to conclude.

Consequently the sequence $(|u_1^n|u_1^n)_{n\geq 1}$ is bounded in $L^2(0,t,L^{\frac{3}{2}}(\Omega))$. So the sequence $(u_1^n)_{n\geq 1}$ satisfies :

$$\begin{aligned}
&| < \partial_t u_1^n, \varphi_1^n >_{X,X'} | \leq | \int_\Omega (\mathbf{A}_1(t,x)\nabla u_1^n \nabla \varphi_1^n + \mathbf{B}_1(t,x)\nabla u_1^n \varphi_1^n) dx| \\
&\gamma| \int_{\partial\Omega} \beta_1(t,x) u_1^n \varphi_1^n d\sigma| + | \int_\Omega (k_1(t,x)u_1^n + q(t,x)|u_1^n|u_1^n)\varphi_1^n dx| \\
&\qquad + | \int_\Omega (k_2(t,x)u_2^n + k_3(t,x)u_3^n)\varphi_1^n dx| + | \int_\Omega f(t,x)\varphi_1^n dx|.
\end{aligned}$$

Combining Hölder inequality, the first two inequalities of lemma 3.3, the boundedness of the sequence $(u_i^n)_{n\geq 1}$ in $L^4(0,t,L^3(\Omega))$, the continuity of the trace and the continuous injection of $L^2(0,t,H^1(\Omega))$ in $L^2(0,t,L^6(\Omega))$, we prove the existence of $C_3 > 0$, independent of n, such that :

$$| \int_0^t < \partial_t u_1^n, \varphi_1^n >_{X,X'} dt| \leq C_3 \|\varphi_1^n\|_{L^2(0,t,X)}. \quad (3.3.16)$$

Similar inequalities hold also for sequences $(\partial_t u_i^n)_{n\geq 1}$, $i = 2,3$ which prove the last assertion of lemma 3.3. □

Using the estimates of Lemma 3.3, we deduce that $\rho^n = T$, which extends each weak solution u_i^n to $[0,T]$. Now we can prove Theorem 3.1.

Proof of Theorem 3.1. As mentioned above, the proof consists in three steps.
Step 1. *Existence of the weak solution.* Since the sequences $(u_i^n)_{n\geq 1}$ are bounded in $L^2(0,T,X)$ and their time-derivatives are bounded in $L^2(0,T,X')$, there exists by the Aubin-Lions lemma (Lemma 2) a subsequence (not relabeled) such that :

$$\begin{cases} u_i^n \to u_i \text{ in } L^2(\Omega_T), \quad u_i^n \to u_i \text{ a.e. in } \Omega_T \\ \nabla u_i^n \rightharpoonup \boldsymbol{\xi}_i \text{ in } (L^2(\Omega_T))^3 \\ \partial_t u_i^n \rightharpoonup \psi_i \text{ in } L^2(0,T,X'). \end{cases} \tag{3.3.17}$$

To prove that $\nabla u_i = \boldsymbol{\xi}_i$, we take a test function $\varphi \in (\mathcal{D}(\Omega_T))^3$, so that :

$$\int_0^T \int_\Omega \nabla u_i^n \varphi \; dxdt = -\int_0^T \int_\Omega u_i^n \nabla\varphi \; dxdt$$

Taking the limit when $n \to \infty$ of both sides of this equation, we obtain

$$\int_0^T \int_\Omega \boldsymbol{\xi}_i \varphi \; dxdt = -\int_0^T \int_\Omega u_i \nabla\varphi \; dxdt = \int_0^T \int_\Omega \nabla u_i \varphi \; dxdt,$$

and we conclude by a density argument. To prove that $\partial_t u_i = \psi_i$, we use a similar computation for the derivative with respect to time, with test function $\varphi \in C_c^1(0,T,X)$. Thus we have

$$\begin{aligned} &u_i^n \rightharpoonup u_i \text{ in } L^2(0,T,X), \; \partial u_i^n \rightharpoonup \partial u_i \text{ in } L^2(0,T,X') \\ &\quad q(t,x)|u_1^n|u_1^n \rightharpoonup q(t,x)|u_1|u_1 \text{ in } L^2(0,T,L^{\frac{3}{2}}(\Omega)), \end{aligned}$$

where the last assertion is a straightforward consequence of the upper bound of sequence $|u_1^n|u_1^n$ in $L^2(0,t,L^{\frac{3}{2}}(\Omega))$ and the a.e. convergence of the sequence $(u_1^n)_{n\geq 1}$ in Ω_T.
Finally, integrating over $(0,T)$ in (3.3.6), (3.3.7), (3.3.8), letting $n \to \infty$ and using (3.3.17), we conclude that the limit $\mathbf{u}$ satisfies the first equation of (3.3.1). It remains to prove that $\mathbf{u}$ satisfies also the initial conditions. Using the initial conditions of the approximate solution (3.3.4),

$$u_i^n(0,x) := \sum_{j=1}^n {}_{L^2} < u_{i,0}, w_j >_{L^2} w_j \tag{3.3.18}$$

which converges to $u_{i,0}$ when $n \to \infty$. For any test function $\varphi \in C^1(0,T,X)$ such that $\varphi(T) = 0$, we have :

$$\int_0^T < \partial_t u_i^n, \varphi >_{X,X'} dt = -\int_0^T \int_\Omega u_1^n \, \partial_t\varphi dxdt - \int_\Omega u_1^n(0,x)\varphi(0,x)dx$$

A density argument after taking the limit in the previous equation, when $n \to \infty$ gives the boundary condition of (3.3.1).

Step 2. *Uniqueness of the weak solution.* Let $\mathbf{u} = (u_1, u_2, u_3)$ and $\mathbf{v} = (v_1, v_2, v_3)$ be two weak solutions of (3.2.2) and let $\mathbf{z} = (z_1, z_2, z_3) = \mathbf{u} - \mathbf{v}$. Then $\mathbf{z}(0) = \mathbf{0}$ in $\mathbf{L}^2(\Omega)$.

From [39], we have the following inequality :

$$(|u_1|u_1 - |u_2|u_2)(u_1 - u_2) \geq 0. \tag{3.3.19}$$

Then $\mathbf{z}$ verifies :

$$\begin{aligned} &< \partial_t z_1, \varphi_1 >_{X,X'} + \int_\Omega \big(\mathbf{A}_1(t,x)\nabla z_1 \nabla \varphi_1 + \mathbf{B}_1(t,x)\nabla z_1 \varphi_1\big)dx \\ &+ \gamma \int_{\partial\Omega} \beta_1(t,x) z_1 \varphi_1 d\sigma + \int_\Omega (k_1(t,x)z_1 + q(t,x)(|u_1|u_1 - |u_2|u_2)\varphi_1 dx \\ &\qquad = \int_\Omega (k_2(t,x)z_2 + k_3(t,x)z_3)\varphi_1 dx \end{aligned}$$

$$\begin{aligned} &< \partial_t z_2, \varphi_2 >_{X,X'} + \int_\Omega \big(\mathbf{A}_2(t,x)\nabla z_2 \nabla \varphi_2 + \mathbf{B}_2(t,x)\nabla z_2 \varphi_2\big)dx \\ &+ \gamma \int_{\partial\Omega} \beta_2(t,x) z_2 \varphi_2 d\sigma + \int_\Omega (k_2(t,x) + k_4(t,x)) z_2 \varphi_2 dx \\ &\qquad = \int_\Omega k_1(t,x) z_1 \varphi_2 dx \end{aligned}$$

$$\begin{aligned} &< \partial_t z_3, \varphi_3 >_{X,X'} + \int_\Omega \big(\mathbf{A}_3(t,x)\nabla z_3 \nabla \varphi_3 + \mathbf{B}_3(t,x)\nabla z_3 \varphi_3\big)dx \\ &+ \gamma \int_{\partial\Omega} \beta_3(t,x) z_3 \varphi_3 d\sigma + \int_\Omega k_3(t,x) z_3 \varphi_3 dx \\ &\qquad = \int_\Omega k_4(t,x) z_2 \varphi_3 dx \end{aligned}$$

Letting $\varphi_i = z_i$ and using the Hölder's and Young's inequalities, we obtain like in (3.3.12) the following inequality :

$$\frac{d}{dt}J(t) \leq CJ(t),$$

where $J(t) = \|z_1(t)\|^2_{L^2} + \|z_2(t)\|^2_{L^2} + \|z_3(t)\|^2_{L^2}$. Since $J(0) = 0$

$$J(t) = 0, \quad \forall t \in [0, T]$$

by Gronwall inequality and the conclusion follows.
As (3.2.2) has an unique weak solution, we deduce that the whole sequence of approximate solutions of step 1 converges.
Step 3. *Nonnegativity of the weak solution.* We use here the same idea as Efendiev and Sonner ([63]). Given $u \in H^1(\Omega)$, define $u^+ = max(u, 0)$ and $u^- = max(-u, 0)$. Then u^- and u^+ belong to $H^1(\Omega)$ (cf. [64]). The first equation of (3.3.1)$(i = 1)$ gives :

$$\begin{aligned}
&< \partial_t u_1, \varphi_1 >_{X,X'} + \int_\Omega (\mathbf{A}_1(t,x)\nabla u_1 \nabla \varphi_1 + \mathbf{B}_1(t,x)\nabla u_1\, \varphi_1)dx \\
&+ \int_\Omega q(t,x)|u_1|u_1\varphi_1 dx + \gamma \int_{\partial\Omega} \beta_1(t,x)u_1\, \varphi_1 d\sigma \\
&\quad = \int_\Omega (-k_1(t,x)u_1 + k_2(t,x)u_2 + k_3(t,x)u_3)\varphi_1 dx + \int_\Omega f(t,x)\varphi_1 dx.
\end{aligned}$$

Taking $\varphi_1 = -u_1^-$ we obtain :

$$\begin{aligned}
&< \partial_t u_1^-, u_1^- > + \int_\Omega (\mathbf{A}_1(t,x)\nabla u_1^- \nabla u_1^- + \mathbf{B}_1(t,x)\nabla u_1^-\, u_1^-)dx \\
&+ \gamma \int_{\partial\Omega} \beta_1(t,x)(u_1^-)^2 d\sigma + \int_\Omega (k_1(t,x)u_1^- + q(t,x)|u_1|u_1^-)u_1^- dx \\
&\qquad\qquad = -\int_\Omega (k_2(t,x)u_2 + k_3(t,x)u_3 + f(t,x))u_1^- dx.
\end{aligned}$$

By the coercivity assumption and Hölder's inequality, we deduce that :

$$< \partial_t u_1^-, u_1^- > \leq C\|u_1^-\|^2_{L^2(\Omega)} - \int_\Omega (k_2(t,x)u_2 + k_3(t,x)u_3 + f(t,x))u_1^- dx$$

A sufficient condition to have a nonnegative solution is the nonnegativity of the term

$$k_2(t,x)u_2 + k_3(t,x)u_3, \tag{3.3.20}$$

because $f(t,x)$ is already nonnegative. Indeed in this case we have :

$$\frac{1}{2}\partial_t \|u_1^-\|^2_{L^2(\Omega)} \leq C\|u_1^-\|^2_{L^2(\Omega)}. \tag{3.3.21}$$

As the initial condition $u_1^-(0)$ is zero, we obtain by Gronwall inequality that $\|u_1^-\|^2_{L^2(\Omega)} = 0$ and thus $u_1^- = 0$ a.e. in Ω. Similar results hold for u_2 and u_3, under similar assumptions of the right hand side term of the corresponding

equation.
We then consider the system of equation (3.2.2), where we replace the right hand side term $\mathbf{g}^+$ with $\tilde{\mathbf{g}}$ defined by :

$$\tilde{g}_i(t,x,\mathbf{u}) = g_i^+(t,x,u_i,|u_j|) \quad j \neq i. \tag{3.3.22}$$

We thus obtain a new system which admits a nonnegative weak solution $\tilde{u}$. But $\tilde{u}$ is also a weak solution of the initial system (3.2.2). Using uniqueness of solution, we deduce that u is nonnegative.

□

Assume once again that conditions (3.2.3)-(3.2.8) are fulfilled.

Remark 3.2. *Using the above theorem, we deduce that for every f in $L^2(0,T,X')$ the initial value problem*

$$\begin{cases} \frac{\partial u_i}{\partial t} - div(\mathbf{A}_i(t,x)\nabla u_i) + \mathbf{B}_i(t,x)\nabla u_i = g_i(t,x,\mathbf{u}), & \text{in } \Omega_T \\ \gamma\left(\mathbf{A}_i(t,x)\nabla u_i\right)\cdot\nu + \beta_i(t,x)u_i = 0, & \text{on } \Sigma_T := (0,T)\times\partial\Omega \\ u_i(0) = u_{i,0} & \text{in } \Omega \end{cases} \tag{3.3.23}$$

has a unique weak nonnegative soldivution, where $\mathbf{g}(t,x,\mathbf{u})$ is identical to $\mathbf{g}^+(t,x,\mathbf{u})$ except for the quadratic term $-q(t,x)|u_1|u_1$, which becomes $-q(t,x)u_1^2$ like in the ODE first model.

Definition 3.2. *A function $\tilde{\mathbf{u}} \in \mathbf{W}$ is said to be an upper weak solution of problem (3.2.2) if, for all i :*

$$\begin{aligned} \frac{\partial \tilde{u}_i}{\partial t} - div(\mathbf{A}_i(t,x)\nabla\tilde{u}_i) + \mathbf{B}_i(t,x)\nabla\tilde{u}_i &\geq g_i^+(t,x,\tilde{\mathbf{u}}) \text{ in } \Omega_T, \\ \gamma\left(\mathbf{A}_i(t,x)\nabla\tilde{u}_i\right)\cdot\nu + \beta_i(t,x)\tilde{u}_i &\geq 0 \qquad \text{on } \Sigma_T, \\ \tilde{u}_i(0,x) &\geq u_{i,0} \qquad \text{in } \Omega \end{aligned} \tag{3.3.24}$$

Similarly, $\hat{\mathbf{u}} \in \mathbf{W}$ is called a lower weak solution if it is satisfies the inequalities in (3.3.24) in reverse order.

Remark 3.3. *With the same assumptions as in Theorem 1, if $\tilde{\mathbf{u}}$ is an upper weak solution of the initial boundary problem (3.2.2), then $\tilde{\mathbf{u}}$ is nonnegative ; the proof is exactly the same as the proof of the nonnegativity of the weak solution.*

Lemma 3.4 (Comparison lemma)**.** *Assume that conditions (3.2.3)-(3.2.8) hold and let $\mathbf{u} \in \mathbf{W}$ be a weak solution, and let $\tilde{\mathbf{u}} \in \mathbf{W}$, respectively $\hat{\mathbf{u}} \in \mathbf{W}$, be an upper weak solution, respectively a lower weak solution , of the initial*

boundary problem (3.2.2). Then the functions $\mathbf{u},\ \tilde{\mathbf{u}},\ \hat{\mathbf{u}}$ *possess the following monotonicity property :*

$$\hat{\mathbf{u}} \leq \mathbf{u} \leq \tilde{\mathbf{u}} \quad \text{in } \Omega_T \tag{3.3.25}$$

Proof. If $\mathbf{u},\ \tilde{\mathbf{u}}$ are respectively a weak solution and an upper weak solution of (3.2.2), then they satisfy :

$$\begin{aligned}
&< \partial_t(\tilde{u}_i - u_i), \varphi_i >_{X,X'} \\
&+ \int_\Omega (\mathbf{A}_i(t,x)\nabla(\tilde{u}_i - u_i)\,\nabla\varphi_i + \mathbf{B}_i(t,x)\nabla(\tilde{u}_i - u_i)\,\varphi_i dx \\
&+ \delta_{i1}\int_\Omega q(t,x)(|\tilde{u}_1|\tilde{u}_1 - |u_1|u_1)\varphi_1 dx + \gamma\int_{\partial\Omega}\beta_i(t,x)(\tilde{u}_i - u_i)\,\varphi_i d\sigma \\
&\geq \int_\Omega \sum_{j=1}^{3}\kappa_{ij}(t,x)(\tilde{u}_j - u_j)\,\varphi_i dx, \\
&(\tilde{u}_i - u_i)(0,x) \geq 0 \quad \text{in } \Omega
\end{aligned}$$

for all $\varphi_i \in L^2_+(0,T,X)$, where δ_{i1} is the Kronecker symbol and $\kappa_{ij}(t,x)$ are the entries of the following matrix :

$$\mathbf{K} := \begin{pmatrix} -k_1(t,x) & k_2(t,x) & k_3(t,x) \\ k_1(t,x) & -(k_2(t,x)+k_4(t,x)) & 0 \\ 0 & k_4(t,x) & -k_3(t,x) \end{pmatrix}.$$

Then $\mathbf{w} := \tilde{\mathbf{u}} - \mathbf{u}$ is an upper solution for a similar initial boundary problem, where the quadratic term $q(t,x)(|\tilde{u}_1|\tilde{u}_1 - |u_1|u_1)$ has the same sign as w_1 thanks to (3.3.19). Therefore, by the above remark, $\mathbf{w}$ is nonnegative. Similarly, $\mathbf{u} - \hat{\mathbf{u}}$ is also nonnegative and this completes the proof. □

Remark 3.4. *As every weak solution of the initial boundary problem (3.2.2) is also an upper solution or a lower solution of the same problem, we deduce that if* $\mathbf{u}_1,\ \mathbf{u},\ \mathbf{u}_2$ *are three weak solutions satisfying the initial inequalities :*

$$\mathbf{u}_1(0,x) \leq \mathbf{u}(0,x) \leq \mathbf{u}_2(0,x) \quad \text{in } \ \Omega,$$

then they satify :

$$\mathbf{u}_1(t,x) \leq \mathbf{u}(t,x) \leq \mathbf{u}_2(t,x) \quad \text{in } \ \Omega_T,$$

3.4 Periodic solutions.

When modelling the bio-geochemical transformations of SOC, we take into account the effects of temperature, soil moisture, and external inputs in organic material. To compute the long-term behavior of the soil carbon dynamics model, assuming periodic different time-dependent parameters (that take into account seasonal variations) is necessary in many applications. The purpose of this section is to consider this important case.
A periodic behavior of solutions of parabolic boundary value problems arises in many biological, chemical and physical systems, and various methods have been proposed for the study of the existence and qualitative property of periodic solutions. We will apply the method of upper and lower weak solutions and its associated monotone iterations to a coupled system of semilinear parabolic equations. The method is classical and has been successfully used by many authors (see [65], [66], [67] and references given there).
Let us assume that, for each $x \in \Omega$, the matrix functions $\mathbf{A}_i$, the vector functions $\mathbf{B}_i$ and the functions g_i^+ are T-time periodic, for some $T > 0$. We are concerned in this section with the existence of a weak solution $\mathbf{u} \in \mathbf{W}$, of the periodic parabolic system :

$$\begin{aligned} \frac{\partial u_i}{\partial t} - div(\mathbf{A}_i(t,x)\nabla u_i) + \mathbf{B}_i(t,x)\nabla u_i &= g_i^+(t,x,\mathbf{u}),\ (t,x) \in \Omega_T, \\ \gamma\left(\mathbf{A}_i(t,x)\nabla u_i\right)\cdot\nu + \beta_i(t,x)u_i &= 0, \qquad (t,x) \in \Sigma_T, \quad (3.4.1) \\ \mathbf{u}(0,x) &= \mathbf{u}(T,x), \qquad x \in \Omega \end{aligned}$$

where we assume that $f \in L^\infty_+(\Omega_T)$ is T-time periodic and that conditions (3.2.3)-(3.2.7) hold. If such a solution $\mathbf{u}$ exists then the periodic condition :

$$\mathbf{u}(t,x) = \mathbf{u}(t+T,x), \quad (t,x) \in \Omega_T$$

follows obviously from the T periodicity in time of coefficients and the uniqueness of the solution with a prescribed initial condition.

Definition 3.3. *A function $\tilde{\mathbf{u}} \in \mathbf{W}$ is said to be an upper solution of problem (3.4.1) if, for all i :*

$$\begin{aligned} \frac{\partial \tilde{u}_i}{\partial t} - div(\mathbf{A}_i(t,x)\nabla \tilde{u}_i) + \mathbf{B}_i(t,x)\nabla \tilde{u}_i &\geq g_i^+(t,x,\tilde{\mathbf{u}}) \quad \text{in } \Omega_T, \\ \gamma\left(\mathbf{A}_i(t,x)\nabla \tilde{u}_i\right)\cdot\nu + \beta_i(t,x)\tilde{u}_i &\geq 0 \quad \text{on } \Sigma_T, \quad (3.4.2) \\ \tilde{u}_i(0,x) &\geq \tilde{u}_i(T,x) \quad \text{in } \Omega \end{aligned}$$

A function $\hat{\mathbf{u}} \in \mathbf{W}$ is called a lower solution if it is satisfies the inequalities in (3.4.2) in reverse order.

A pair of upper and lower solutions $\hat{\mathbf{u}}$, $\tilde{\mathbf{u}}$ are said to be *ordered* if $\hat{\mathbf{u}} \leq \tilde{\mathbf{u}}$ in Ω_T. Problem (3.4.1) has an obvious lower solution, viz. $\hat{\mathbf{u}} \equiv \mathbf{0}$, because f is a nonnegative function. If we assume that there exists a constant $C_{\min} > 0$ such that :

$$C_{\min} \leq k_3(t,x),\ k_2(t,x) + k_4(t,x),\ q(t,x) \quad \text{in } \Omega_T, \tag{3.4.3}$$

then problem (3.4.1) has also a constant upper solution $\tilde{\mathbf{u}} \equiv \mathbf{M}$. Indeed, if $\mathbf{M} = (M_1, M_2, M_3)$ is a constant upper solution, it must verify :

$$g^+(t,x,\mathbf{M}) \leq \mathbf{0}. \tag{3.4.4}$$

A straightforward calculation shows that, if we let $c := \frac{C_{\max}}{C_{\min}} > 0$, the constant vector $\mathbf{M} := (d, cd, c^2 d)$ verifies the inequality (3.4.4) for all $d \geq d_0 > 0$, where d_0 is the positive root of the quadratic equation :

$$x^2 - (c^2 + c^3)x - c = 0. \tag{3.4.5}$$

As $M_i > 0$ for all i we deduce that $\hat{\mathbf{u}}$, $\tilde{\mathbf{u}}$ are ordered.
In order to use the classical monotone iteration process for our problem (3.4.1) (cf. [66]), we remark that we can add an operator $D_i u_i$ to the left- and right-hand sides of the first equation of (3.4.1), with constants $D_i > 0$ large enough, that the operator :

$$\mathbf{Lu} := \begin{pmatrix} -div(\mathbf{A}_1(t,x)\nabla u_1) + \mathbf{B}_1(t,x)\nabla u_1 + D_1 u_1 + q(t,x)|u_1|u_1 \\ -div(\mathbf{A}_2(t,x)\nabla u_2) + \mathbf{B}_2(t,x)\nabla u_2 + D_2 u_2 \\ -div(\mathbf{A}_3(t,x)\nabla u_3) + \mathbf{B}_3(t,x)\nabla u_3 + D_3 u_3 \end{pmatrix}$$

is monotone and coercive and the matrix function $\mathbf{F}$ defined by

$$\mathbf{F}(t,x) := \begin{pmatrix} -k_1(t,x) + D_1 & k_2(t,x) & k_3(t,x) \\ k_1(t,x) & -k_2(t,x) - k_4(t,x) + D_2 & 0 \\ 0 & k_4(t,x) & -k_3(t,x) + D_3 \end{pmatrix},$$

has nonnegative coefficients in Ω_T.
Indeed, if D_i are large enough, there exists a constant $C > 0$ such that for all i :

$$\begin{aligned} &< L_i u_i - L_i v_i, u_i - v_i >_{X,X'} \\ &= \int_\Omega \mathbf{A}_i(t,x)\nabla(u_i - v_i)\nabla(u_i - v_i) + \mathbf{B}_i(t,x)\nabla(u_i - v_i)(u_i - v_i)dx \\ &+ \int_\Omega D_i(u_i - v_i)^2 dx + \gamma \int_{\partial\Omega} \beta_i(t,x)(u_i - v_i)^2 d\sigma \\ &+ \delta_{i1} \int_\Omega q(t,x)(|u_1|u_1 - |v_1|v_1)(u_1 - v_1)dx \geq C\|u_i - v_i\|_X^2, \end{aligned} \tag{3.4.6}$$

thanks to Young's and Hölder's inequalities and to the monotonicity property (3.3.19). Let

$$\mathbf{h}(t,x,\mathbf{u}) := \mathbf{F}(t,x)\ \mathbf{u} + \begin{pmatrix} f(t,x) \\ 0 \\ 0 \end{pmatrix}.$$

Because all the coefficients of the matrix $\mathbf{F}$ are nonnegative functions, we deduce the following monotonicity property of $\mathbf{h}$:

$$\mathbf{h}(t,x,\mathbf{u}) \geq \mathbf{h}(t,x,\mathbf{v}), \qquad \text{for all } \mathbf{u},\mathbf{v} \in \mathbf{W} \ \text{ such that } \mathbf{u} \geq \mathbf{v}.$$

The system (3.4.1) has now the equivalent form :

$$\begin{array}{ll} \partial_t \mathbf{u} + \mathbf{L}\mathbf{u} = \mathbf{h}(t,x,\mathbf{u}) & \text{in } \Omega_T, \\ \mathscr{B}\mathbf{u} = \mathbf{0} & \text{on } \Sigma_T, \\ \mathbf{u}(0,x) = \mathbf{u}(T,x) & \text{in } \Omega, \end{array} \tag{3.4.7}$$

where $\mathscr{B}_i u_i := \gamma\,(\mathbf{A}_i(t,x)\nabla u_i)\cdot\nu + \beta_i(t,x)u_i$.
Starting from either $\mathbf{u}^{(0)} = \tilde{\mathbf{u}}$ or $\mathbf{u}^{(0)} = \hat{\mathbf{u}}$, we construct a sequence $\mathbf{u}^{(m)} \in \mathbf{W}$ by solving the uncoupled system :

$$\begin{array}{ll} \partial_t u_i^{(m)} + L_i u_i^{(m)} = h_i(t,x,\mathbf{u}^{(m-1)}) & \text{in } \Omega_T, \\ \mathscr{B}_i u_i^{(m)} = 0 & \text{on } \Sigma_T, \\ u_i^{(m)}(0,x) = u_i^{(m-1)}(T,x) & \text{in } \Omega. \end{array} \tag{3.4.8}$$

Since the operator $\mathbf{L}$ is continuous from $(L^2(0,T,X))^3$ with the strong topology, into $(L^2(0,T,X'))^3$ with the weak topology, it follows that $\mathbf{L}$ is a hemicontinous mapping from $(L^2(0,T,X))^3$ into $(L^2(0,T,X'))^3$. Since $\mathbf{L}$ is also a monotone coercive operator by ([39] see Theorem 2.7.1 and Remark 2.7.8), we deduce the existence of a unique solution of (3.4.8) in $\mathbf{W}$. So the sequence $(\mathbf{u}^{(m)})_{m\geq 0}$ is well defined in $\mathbf{W}$. Denote the sequence by $(\overline{\mathbf{u}}^{(m)})_{m\geq 0}$ when $\mathbf{u}^{(0)} = \tilde{\mathbf{u}}$ and by $(\underline{\mathbf{u}}^{(m)})_{m\geq 0}$ when $\mathbf{u}^{(0)} = \hat{\mathbf{u}}$ and refer to them as maximal and minimal sequences, respectively.

Lemma 3.5. *The maximal and minimal sequences $(\overline{\mathbf{u}}^{(m)})_{m\geq 0}$ and $(\underline{\mathbf{u}}^{(m)})_{m\geq 0}$ possess the monotonicity property*

$$\mathbf{0} \equiv \hat{\mathbf{u}} \leq \underline{\mathbf{u}}^{(m)} \leq \underline{\mathbf{u}}^{(m+1)} \leq \overline{\mathbf{u}}^{(m+1)} \leq \overline{\mathbf{u}}^{(m)} \leq \tilde{\mathbf{u}} \equiv \mathbf{M} \quad \textit{in} \ \ \Omega_T. \tag{3.4.9}$$

Proof. The key argument is the following monotonicity property : if we have

$$\begin{array}{ll} \partial_t u_i + L_i u_i \geq \partial_t v_i + L_i v_i & \text{in } \Omega_T, \\ \mathscr{B}_i(u_i - v_i) = 0 & \text{on } \Sigma_T, \\ u_i(0,x) \geq v_i(0,x) & \text{in } \Omega, \end{array} \tag{3.4.10}$$

then $u_i \geq v_i$ in Ω_T. This monotonicity property will be the necessary ingredient for a proof by induction and it is a straightforward consequence of the comparison lemma (Lemma 4). The rest of the proof is standard (see for example [66], Lemma 2.1). □

Theorem 3.2. *Assume that assumptions (3.2.3)-(3.2.8) and (3.4.3) hold. Then the sequence* $(\overline{\mathbf{u}}^{(m)})_{m\geq 0}$ *given by (3.4.8) with* $\overline{\mathbf{u}}^{(0)} = \mathbf{M}$ *converges in* $\mathbf{W}$*, monotonically from above, to a maximal weak periodic solution* $\overline{\mathbf{u}}$ *of the problem (3.4.1), and the sequence* $(\underline{\mathbf{u}}^{(m)})_{m\geq 0}$ *with* $\underline{\mathbf{u}}^{(0)} = \mathbf{0}$ *converges in* $\mathbf{W}$*, monotonically from below, to a minimal weak periodic solution* $\underline{\mathbf{u}}$*. Moreover,*

$$\mathbf{0} \leq \underline{\mathbf{u}}^{(m)} \leq \underline{\mathbf{u}} \leq \overline{\mathbf{u}} \leq \overline{\mathbf{u}}^{(m)} \leq \mathbf{M} \quad \text{in } \Omega_T. \tag{3.4.11}$$

Proof. The sequences $(\overline{\mathbf{u}}^{(m)})_{m\geq 0}$ and $(\underline{\mathbf{u}}^{(m)})_{m\geq 0}$ are monotone and bounded from below and above a.e. in Ω_T

$$\mathbf{0} \leq \underline{\mathbf{u}}^{(m)} \leq \overline{\mathbf{u}}^{(m)} \leq \mathbf{M}.$$

Therefore, by Beppo Levi's theorem and Fatou's lemma, $(\overline{\mathbf{u}}^{(m)})_{m\geq 0}$, respectively $(\underline{\mathbf{u}}^{(m)})_{m\geq 0}$, converges a.e. in Ω_T to a limit function $\overline{\mathbf{u}}$, respectively $\underline{\mathbf{u}}$, and the following inequality is verified a.e. in Ω_T :

$$\mathbf{0} \leq \underline{\mathbf{u}}^{(m)} \leq \underline{\mathbf{u}} \leq \overline{\mathbf{u}} \leq \overline{\mathbf{u}}^{(m)} \leq \mathbf{M}.$$

Moreover the sequences $(\overline{\mathbf{u}}^{(m)})_{m\geq 0}$, respectively $(\underline{\mathbf{u}}^{(m)})_{m\geq 0}$, strongly converges in $(L^2(\Omega_T))^3$ to $\overline{\mathbf{u}}$, respectively $\underline{\mathbf{u}}$. As the sequence $(\overline{\mathbf{u}}^{(m)})_{m\geq 0}$ is a.e. uniformly bounded and the operator $\mathbf{L}$ is coercive, the sequence $(\overline{\mathbf{u}}^{(m)})_{m\geq 0}$ is bounded in $\mathbf{W}$, just the sequence of approximate solutions was bounded as the consequence of Lemma 3. So , like in part (i) of the proof of Theorem 1, there exists a subsequence (not relabeled) such that

$$\nabla \overline{u}_i^{(m)} \rightharpoonup \nabla \overline{u}_i \quad \text{in } (L^2(\Omega_T))^3, \qquad \partial_t \overline{u}_i^{(m)} \rightharpoonup \partial_t \overline{u}_i \quad \text{in } L^2(0,T,X'),$$
$$q(t,x)|\overline{u}_1^{(m)}|u_1^{(m)} \rightharpoonup q(t,x)|\overline{u}_1|\overline{u}_1 \text{ in } L^2(0,T,L^{\frac{3}{2}}(\Omega)), \quad \text{for all } i = 1,2,3.$$

Thanks to the definition of $\overline{\mathbf{u}}$, these convergence results hold for the entire sequence.
Passing now to the limit as $m \to \infty$ in (3.4.8), shows that the limit $\overline{\mathbf{u}}$ satisfies the first two equations of problem (3.4.7) or (3.4.1). As in the proof of Theorem 1, we obtain the following convergences at times 0 and T :

$$\overline{\mathbf{u}}^{(\mathbf{m})}(0) \rightharpoonup \overline{\mathbf{u}}(0), \quad \overline{\mathbf{u}}^{(\mathbf{m})}(T) \rightharpoonup \overline{\mathbf{u}}(T) \quad \text{in } L^2(\Omega), \quad \text{when } m \to \infty.$$

Finally we deduce the periodicity condition of $\overline{\mathbf{u}}$ from the equality :

$$\overline{\mathbf{u}}^{(m)}(0,x) = \overline{\mathbf{u}}^{(m-1)}(T,x).$$

A similar proof indicates that $\underline{\mathbf{u}}$ is periodic too. To establish the maximal and minimal property of the solutions $\overline{\mathbf{u}}$ and $\underline{\mathbf{u}}$, we proceed like in ([66], Theorem 2.1.). More specifically every solution $\mathbf{u}$ of (3.4.7) such that $\hat{\mathbf{u}} \leq \mathbf{u} \leq \tilde{\mathbf{u}}$ is an upper solution as well as a lower solution. By considering $\mathbf{u}$ and $\hat{\mathbf{u}}$ as a pair of ordered upper and lower solution, we infer from Lemma 4 that $\hat{\mathbf{u}} \leq \underline{\mathbf{u}}^{(m)} \leq \mathbf{u}$ for every m. Letting $m \to \infty$ gives $\underline{\mathbf{u}} \leq \mathbf{u}$. A similar argument using $\tilde{\mathbf{u}}$, $\mathbf{u}$ as ordered upper and lower solution leads to $\mathbf{u} \leq \overline{\mathbf{u}}$. This completes the proof. □

Asymptotic stability of periodic solution.

It was shown in Theorem 2 that the existence of a pair of ordered upper and lower weak solutions ensures the existence of a periodic weak solution. Moreover, we obtained the existence of a maximal and a minimal periodic weak solutions, but there is no a priori reason to think that they coincide. As one of the purpose of such a model is to provide answers to critical theoretical scenarii of global climate change, we need to compute the long-term behaviour of the SOC, in a cyclic variation case. So we are interested in the existence of cases where the periodic solution is unique and asymptotically stable, which means that it is an attractor for any other solution when time goes to infinity.
We limit our discussion to a simplified, but realistic model, where we consider only diffusion effects (there are no longer advection terms, i.e., $\mathbf{B}_i = \mathbf{0}$) and the elliptic and boundary operators are given in the form :

$$\mathbf{A}_i u_i \equiv D_i \Delta u_i, \quad \mathscr{B}_i u_i \equiv \mathscr{B} u_i \equiv \alpha \frac{\partial u_i}{\partial \nu} + \beta u_i \quad i = 1,2,3,$$

where $D_i > 0$, $\alpha \geq 0$, $\beta \geq 0$ are all constants with $\alpha + \beta > 0$. We consider also a simplified reaction term, derived from the initial ordinary differential equation system (3.2.1) (corresponding to the MOMOS model) :

$$\mathbf{g}^+(t,x,\mathbf{u}) = g(t)\mathbf{K}_0\mathbf{u} + \begin{pmatrix} -g(t)\ q\ |u_1|u_1 \ + \ f(t,x) \\ 0 \\ 0 \end{pmatrix},$$

with :

$$\mathbf{K}_0 := \begin{pmatrix} -k_1 & k_2 & k_3 \\ k_1 & -(k_2+k_4) & 0 \\ 0 & k_4 & -k_3 \end{pmatrix},$$

where $k_1, \ldots, k_4, q$ are positive constants, f a nonnegative scalar function satisfying (3.2.8) and g a positive function such that there exist two positive constants $C_{\min}$, $C_{\max}$ with $C_{\min} \leq g \leq C_{\max}$ on $(0,T)$. The periodic problem reads now :

$$\begin{array}{ll} \partial_t u_i - D_i \Delta u_i, = \mathsf{g}_i^+(t,x,\mathbf{u}) & \text{in } \Omega_T, \\ \mathscr{B} u_i = 0 & \text{on } \Sigma_T, \\ u_i(0,x) = u_i(T,x) & \text{in } \Omega. \end{array} \tag{3.4.12}$$

It is well known that the smallest eigenvalue λ_0 of the eigenvalue problem

$$\Delta\phi + \lambda\phi = 0 \quad \text{in } \Omega, \qquad \mathscr{B}\phi = 0 \quad \text{on } \partial\Omega, \tag{3.4.13}$$

is nonnegative and its corresponding eigenfunction ϕ is positive in Ω. In fact, $\lambda_0 > 0$ if $\beta > 0$ (for either Dirichlet or Robin boundary conditions) and $\lambda_0 = 0$ if $\beta = 0$ (for Neumann boundary conditions).

Theorem 3.3. *Let $\mathbf{u}^\star = (u_1^\star, u_2^\star, u_3^\star)$ be a given periodic solution of (3.4.12) such that $c \leq u_1^\star$ in Ω_T, with a positive constant c. Let $\mathbf{u}$ be a solution of (3.4.12) with the condition $\mathbf{u}(0,x) = \mathbf{u}(T,x)$, $x \in \Omega$ be replaced with $\mathbf{u}(0,x) = \mathbf{u}_0(x)$, $x \in \Omega$. Assume that there exist two constant vectors $\mathbf{m} \geq \mathbf{0}$, $\mathbf{M} \geq \mathbf{0}$ such that u_0 satisfies*

$$\mathbf{0} \leq -\mathbf{m}\,\phi(x) + \mathbf{u}^\star(0,x) \leq \mathbf{u}_0 \leq \mathbf{M}\,\phi(x) + \mathbf{u}^\star(0,x) \quad \textit{for almost every } x \in \Omega.$$

Assume that all the data of problem (3.4.12) are T-periodic in time. Then there exists $\varepsilon > 0$ such that :

$$|\mathbf{u}^\star(t,x) - \mathbf{u}(t,x)| \leq \mathbf{M} e^{-\varepsilon t}\phi(x) \quad \textit{for all } t > 0 \quad \textit{and a.e } x \in \Omega. \tag{3.4.14}$$

For proving Theorem 3 the following lemma is needed :

Lemma 3.6. *Let α be a real constant and $k_3, \ldots, k_6$ be four nonnegative constants. The eigenvalues of the following matrix*

$$\mathbf{K}_\alpha := \begin{pmatrix} -k_3 - \alpha & k_4 & k_5 \\ k_3 & -(k_4 + k_6) & 0 \\ 0 & k_6 & -k_5 \end{pmatrix} \tag{3.4.15}$$

have strictly negative real parts if $\alpha > 0$.

Proof. The matrix $\mathbf{K}_\alpha$ has negative diagonal terms and positive off-diagonal elements. The sum of elements of each column is zero or $-\alpha$ for the first

column. Then, by Gerschgorin's theorem [60], each eigenvalue of matrix $\mathbf{K}_\alpha$ belongs to one of the disks :

$$\{z \in \mathbb{C} \ / \ |z + k_{ii}| \leq k_{ii}\} \quad i \in \{1, 2, 3\},$$

where $-k_{ii}$ are the diagonal terms of $\mathbf{K}_\alpha$. Thus, the eigenvalues of matrix $\mathbf{K}_\alpha$ are zero or have strictly negative real parts. Because zero cannot be an eigenvalue of $\mathbf{K}_\alpha$, then we conclude. □

Furthermore $\mathbf{K}_\alpha$ is an essentially nonegative matrix thus, it exists a positive constant a_α such that $\mathbf{K}_\alpha + a_\alpha \mathbf{I}$ is a nonnegative matrix. Since $(\mathbf{K}_\alpha + a_\alpha \mathbf{I})^2$ is a positive matrix, we deduce that the matrix $\mathbf{K}_\alpha + a_\alpha \mathbf{I}$ is also irreducible. Then it follows from the Perron-Frobenius theorem for irreducible nonegative matrix that there exists a real eigenvalue of matrix $\mathbf{K}_\alpha$ with a positive eigenvector, which is the largest one among real parts of all other eigenvalues of $\mathbf{K}_\alpha$. This special eigenvalue termed as $r(\mathbf{K}_\alpha)$ and called the Perron-Frobenius eigenvalue of $\mathbf{K}_\alpha$, is negative thanks to Lemma 6. We deduce from the Collatz-Wieland formula (see for example [68], p.665) that $(\mathbf{K}_\alpha \mathbf{X})_i \leq r(\mathbf{K}_\alpha)\, X_i$ for all non-negative non-zero vectors $\mathbf{X}$, such that $X_i \neq 0$. Then the solution of the differential equation $\mathbf{X}'(t) = \mathbf{K}_\alpha \ \mathbf{X}(t)$ with $\mathbf{X}(0) = \mathbf{X}_0 \geq \mathbf{0}$ is such that :

$$\mathbf{0} \leq \mathbf{X}(t) \leq e^{-\varepsilon t} \mathbf{X}_0 \quad \text{for all } t > 0, \tag{3.4.16}$$

where $0 < \varepsilon = -r(\mathbf{K}_\alpha)$.

Proof of Theorem 3.3. Let $\tilde{u}_i = u_i^\star + p_i(t)\phi(x), \ i = 1, 2, 3$, where $0 \leq p_i$ is a function to be determined. Then $\tilde{\mathbf{u}} = (\tilde{u}_1, \tilde{u}_2, \tilde{u}_3)$ satisfies the boundary and initial conditions of (3.4.2) if

$$\begin{aligned} u_i^\star(0, x) + p_i(0)\phi(x) &\geq u_i^\star(T, x) + p_i(T)\phi(x) \quad \text{in } \Omega \\ \alpha \frac{\partial u_i^\star}{\partial \nu} + \alpha\, p_i \frac{\partial \phi}{\partial \nu} + \beta(u_i^\star + p_i\, \phi) &\geq 0 \quad \text{in } \Sigma_T \end{aligned}$$

Since $\mathbf{u}^\star$ is a solution of (3.4.12) and ϕ a solution of (3.4.13), the above inequalities are satisfied if $p_i(0) \geq p_i(T)$. Thanks to (3.4.13), the differential inequalities in (3.4.2) are satified if

$$\begin{aligned} &\partial_t u_i^\star - D_i \Delta u_i^\star + (p_i' + \lambda_0\, D_i\, p_i)\phi \geq \\ &\quad g(t) \ \sum_{j=1}^{3} K_{ij}^0 (u_j^\star + p_j \phi) - \delta_{i1}\ g(t)\, q (u_1^\star + p_1 \phi)^2 + f(t, x) \quad \text{in } \Omega_T, \end{aligned}$$

where K_{ij}^0 denote the coefficients of the matrix $\mathbf{K}_0$. This inequality is equivalent to

$$p_i' + \lambda_0 D_i\, p_i \geq g(t)\, \sum_{j=1}^{3} K_{ij}^0 p_j - \delta_{i1}\; g(t)\, q(2\, u_1^\star + p_1\phi)\, p_1. \tag{3.4.17}$$

Since $c \leq 2\, u_1^\star + p_1\phi$ a.e. in Ω_T, the last inequalities may be expressed in the form

$$\mathbf{p}' \geq \Big(g(t)\mathbf{K}_{qc} - \lambda_0\mathbf{D}\Big)\mathbf{p},$$

where $\mathbf{D}$ is the diagonal matrix $\mathrm{diag}(D_1, D_2, D_3)$. We choose $\mathbf{p}$ as the solution of the equation $\mathbf{p}' = g(t)\mathbf{K}_{qc}\mathbf{p}$ with $\mathbf{p}(0) = \mathbf{M}$, so that $\tilde{\mathbf{u}} = \mathbf{u}^\star + \mathbf{p}\phi$ is an upper solution of (3.4.12). Since $0 < g(t) \leq C_{\max}$, $0 < t$ the following change of variable $\tau(t) = \int_0^t \frac{1}{g(\sigma)} d\sigma$ gives the following equivalent differential system for $\mathbf{p}$:

$$\frac{d\mathbf{p}}{d\tau} = \mathbf{K}_{qc}\mathbf{p} \quad \text{ with } \mathbf{p}(0) = \mathbf{M}.$$

Thanks to (3.4.16), there exists $\varepsilon' > 0$ such that

$$\mathbf{0} \leq \mathbf{p}(t) \leq \mathbf{M}e^{-\varepsilon'\tau(t)} \leq \mathbf{M}e^{-\varepsilon' t \frac{1}{C_{\max}}}, \quad t > 0.$$

By choosing $\varepsilon = \frac{\varepsilon'}{C_{\max}}$, we infer that $\mathbf{p}(0) \geq \mathbf{p}(T)$ and

$$0 \leq \mathbf{p}(t) \leq \mathbf{M}e^{-\varepsilon t}, \quad t > 0.$$

A similar argument shows that $\hat{\mathbf{u}} = \mathbf{u}^\star - \mathbf{w}\phi$ is also a lower solution for the same system, where $\mathbf{w}$ is the solution of the equation $\mathbf{w}' = g(t)\mathbf{K}_{qc}\mathbf{w}$ with $\mathbf{w}(0) = \mathbf{m}$ and $0 \leq \mathbf{w}(t) \leq \mathbf{m}e^{-\varepsilon t}$. By Theorem 2, there exists a maximal solution $\overline{\mathbf{u}}$ and a minimal solution $\underline{\mathbf{u}}$ such that

$$\mathbf{u}^\star - \mathbf{w}\phi \leq \underline{\mathbf{u}} \leq \mathbf{u}^\star \leq \overline{\mathbf{u}} \leq \mathbf{u}^\star + \mathbf{p}\phi \quad \text{ a.e. in } \Omega_T.$$

Moreover, if the periodic initial condition in (3.4.12) is replaced with the initial condition $\mathbf{u}(0,x) = \mathbf{u}_0\ x \in \Omega$, then the pair $\underline{\mathbf{u}}$, $\overline{\mathbf{u}}$ are also upper and lower solutions of the corresponding initial-boundary problem if $\mathbf{u}^\star(0,x) - \mathbf{w}(0)\phi(x) \leq \mathbf{u}_0(x) \leq \mathbf{u}^\star(0,x) + \mathbf{p}(0)\phi(x)$. By the comparison lemma, the unique solution $\mathbf{u}$ of the problem (3.4.12) with $\mathbf{u}(0,x) = \mathbf{u}_0(x)\ x \in \Omega$, satisfies the relation (3.4.14), which proves the theorem. □

Remark 3.5. *The condition* $0 < c \leq u_1^\star$ *in needed in order to ensure that all the eigenvalues of the essentially nonnegative matrix* $\mathbf{K}_{qc}$ *have a strictly negative real part. If* $\lambda_0 > 0$ *(which means that we are not in the case*

of Neumann boundary conditions), we can choose p as the solution of the differential system :

$$\mathbf{p}' = g(t)(\mathbf{K}_0 - \frac{\lambda_0}{C_{max}}\mathbf{D})\mathbf{p},$$

with $\mathbf{p}(0) = \mathbf{M}$*, so as to satisfy (3.4.17), which is equivalent to*

$$p_i' \geq g(t)\ \sum_{j=1}^{3} \big(K_{ij}^0 - \lambda_0 \frac{1}{g(t)}\delta_{ij} D_i\big) p_j - \delta_{i1}\ g(t)\, q(2\, u_1^\star + p_1\phi)\, p_1,\ \ t > 0.$$

Since matrix $\mathbf{K}_0 - \frac{\lambda_0}{C_{max}}\mathbf{D}$ *has like* $\mathbf{K}_{qc}$ *all its eigenvalues with a strictly negative real part, we can again conclude, without any condition on* $u_1^\star$*.*

We remarked that $\hat{\mathbf{u}} = \mathbf{0}$ is a lower weak solution of the periodic problem (3.4.12). Initializing the iterative procedure with this lower solution, Theorem 2 guarantees the existence of a minimal weak periodic solution of (3.4.12), which we denote $\underline{\mathbf{u}}$.

Lemma 3.7. *Suppose that* $0 < C' \leq f(t,x)$*,* $(t,x) \in \Omega_T$*. Then there exists a constant vector* $\mathbf{m} > \mathbf{0}$ *such that* $\mathbf{m}\phi \leq \underline{\mathbf{u}}$ *a.e. in* Ω_T*.*

Proof. We prove that there exists a vector field $\mathbf{0} \leq \mathbf{p} := \mathbf{p}(t)$ such that $\mathbf{p}\phi$ is a lower solution of (3.4.1). For this purpose the vector field $\mathbf{p}\,\phi$ should satisfy

$$p_i' + \lambda_0 D_i\, p_i \leq g(t)\ \sum_{j=1}^{3} K_{ij}^0 p_j - \delta_{i1}\ g(t)\, q\ p_1^2\, \phi + f(t,x), \quad (t,x) \in \Omega_T$$

$p_i(0) \leq p_i(T)$ and the boundary condition on Σ_T, which are automatically satified. As $\phi \in \mathcal{C}^\infty(\Omega)$ is bounded in Ω, we denote $\phi_{\max}$ its upper bound. Let $\mathbf{p} = (p_i)$ the solution of the following initial value problem for a system of ordinary differential equations :

$$\begin{cases} p_i' = g(t) \sum_{j=1}^{3} \big(K_{ij}^0 - \lambda_0 \frac{1}{C_{\min}}\delta_{ij} D_i\big) p_j \\ \qquad\qquad\qquad\qquad -\delta_{i1}\ g(t)\, q\, \phi_{\max}\, p_1^2 + C', \\ p_i(0) = 0 \end{cases} \tag{3.4.18}$$

with $p_i(0) = 0$. We already proved in ([61]) that this problem has a unique positive global solution, for all $t \geq 0$, which converges to a periodic unique solution $\mathbf{p}_{\text{per}}$ of (3.4.18), where the initial condition is replaced with a periodic condition at 0 and T. Thus $\mathbf{p}(t)\phi(x)$ $(t,x) \in \Omega_T$, is a lower solution of (3.4.1) and since

$$\mathbf{0} = \mathbf{p}(0)\phi(x) \leq \underline{\mathbf{u}}(0,x) \quad \text{ in } \Omega,$$

we deduce by the comparison lemma that $\mathbf{p}\phi \leq \underline{\mathbf{u}}$ in $\mathbb{R}^+ \times \Omega$. Since $\mathbf{p}_{\text{per}}\,\phi$ and $\underline{\mathbf{u}}$ are both periodic in time and since $\mathbf{p}$ converges to $\mathbf{p}_{\text{per}}$ when $t \to \infty$, it follows that $\mathbf{p}_{\text{per}}\,\phi \leq \underline{\mathbf{u}}$ in Ω_T.
It is sufficient now to prove that there exists $\mathbf{m} > \mathbf{0}$ such that $\mathbf{m} \leq \mathbf{p}_{\text{per}}$ in $[0,T]$. Now, if we denote $D_i' = \frac{\lambda_0}{C_{\min}} D_i$, a straightforward calculation gives that

$$\mathbf{m}^\delta := (\delta, \frac{k_1}{k_2+k_4+D_2'}\delta,\ \frac{k_4}{k_3+D_3'}\,\frac{k_1}{k_2+k_4+D_2'}\delta)$$

is a constant lower solution for (3.4.18) for any δ, with $0 < \delta \leq \delta_0$, where δ_0 is the unique positive square root of a particular quadratic polynomial. By the comparison lemma for such a differential system ([28], proposition 1.1) we deduce that $\mathbf{m}^\delta$ is the lower bound of the unique solution $\mathbf{p}^\delta$ of (3.4.18), with the initial condition $\mathbf{p}^\delta(0) = \mathbf{m}^\delta$. As the limit of $\mathbf{p}^\delta(t)$ as $t \to \infty$ is also $\mathbf{p}_{\text{per}}$, we deduce that $\mathbf{m}^\delta \leq \mathbf{p}_{\text{per}}$ in Ω_T, which complets the proof. □

Theorem 3.4. *The periodic problem (3.4.12) has a unique periodic weak solution* $\underline{\mathbf{u}}$ *in* $\mathbf{W}$*, with periodic initial condition in* $L^\infty(\Omega)$*. For any other solution* $\mathbf{u}$ *of the corresponding initial-boundary problem for which there exist two constant vectors,* $\mathbf{M} \geq \mathbf{0}$*,* $\mathbf{m} \geq \mathbf{0}$*, such that* u_0 *satisfies*

$$\mathbf{0} \leq -\mathbf{m}\,\phi(x) + \underline{\mathbf{u}}(0,x) \leq \mathbf{u}_0 \leq \mathbf{M}\,\phi(x) + \underline{\mathbf{u}}(0,x), \quad \textit{for almost every } x \in \Omega,$$

there exists $\varepsilon > 0$ *such that*

$$|\underline{\mathbf{u}}(t,x) - \mathbf{u}(t,x)| \leq \mathbf{M}e^{-\varepsilon t}\phi(x), \ \textit{for all } t > 0 \ \textit{ and almost every } x \in \Omega.$$

Proof. If $\mathbf{u}^\star$ is a periodic weak solution of (3.4.12), we conclude thanks to Theorem 2 that $\underline{\mathbf{u}} \leq \mathbf{u}^\star$ a.e. in Ω_T. Since $\mathbf{u}^\star(0,x) \in L^\infty(\Omega)$ and $\phi \in \mathcal{C}^\infty(\Omega)$, there exists a constant vector $\mathbf{M} > \mathbf{0}$ such that $\mathbf{u}^\star(0,x) \leq \mathbf{M}\phi(x) + \underline{\mathbf{u}}(0,x)$ for almost all $x \in \Omega$. The periodic functions $\mathbf{u}^\star$, $\underline{\mathbf{u}}$ belong to $\mathcal{C}(0,T,L^2(\Omega))$ and the convergence

$$||\mathbf{u}^\star(0,\cdot) - \underline{\mathbf{u}}(0,\cdot)||_{L^2(\Omega)} = ||\mathbf{u}^\star(nT,\cdot) - \underline{\mathbf{u}}(nT,\cdot)||_{L^2(\Omega)} \to 0 \quad \text{when } n \to \infty$$

means that the two periodic solutions have the same initial condition at $t = 0$. Hence they coincide.
The last assertion of the theorem is a straightforward consequence of Theorem 3. □

Remark 3.6. *If the function* f *is Hölder continuous in* $[0,\infty) \times \overline{\Omega}$ *then the problem (3.4.12) has periodic classical solutions and from Theorem 4*

it follows that the periodic solution is unique in this case. Besides, it is an attractor for any other solution of the initial-boundary problem if there exists one constant vector $\mathbf{m} \geq \mathbf{0}$ *such that* $\mathbf{0} \leq -\mathbf{m}\,\phi(x) + \underline{\mathbf{u}}(0,x) \leq \mathbf{u}_0$.

Chapitre 4

Homogenization of a spatially distributed model.

Abstract

We deal here with the previous model of soil carbonic dynamics which is a spatial version of Modelling Organic changes by Micro-Organisms of Soil model, recently introduced by M. Pansu and his group. From a mathematical point of view this new model is a reaction-diffusion-advection system with a quadratic reaction term. In this section the model entries are heterogeneous and periodic in space, with a small period ϵ. This space periodicity aims at modelling the scale patterns of agricultural fields. The goal of this chapter is to give an equivalent homogeneous model when ε goes to zero.

4.1 Introduction

The compartmental MOMOS model (Modelling Organic changes by Micro-Organisms of Soil, [23], [24]) was selected because it focuses on the role of soil microbial biomass. It is written like a nonlinear ordinary differential system and has been proved to be mathematically valid providing a unique solution ([61]). Moreover, if the carbon inputs are periodic, there is a unique periodic solution which is also a global attractor for any other solution of this periodic model.

In [69] we improved the initial model, which was not spatially distributed, by adding diffusion and advection terms while keeping the reaction term unchanged. We proved that this new model, a reaction-diffusion-advection system, had a unique weak solution. We was looking for weak solutions because initial inputs are objectively not regular enough to allow more "re-

gular" solutions. When we assumed periodicity of model entries, we proved that there exists a maximal and a minimal periodic solution of this system. In a very particular case the minimal and the maximal periodic solution coincide and become a global attractor for any other solution of the periodic system.

In this paper, we deal with a soil which is "heterogeneous" and periodic to a small space scale called "microscopic". An example for such a soil is a cultivated area of cereals, where the "microscopic" pattern is the assembly of a cereal roots and a square piece of ground around it. In this case being "heteregeneous" means having different inputs in the ground part and in the cereal roots part. By using homogenization theory we finally obtain a "macroscopic" behaviour of a "homogeneous" system with inputs which are a subtle mixture of the heterogeneous inputs (see equations (4.3.3) and (4.3.4) bellow). For example the homogenized advection term depends not only on the initial advection term but also on the diffusive term. We say that the homogenization of the advection is "relative to the diffusion".

This "macroscopic" system behaviour will be equivalent, when the "microscopic" pattern is "small enough", with the initial system behaviour.

4.2 Mathematical preliminaries and notations.

Let Ω be the domain occupied by the cultivated area of cereals, a bounded open subset of $\mathbb{R}^2$ with smooth boundary $\partial\Omega$. Let ν denote the outward unit normal vector along $\partial\Omega$. Let $T > 0$ and $\Omega_T := (0,T) \times \Omega$, and let :

$$H^1(\Omega) := \{u \in L^2(\Omega), \nabla u \in L^2(\Omega; \mathbb{R}^N))\},$$

$$H_0^1(\Omega) := \{u \in H^1(\Omega),\ u = 0 \text{ on } \partial\Omega \text{ a.e.}\}.$$

If X is a Banach space,

$$L^p(0,T,X) := \{u : (0,T) \to X \text{ mesurable}, \|u(t,.)\|_X \in L^p(0,T)\},$$

and $C([0,T],X)$ denotes the space of continuous functions $u : [0,T] \to X$.

Let the reference cell Y be defined $Y = [0,l_1] \times [0,l_2] \subset \mathbb{R}^2$ and let $Y_1, Y_2 \subset Y$ such that

$$\overline{Y} = \overline{Y}_1 \cup \overline{Y}_2 \qquad Y_1 \cap Y_2 = \varnothing$$

Let $\varepsilon > 0$ be a parameter which takes its values in a sequence which tends to zero and set

$$\Omega_\rho^\varepsilon = \{x/\ \chi_\rho(\frac{x}{\varepsilon}) = 1\}$$

where χ_ρ for $\rho = 1, 2$ is the characteristic function of the set Y_ρ extended by periodicity with period Y. By this construction, the set Ω is covered by a pavement of cells of the form $\varepsilon Y = \varepsilon Y_1 \cup \varepsilon Y_2$. When taking $\varepsilon \to 0$ the cells εY covering Ω are smaller and smaller and their number goes to ∞. A coefficient h of this problem is such that :

$$h^\varepsilon(x) := h_1 \chi_1(\frac{x}{\varepsilon}) + h_2 \chi_2(\frac{x}{\varepsilon}),$$

where $h_1,\ h_2$ are the two different constant values of coefficient h in Y_1 and Y_2.

Definition 4.1. *The function f is called $Y-$ periodic if and only if*

$$f(x + k l_\alpha e_\alpha) = f(x) \quad \text{a.e. in } \mathbb{R}^2 \quad \forall k \in \mathbb{Z} \quad \alpha = 1, 2,$$

where $\{e_1, e_2\}$ is the canonical base in $\mathbb{R}^2$.

Definition 4.2. *Let ω be a bounded open set in $\mathbb{R}^2$ and f a function in $L^1(\omega)$. The mean value of f over ω is the real number $\mathcal{M}_\omega(f)$ given by :*

$$\mathcal{M}_\omega(f) = \frac{1}{|\omega|} \int_\omega f(x) dx$$

Next we recall an useful result (for a proof see for example [32] Th 2.6.) :

Lemma 4.1. *Let $1 \leq p \leq \infty$ and f be a $Y-$periodic function in $L^p(Y)$. Set $f^\varepsilon(x) = f(\frac{x}{\varepsilon})$ a.e. in $\mathbb{R}^2$. Then, if $p < \infty$ as $\varepsilon \to 0$*

$$f^\varepsilon \rightharpoonup \mathcal{M}_Y(f) \quad \text{weakly in } L^p(\omega)$$

for any bounded open subset $\omega \subset \mathbb{R}^2$.
If $p = \infty$, one has

$$f^\varepsilon \rightharpoonup \mathcal{M}_Y(f) \quad \text{weakly } \star \text{ in } L^\infty(\mathbb{R}^2).$$

It is understood once and for all that, save when otherwise specified, Latin and Greek indices range respectively in $\{1, 2, 3\}$ and $\{1, 2\}$ and the summation convention with respect to repeated indices is used only for Greek Indices. The Euclidean norm and the inner product in $\mathbb{R}^2$ are denoted by the symbol $|\ |$ and $\cdot$ respectively.

Let us introduce the following reaction-diffusion-advection initial problem :

$$\begin{cases} \frac{\partial u_{i,\varepsilon}}{\partial t} - \operatorname{div}(\mathbf{A}_i^\varepsilon(x)\nabla u_{i,\varepsilon}) + \mathbf{B}_i^\varepsilon(x)\nabla u_{i,\varepsilon} = g_i^\varepsilon(t,x,\mathbf{u}_\varepsilon), (t,x) \in \Omega_T \\ \gamma\,(\mathbf{A}_i^\varepsilon(x)\nabla u_{i,\varepsilon})\cdot\nu + \beta_i(t,x)u_{i,\varepsilon} = 0, (t,x) \in \Sigma_T := (0,T)\times\partial\Omega \\ u_{i,\varepsilon}(0,x) = u_i^0(x) \quad \text{ in } \Omega \end{cases} \tag{4.2.1}$$

where $\mathbf{A}_i$ is a Y-periodic diffusion matrix field and $\mathbf{B}_i$ a Y-periodic transport vector field, for each i. We set $\mathbf{A}_i^\varepsilon(x) = \mathbf{A}_i(\frac{x}{\varepsilon})$ and $\mathbf{B}_i^\varepsilon(x) = \mathbf{B}_i(\frac{x}{\varepsilon})$, a.e. on $\mathbb{R}^2$. The boundary conditions are of either Dirichlet type ($\gamma = 0,\ \beta_i \equiv 1$) or of Neumann-Robin type ($\gamma = 1,\ \beta_i(t,x) \geq 0$). The right hand side term of (4.2.1) is $\mathbf{g}^\varepsilon(t,x,\mathbf{u}_\varepsilon) = (g_i^\varepsilon(t,x,\mathbf{u}_\varepsilon))_{i=1,2,3}$

$$\mathbf{g}^\varepsilon := \begin{pmatrix} -k_1^\varepsilon(t,x)u_{1,\varepsilon} - q^\varepsilon(t,x)|u_{1,\varepsilon}|u_{1,\varepsilon} + k_2^\varepsilon(t,x)u_{2,\varepsilon} + k_3^\varepsilon(t,x)u_{3,\varepsilon} + f(t,x) \\ k_1^\varepsilon(t,x)u_{1,\varepsilon} - (k_2^\varepsilon(t,x) + k_4^\varepsilon(t,x))u_{2,\varepsilon} \\ k_4^\varepsilon(t,x)u_{2,\varepsilon} - k_3^\varepsilon(t,x)u_{3,\varepsilon} \end{pmatrix},$$

where k_j, for all $j = 1,2,3,4$ and q are Y-periodic functions. We set $k_j^\varepsilon(x) = k_j(\frac{x}{\varepsilon})$ and $q^\varepsilon(x) = q(\frac{x}{\varepsilon})$, a.e. on $\mathbb{R}^2$.

We assume that for all i the diffusion matrix fields $\mathbf{A}_i$ are bounded, symmetric and coercive :

$$\begin{cases} \mathbf{A}_i := \big((A_i)_{\alpha\beta}\big)_{\alpha,\beta=1,2} \in L^\infty(Y)^{2\times 2}, \\ \mathbf{A}_i\,\zeta\cdot\zeta \geq a|\zeta|^2, \quad \forall\zeta\in\mathbb{R}^2, \text{ a.e in } Y, \text{ with } a>0, \\ |\mathbf{A}_i\,\zeta| \leq b\,|\zeta|, \quad \forall\zeta\in\mathbb{R}^2, \text{ a.e in } Y, \text{ with } b>0 \end{cases} \tag{4.2.2}$$

and the transport vector fields $\mathbf{B}_i$ are bounded :

$$\mathbf{B}_i := \big((B_i)_\alpha\big)_{\alpha=1,2} \in L^\infty(Y)^2, \quad |(B_i)_\alpha| \leq c \quad \text{a.e in } Y, \ \text{ for all } \alpha. \tag{4.2.3}$$

The functions k_j and q are assumed to be nonnegative-valued and bounded for all $j = 1,2,3,4$:

$$k_j,\ q \in L^\infty(Y_T),\ 0 \leq k_j, q \leq C_{\max} \text{ a.e on } \ Y_T, \ \text{ where } Y_T := (0,T)\times Y, \tag{4.2.4}$$

for some constant $C_{\max} > 0$. The functions β_i are assumed to be nonnegative-valued and bounded for all i :

$$\beta_i \in L^\infty(\Sigma_T), \quad 0 \leq \beta_i \leq C_{\max} \text{ a.e } \ on\ \Sigma_T, \ \text{ where } \Sigma_T := (0,T)\times\partial\Omega. \tag{4.2.5}$$

Finally we assume that the initial data and input are nonnegative and bounded :

$$u_i^0 \in L^2_+(\Omega), \quad f \in L^2_+(\Omega_T), \quad f(t,x) \leq C_{\max} \text{ a.e } \ on\ \Omega_T. \tag{4.2.6}$$

4.3 The homogenization result.

Hereafter the space X will be equal to $H^1(\Omega)$ if the boundary conditions are of Neumann-Robin type ($\gamma = 1$) and to $H_0^1(\Omega)$ if the boundary conditions are of Dirichlet type ($\gamma = 0$). We define the vector valued space :

$$\mathbf{W} := \{\mathbf{u} = (u_1, u_2, u_3)/\ \mathbf{u} \in (L^2(0,T,X)^3,\ \partial_t \mathbf{u} \in (L^2(0,T,X'))^3\}.$$

Definition 4.3. *A weak solution of (4.2.1) is a vector field* $\mathbf{u}_\varepsilon$ *in* $\mathbf{W}$ *that satisfies :*

$$\begin{aligned}
&\int_0^T < \partial_t u_{i,\varepsilon}, \varphi_i >_{X,X'} dt + \int_0^T \int_\Omega (\mathbf{A}_i^\varepsilon(x)\nabla u_{i,\varepsilon}\nabla\varphi_i + \mathbf{B}_i^\varepsilon(x)\nabla u_{i,\varepsilon}\,\varphi_i)dxdt \\
&+ \gamma \int_0^T \int_{\partial\Omega} \beta_i(t,x) u_{i,\varepsilon}\,\varphi_i d\sigma dt = \int_0^T \int_\Omega g_i^\varepsilon(t,x,\mathbf{u}_\varepsilon)\varphi_i dxdt, \\
&u_{i,\varepsilon}(0) = u_{i,0} \quad \text{in } \Omega
\end{aligned}$$

for all $\varphi_i \in L^2(0,T,X)$.

The existence and uniqueness of $\mathbf{u}_\varepsilon$, which is nonnegative, is given in theorem 1 of [69].

Theorem 4.1. *Assume that (4.2.2)-(4.2.6) hold. Then* $\mathbf{u}_\varepsilon$ *satisfies :*

$$\begin{cases}
(i)\ \mathbf{u}_\varepsilon \rightharpoonup \mathbf{u} \text{ weakly in } \mathbf{W}, \\
(ii)\ \mathbf{A}_i^\varepsilon \nabla u_{i,\varepsilon} \rightharpoonup \mathbf{A}_i^0 \nabla u_i \text{ weakly in } (L^2(\Omega_T))^2, \\
(iii)\ \mathbf{B}_i^\varepsilon \nabla u_{i,\varepsilon} \rightharpoonup \mathbf{B}_i^0 \nabla u_i \text{ weakly in } L^2(\Omega_T),
\end{cases} \tag{4.3.1}$$

where $\mathbf{u}$ *is the solution of the following limit problem :*

$$\begin{cases}
\frac{\partial u_i}{\partial t} - div(\mathbf{A}_i^0 \nabla u_i) + \mathbf{B}_i^0 \nabla u_i = g_i^0(t,x,\mathbf{u}), \quad (t,x) \in \Omega_T \\
\gamma\,(\mathbf{A}_i^0 \nabla u_i)\cdot\nu + \beta_i(t,x)u_i = 0, \quad (t,x) \in \Sigma_T \\
u_i(0,x) = u_i^0(x) \quad \text{in } \Omega,
\end{cases} \tag{4.3.2}$$

where $\mathbf{c}_i^0 := \big((A_i^0)_{\alpha\rho}\big)_{\alpha,\rho=1,2}$ *is the matrix given by :*

$$(A_i^0)_{\alpha\rho} := \mathcal{M}_Y\big((A_i)_{\alpha\rho}\big) - \mathcal{M}_Y\Big((A_i)_{\tau\rho}(\frac{\partial \chi_\alpha^i}{\partial y_\tau})\Big), \tag{4.3.3}$$

$\mathbf{B}_i^0 = \big((B_i^0)_\alpha\big)_{\alpha=1,2}$ *is the vector given by :*

$$(B_i^0)_\alpha = \mathcal{M}_Y\big((B_i)_\alpha\big) - \mathcal{M}_Y\big((\mathbf{B}_i \cdot \nabla\chi_\alpha^i)\big) \tag{4.3.4}$$

and the vector field $\boldsymbol{\chi}^i = (\chi^i_\alpha)_{\alpha=1,2}$ *is such that* χ^i_α *is the unique solution of the following problem ([32] theorem 4.27) :*

$$\begin{cases} -div\,({}^t\mathbf{A}_i(y)\nabla\chi^i_\alpha) = -div\,({}^t\mathbf{A}_i(y)\,e_\alpha), \quad y \in Y, \\ \chi^i_\alpha \quad Y - periodic\ , \\ \mathcal{M}_Y(\chi^i_\alpha) = 0, \end{cases} \tag{4.3.5}$$

where $\{e_1, e_2\}$ *is the canonical basis for the euclidean space* $\mathbb{R}^2$*. The vector field* $\mathbf{g}^0(t,x,\mathbf{u}) = \left(g^0_i(t,x,\mathbf{u})\right)_{i=1,2,3}$ *is given by*

$$\mathbf{g}^0 := \begin{pmatrix} -k^0_1(t)u_1 - q^0(t)|u_1|u_1 + k^0_2(t)u_2 + k^0_3(t)u_3 + f(t,x) \\ k_1 0(t)u_1 - (k^0_2(t) + k^0_4(t))u_2 \\ k^0_4(t)u_2 - k^0_3(t)u_3 \end{pmatrix},$$

where coefficient functions k^0_j *and* q^0 *denote the mean values over* Y *of functions* k_j *and* q*, for all* $j = 1,2,3,4$*.*

Proof. Observe first that thanks to hypothesis (4.2.2)-(4.2.6) and using the same estimates as in lemma 3 [69] we have :

$$||u_{i,\varepsilon}||_W + ||u_{i,\varepsilon}||_{L^\infty(0,T,L^2(\Omega))} \leq C \tag{4.3.6}$$

where $C > 0$ is independent of ε. Moreover if we introduce the vector field $\boldsymbol{\xi}^\varepsilon_i$ and the function θ^ε_i defined by :

$$\boldsymbol{\xi}^\varepsilon_i(t,x) := \mathbf{A}^\varepsilon_i(x)\nabla u_{i,\varepsilon}(t,x) \quad \text{ and } \quad \theta^\varepsilon_i(t,x) := \mathbf{B}^\varepsilon_i(x)\cdot\nabla u_{i,\varepsilon}(t,x)$$

from (4.3.6) and assumptions on $\mathbf{A}^\varepsilon_i$ and $\mathbf{B}^\varepsilon_i$ one has

$$||\boldsymbol{\xi}^\varepsilon_i||_{(L^2(\Omega_T))^2} \leq C_1, \qquad ||\theta^\varepsilon_i||_{L^2(\Omega_T)} \leq C_1,$$

with constant C_1 independent of ε. Consequently there exists a subsequence, still denoted by ε such that for all i

$$\begin{cases} (i)\ \mathbf{u}_\varepsilon \rightharpoonup \mathbf{u} \text{ weakly } \star \text{ in } (L^\infty(0,T,L^2(\Omega)))^3, \\ (ii)\ \mathbf{u}_\varepsilon \rightharpoonup \mathbf{u} \text{ weakly in } (L^2(0,T,X))^3, \\ (iii)\ \mathbf{u}_\varepsilon \to \mathbf{u} \text{ strongly in } (L^q(\Omega_T))^3 \text{ for all } q \in [2,4) \\ (iv)\ \mathbf{u'}_\varepsilon \rightharpoonup \mathbf{u'} \text{ weakly in } (L^2(0,T,X'))^3, \\ (v)\ \boldsymbol{\xi}^\varepsilon_i \rightharpoonup \boldsymbol{\xi}_i \text{ weakly in } (L^2(\Omega_T))^2, \\ (vi)\ \theta^\varepsilon_i \rightharpoonup \theta_i \text{ weakly in } L^2(\Omega_T), \end{cases} \tag{4.3.7}$$

where we have used the compact injection $W \hookrightarrow L^2(\Omega_T)$ and the interpolation tecqniques for proving the strong convergence of $\mathbf{u}_\varepsilon$ toward $\mathbf{u}$ in all spaces $(L^q(\Omega_T))^3$ with $2 \leq q < 4$.
Then $\boldsymbol{\xi}_i^\varepsilon$ and θ_i^ε satisfy

$$\begin{aligned}
&\int_0^T \int_\Omega \boldsymbol{\xi}_i^\varepsilon \cdot \nabla v(x)\varphi(t)dxdt + \int_0^T \int_\Omega \theta_i^\varepsilon v(x)\varphi(t)dxdt \\
&= \gamma \int_0^T \int_{\partial\Omega} \beta_i u_{i,\varepsilon} v(x)\varphi(t)d\sigma dt + \int_0^T \int_\Omega g_i^\varepsilon(x,t,\mathbf{u}_\varepsilon)v(x)\varphi(t)dxdt \\
&\quad - \int_0^T < \partial_t u_{i,\varepsilon}, v >_{X,X'} \varphi(t)dt, \quad \forall v \in H^1(\Omega) \text{ and } \forall \varphi \in \mathcal{D}(0,T).
\end{aligned} \tag{4.3.8}$$

We pass to the limit in ε. Thanks to Lemma 1 we obtain that $\boldsymbol{\xi}_i$ and θ_i satify

$$\begin{aligned}
&< \partial_t u_i, v >_{X,X'} + \int_\Omega \boldsymbol{\xi}_i \cdot \nabla v \, dx + \int_\Omega \theta_i v \, dx - \gamma \int_{\partial\Omega} \beta_i u_i v(x) \, d\sigma \\
&\quad = \int_0^T \int_\Omega g_i^0(x,t,\mathbf{u}) v \, dx \quad \text{in } \mathcal{D}'(0,T), \qquad \forall v \in H^1(\Omega).
\end{aligned} \tag{4.3.9}$$

In this point we only have to prove that

$$\begin{cases}
(i) \;\; \boldsymbol{\xi}_i = \mathbf{A}_i^0 \nabla u_i, \\
(ii) \; \theta_i = \mathbf{B}_i^0 \cdot \nabla u_i, \\
(iii) \; \gamma(\mathbf{A}_i^0 \nabla u_i)\nu + \beta_i u_i = 0 \quad \text{on } \Sigma_T \;\; \text{and} \\
\qquad u_i(0,\cdot) = u_i^0(\cdot) \quad \text{in } \Omega
\end{cases}$$

(i) *Diffusive term* : For this point we will make use of oscillanting test functions defined by Tartar's method ([31], [32]) :

$$w_\alpha^{i,\varepsilon} = \varepsilon w_\alpha^i(\frac{x}{\varepsilon}) = x_\alpha - \varepsilon \chi_\alpha^i(\frac{x}{\varepsilon}).$$

Thus w_α^i is the unique solution of

$$\begin{cases}
-\text{div}\,({}^t\mathbf{A}_i(y)\nabla w_\alpha^i) = 0 \quad y \in Y, \\
w_\alpha^i - y_\alpha \quad Y - \text{periodic}\,, \\
\mathcal{M}_Y(w_\alpha^i - y_\alpha) = 0,
\end{cases} \tag{4.3.10}$$

Let us recall the following convergences (see for example (8.11) [32])

$$\begin{cases}
(i) \;\; w_\alpha^{i,\varepsilon} \rightharpoonup x_\alpha \quad \text{weakly in } H^1(\Omega), \\
(ii) \; w_\alpha^{i,\varepsilon} \to x_\alpha \quad \text{strongly in } L^p(\Omega) \quad \text{for all } p \in [2,\infty),
\end{cases}$$

We introduce also the vector function

$$\boldsymbol{\eta}^{\varepsilon}_{i,\alpha} := ({}^t\mathbf{A}^{\varepsilon}_i)\nabla w^{i,\varepsilon}_{\alpha},$$

which satisfies (see [32] (8.13), (8.14))

$$\boldsymbol{\eta}^{\varepsilon}_{i,\alpha} \rightharpoonup \mathcal{M}_Y\big(({}^t\mathbf{A}^0_i)\nabla w^i_{\alpha}\big) = ({}^t\mathbf{A}^0_i)\mathbf{e}_{\alpha} \ \text{ weakly in } (L^2(\Omega))^2, \tag{4.3.11}$$

with $\mathbf{A}^0_i$ the matrix given in (4.3.3) (see [32] (6.36)) and

$$\int_{\Omega} \boldsymbol{\eta}^{\varepsilon}_{i,\alpha} \cdot \nabla v = 0 \quad \forall v \in H^1_0(\Omega).$$

Let $\psi \in \mathcal{D}(\Omega),\ \varphi \in \mathcal{D}(0,T)$, choose in the previous equation $v = u_{i,\varepsilon}\psi\varphi$ and integrate over $[0,T]$. Then

$$\int_0^T \int_{\Omega} \boldsymbol{\eta}^{\varepsilon}_{i,\alpha} \cdot \nabla u_{i,\varepsilon}\, \psi\, \varphi\, dxdt + \int_0^T \int_{\Omega} \boldsymbol{\eta}^{\varepsilon}_{i,\alpha} \cdot \nabla \psi\, u_{i,\varepsilon}\, \varphi\, dxdt = 0. \tag{4.3.12}$$

Choosing now $v = \psi\, w^{\varepsilon}_{i,\alpha}$ in (4.3.8) ($v_i \in H^1_0(\Omega)$) and subtracting from (4.3.12) we obtain :

$$\begin{aligned} &\int_0^T \int_{\Omega} \boldsymbol{\xi}^{\varepsilon}_i \cdot \nabla \psi\, w^{\varepsilon}_{i,\alpha}\, \varphi\, dxdt - \int_0^T \int_{\Omega} \boldsymbol{\eta}^{\varepsilon}_{i,\alpha} \cdot \nabla \psi\, u_{i,\varepsilon}\, \varphi\, dxdt, \\ &= \int_0^T \int_{\Omega} g^{\varepsilon}_i(x,t,\mathbf{u}_{\varepsilon})\, \psi\, w^{\varepsilon}_{i,\alpha}\varphi\, dxdt - \int_0^T \int_{\Omega} \theta^{\varepsilon}_i \psi\, w^{\varepsilon}_{i,\alpha}\varphi\, dxdt \\ &\qquad - \int_0^T < \partial_t u_{i,\varepsilon}, \psi\, w^{\varepsilon}_{i,\alpha} >_{X,X'} \varphi\, dt. \end{aligned} \tag{4.3.13}$$

We pass to the limit in ε and we obtain :

$$\begin{aligned} &\int_0^T \int_{\Omega} \boldsymbol{\xi}_i \cdot \nabla \psi\, x_{\alpha}\, \varphi\, dxdt - \int_0^T \int_{\Omega} ({}^t\mathbf{A}^0_i\, \mathbf{e}_{\alpha}) \cdot \nabla \psi\, u_i\, \varphi\, dxdt, \\ &= \int_0^T \int_{\Omega} g^0_i(x,t,\mathbf{u})\, \psi\, x_{\alpha}\varphi\, dxdt - \int_0^T \int_{\Omega} \theta_i \psi\, x_{\alpha}\, \varphi\, dxdt \\ &\qquad - \int_0^T < \partial_t u_i, \psi\, x_{\alpha} >_{X,X'} \varphi\, dt. \end{aligned} \tag{4.3.14}$$

Choosing $v = \psi\, x_{\alpha} \in \mathcal{D}(\Omega)$ in (4.3.9) and subtracting it from (4.3.14) gives

$$\begin{aligned} -\int_0^T \int_{\Omega} \boldsymbol{\xi}_i \cdot \nabla x_{\alpha}\, \psi\, \varphi\, dxdt - \int_0^T \int_{\Omega} ({}^t\mathbf{A}^0_i\, \mathbf{e}_{\alpha}) \cdot \nabla \psi\, u_i\, \varphi\, dxdt = 0, \\ \forall \psi \in \mathcal{D}(\Omega),\ \forall \varphi \in \mathcal{D}(0,T). \end{aligned}$$

Since $({}^t\mathbf{A}_i^0\,\mathbf{e}_\alpha)$ is constant in x we get

$$\int_0^T\int_\Omega \boldsymbol{\xi}_i\cdot\mathbf{e}_\alpha\,\psi\,\varphi\,dxdt=\int_0^T\int_\Omega({}^t\mathbf{A}_i^0\,\mathbf{e}_\alpha)\cdot\nabla u_i\,\psi\,\varphi\,dxdt,\\ \forall\psi\in\mathcal{D}(\Omega),\ \forall\varphi\in\mathcal{D}(0,T).$$

Hence

$$\boldsymbol{\xi}_i\cdot\mathbf{e}_\alpha=({}^t\mathbf{A}_i^0\,\mathbf{e}_\alpha)\cdot\nabla u_i=(\mathbf{A}_i^0\,\nabla u_i)\cdot\mathbf{e}_\alpha,$$

which gives

$$\boldsymbol{\xi}_i=\mathbf{A}_i^0\,\nabla u_i$$

(*ii*) *Advection term* : We use here the same ideea as in the study of lower terms for elliptic operators ([30], chapter 13). We set $\theta_i^\varepsilon=(B_i^\varepsilon)_\alpha\,\frac{\partial u_{i,\varepsilon}}{\partial x_\alpha}=\mathbf{B}_i^\varepsilon\cdot\nabla u_{i,\varepsilon}$ and we already noticed that we can extract a subsequence such that

$$\theta_i^\varepsilon\rightharpoonup\theta_i\quad\text{ in } L^2(\Omega_T)\ \text{ weakly }.$$

Then

$$-\mathrm{div}(\mathbf{A}_i^\varepsilon\,\nabla u_{i,\varepsilon})=g_i^\varepsilon-\theta_i^\varepsilon-\partial_t\,u_{i,\varepsilon}\rightharpoonup g_i^0-\theta_i-\partial_t\,u_i\quad\text{ in } L^2(0,T,X')\ \text{ weakly },$$

so that

$$\partial_t\,u_i-\mathrm{div}(\mathbf{A}_i^0\,\nabla u_i)+\theta_i=g_i^0(t,x,\mathbf{u}).$$

We define $\beta_i(y)$ as the unique solution of

$$\begin{cases}-\mathrm{div}\,({}^t\mathbf{A}_i(y)\nabla\beta_i)=-\mathrm{div}\,\mathbf{B}_i\quad\text{ in } Y,\\ \beta_i\qquad Y-\text{periodic }\,,\\ \mathcal{M}_Y(\beta_i)=0,\end{cases}$$

i.e.

$$\begin{cases}\beta_i\in W_{\mathrm{per}}(Y)\quad\text{ such that}\\ \int_\Omega{}^t\mathbf{A}_i\,\nabla\beta_i\cdot\nabla\psi\,dx=\int_\Omega\mathbf{B}_i\cdot\nabla\psi\,dx\qquad\forall\psi\in W_{\mathrm{per}}(Y),\end{cases}\tag{4.3.15}$$

where $W_{\mathrm{per}}(Y):=\{v\in H^1_{\mathrm{per}}(Y),\ \mathcal{M}_Y(v)=0\}$. We denote by $C^\infty_{\mathrm{per}}(Y)$ the subset of $C^\infty(\mathbb{R}^2)$ of Y-periodic functions and of $H^1_{\mathrm{per}}(Y)$ the closure of $C^\infty_{\mathrm{per}}(Y)$ for the H^1 norm.
We define next

$$\gamma_i^\varepsilon:=1+\varepsilon\beta_i^\varepsilon,\quad\text{ where }\beta_i^\varepsilon(x)=\beta_i(\frac{x}{\varepsilon}).\tag{4.3.16}$$

Thus

$$\frac{\partial}{\partial x_\alpha}\beta_i^\varepsilon(x) = \frac{\partial}{\partial y_\alpha}\beta_i(y)\ \frac{1}{\varepsilon},$$

$$-\mathrm{div}_x\,({}^t\mathbf{A}_i^\varepsilon\,\nabla\gamma_i^\varepsilon) = -\mathrm{div}_x\,\mathbf{B}_i^\varepsilon \quad \text{in } \Omega. \tag{4.3.17}$$

Obviously, when ε goes to 0, γ_i^ε converges to 1 weakly in $H^1(\Omega)$ and strongly $L^2(\Omega)$. We choose now $v = \psi\,\gamma_i^\varepsilon$ in (4.3.8) and we multiply the equation (4.3.17) by $\varphi\,\psi\,u_{i,\varepsilon}$ with $\psi \in \mathcal{D}(\Omega)$ and $\varphi \in \mathcal{D}(0,T)$. After subtracting we obtain :

$$\begin{aligned}
&\int_0^T\int_\Omega \boldsymbol{\xi}_i^\varepsilon\cdot\nabla\psi\,\gamma_i^\varepsilon\,\varphi\,dxdt - \int_0^T\int_\Omega ({}^t\mathbf{A}_i^\varepsilon\,\nabla\gamma_i^\varepsilon)\cdot\nabla\psi\,u_{i,\varepsilon}\,\varphi\,dxdt,\\
&\qquad = \int_0^T\int_\Omega g_i^\varepsilon(x,t,\mathbf{u}_\varepsilon)\,\psi\,\gamma_i^\varepsilon\,\varphi\,dxdt - \int_0^T\int_\Omega \theta_i^\varepsilon\,\psi\,\gamma_i^\varepsilon\varphi\,dxdt\\
&+\int_0^T\int_\Omega (\mathrm{div}\,\mathbf{B}_i^\varepsilon)\,\psi\,u_{i,\varepsilon}\,\varphi\,dxdt - \int_0^T < \partial_t u_{i,\varepsilon}, \psi\,w_{i,\alpha}^\varepsilon >_{X,X'}\,\varphi\,dt.
\end{aligned}$$

Passing to the limit in ε gives

$$\begin{aligned}
&\int_0^T\int_\Omega \boldsymbol{\xi}_i\cdot\nabla\psi\,\varphi\,dxdt - \mathcal{M}_Y({}^t\mathbf{A}_i\,\nabla\beta_i)\cdot\int_0^T\int_\Omega \nabla\psi\,u_i\,\varphi\,dxdt\\
&\qquad\qquad + \int_0^T\int_\Omega \theta_i\,\psi\,\varphi\,dxdt\\
&= \int_0^T\int_\Omega g_i^0(x,t,\mathbf{u})\,\psi\,\varphi\,dxdt - \int_0^T < \partial_t u_i, \psi >_{X,X'}\,\varphi\,dt\\
&\qquad -\mathcal{M}_Y(\mathbf{B}_i)\cdot\int_0^T\int_\Omega \nabla\psi\,u_i\,\varphi\,dxdt - \int_0^T\int_\Omega \theta_i\,\psi\,\varphi\,dxdt\\
&= \int_0^T\int_\Omega \boldsymbol{\xi}_i\cdot\nabla\psi\,\varphi\,dxdt - \mathcal{M}_Y(\mathbf{B}_i)\cdot\int_0^T\int_\Omega \nabla\psi\,u_i\,\varphi\,dxdt
\end{aligned}$$

Thus

$$\begin{aligned}
\int_0^T\int_\Omega \theta_i\,\psi\,\varphi\,dxdt &= -\mathcal{M}_Y({}^t\mathbf{A}_i\,\nabla\beta_i)\cdot\int_0^T\int_\Omega \nabla u_i\,\psi\,\varphi\,dxdt\\
&\quad +\mathcal{M}_Y(\mathbf{B}_i)\cdot\int_0^T\int_\Omega \nabla u_i\,\psi\,\varphi\,dxdt
\end{aligned}$$

and

$$\theta_i = \mathcal{M}_Y(\mathbf{B}_i)\cdot\nabla u_i - \mathcal{M}_Y({}^t\mathbf{A}_i\,\nabla\beta_i)\cdot\nabla u_i$$

It remains to verify that the last equality coincides with

$$(B_i^0)_\alpha = \frac{1}{|Y|}\int_Y [(B_i)_\alpha - \mathbf{B}_i \cdot \nabla \chi_\alpha^i]\, dy$$

Choosing $\psi = \chi_\alpha^i$ in equation (4.3.15) and using (4.3.5), the definition of χ_α^i, gives

$$|Y|\mathcal{M}_Y(\mathbf{B}_i \cdot \nabla \chi_\alpha^i) = \int_Y {}^t\mathbf{A}_i \nabla \beta_i \cdot \nabla \chi_\alpha^i = \int_Y \mathbf{A}_i \nabla \chi_\alpha^i \cdot \nabla \beta_i$$
$$\int_Y \mathbf{A}_i \nabla y_\alpha \cdot \nabla \beta_i = |Y|\mathcal{M}_Y({}^t\mathbf{A}_i \cdot \nabla \beta_i)_\alpha$$

So

$$(B_i^0)_\alpha = \mathcal{M}_Y\big((B_i)_\alpha\big) - \mathcal{M}_Y\big((\mathbf{B}_i \cdot \nabla \chi_\alpha^i)\big).$$

(*iii*) *The boundary and initial conditions* :
In problem (4.2.1) the boundary conditions are

$$\gamma(\mathbf{A}_i^\varepsilon \nabla u_{i,\varepsilon})\nu + \beta_i u_{i,\varepsilon} = 0 \quad \text{ on } \Sigma_T.$$

If $\gamma = 0$ we have $u_{i,\varepsilon} = 0$ on Σ_T (Dirichlet conditions) and $u_{i,\varepsilon} = 0 \in W$ with $X = H_0^1(\Omega)$. Then $u_i \in W$ and $u_i = 0$ on Σ_T.

If $\gamma = 1$ (Neumann or Robin conditions) we have

$$0 = \int_{\partial\Omega} \Big(\gamma(\mathbf{A}_i^\varepsilon(x)\nabla u_{i,\varepsilon}(t,x))\nu + \beta_i(t,x)u_{i,\varepsilon}(t,x)\Big)\,\psi\, dx \quad \text{ in } \mathcal{D}'(0,T),$$
$$\forall \psi \in H^{\frac{1}{2}}(\partial\Omega)$$
$$= \int_\Omega (\mathbf{A}_i^\varepsilon(x)\nabla u_{i,\varepsilon} \cdot \nabla \psi + \mathbf{B}_i^\varepsilon(x) \cdot \nabla u_{i,\varepsilon}\, \psi)\, dx + < \partial_t u_{i,\varepsilon}, \psi >_{X,X'}$$
$$- \int_\Omega g_i^\varepsilon(t,x,u_{i,\varepsilon})\, \psi)\, dx + \int_{\partial\Omega} \beta_i(t,x)u_{i,\varepsilon}(t,x)\, \psi\, dx \quad \text{ in } \mathcal{D}'(0,T),$$

where $\psi \in H^{\frac{1}{2}}(\partial\Omega) \mapsto \psi \in H^1(\Omega)$ is a continous linear mapping from $H^{\frac{1}{2}}(\partial\Omega)$ to $H^1(\Omega)$. This gives a precise meaning to the boundary condition and it implies that, when ε goes to 0

$$\gamma(\mathbf{A}_i^\varepsilon\, \nabla u_{i,\varepsilon})\nu + \beta_i\, u_{i,\varepsilon} \rightharpoonup 0 \text{ in } L^2(0,T,H^{-\frac{1}{2}}(\partial\Omega)) \text{ weakly}$$

and

$$0 = \int_\Omega (\mathbf{A}_i^0(x)\nabla u_{i,\varepsilon} \cdot \nabla \psi + \mathbf{B}_i^0(x)\, \nabla u_i\, \psi)\, dx + < \partial_t u_i, \psi >_{X,X'}$$
$$- \int_\Omega g_i^0(t,x,u_i)\, \psi)\, dx + \int_{\partial\Omega} \beta_i(t,x)u_i(t,x)\, \psi\, dx \quad \text{ in } \mathcal{D}'(0,T).$$

Hence

$$\gamma(\mathbf{A}_i \nabla u_i)\nu + \beta_i u_i = 0 \quad \text{on } \Sigma_T$$

and consequently $\mathbf{u}$ satisfies

$$\begin{aligned} &< \partial_t u_i, v >_{X,X'} \\ &+ \int_\Omega (\mathbf{A}_i^0(x)\nabla u_{i,\varepsilon} \cdot \nabla v + \mathbf{B}_i^0(x)\, \nabla u_i\, v)\, dx = \int_\Omega g_i^0(t,x,u_i)\, v\, dx \\ &\qquad - \int_{\partial\Omega} \beta_i(t,x) u_i(t,x)\, v\, dx \quad \text{in } \mathcal{D}'(0,T), \quad \forall v \in H^1(\Omega). \quad (4.3.18) \end{aligned}$$

So

$$\begin{cases} \frac{\partial u_i}{\partial t} - \operatorname{div}(\mathbf{A}_i^0 \nabla u_i) + \mathbf{B}_i^0 \nabla u_i = g_i^0(t,x,\mathbf{u}), & (t,x) \in \Omega_T \\ \gamma\,(\mathbf{A}_i^0 \nabla u_i) \cdot \nu + \beta_i(t,x) u_i = 0, & (t,x) \in \Sigma_T \end{cases}$$

The initial condition
To end this proof we have to show that $\mathbf{u}$ satisfies tha initial condition :

$$\mathbf{u}(0,x) = \mathbf{u}^0(x)$$

We choose $\varphi \in C^\infty([0,Y])$ such that $\varphi(0) = 1$ and $\varphi(T) = 0$ and $v \in H^1(\Omega)$. A density argument after taking the limit in (4.3.18), when ε goes to zero, gives the initial condition. □

Chapitre 5

Continuous quality with age effect model.

5.1 Introduction.

Soil organic matter has multiple benefits to society and the environment : building soil organic matter contributes to climate change mitigation ; it also increases soil fertility, enhances resilience of agricultural systems and so supports rural livelihoods and food security. Soil organic matter (SOM) is the decomposing remains of plant and animal matter. Photosynthesis is the primary source of organic matter—plants synthesize organic compounds by harnessing sunlight. Organic matter in the soil is decomposed by the action of microorganisms (bacteria,fungi). Carbon is the dominant element of soil organic matter (SOM), comprising around 50% of SOM.
When considering the global carbon cycle, soils represent a major reservoir for carbon. It is widely acknowledged that the first meter of soil contains more than twice the amount of carbon in the atmospheric reservoir, where C is dominantly present as carbon dioxide(CO_2)and about three times the amount in the global vegetation cover. Topsoil alone (0-30 cm depth) contains as much carbon as the atmosphere. AsSOC and SOM interact with climate, atmosphere and land-use change, modelling SOM dynamcs is of great importance in order to understand mechanisms that regulate SOM cycles to develop better management practices in order to preserve soils sustainability and reduce CO_2 release.
First SOM Models appeared in 1930's and 1940's with the work of Nikiforoff [11] and Henin and Depuis [12]. They fractionate SOM into several quality and uses fluxes to represent interactions. This led to first compartmental

models in soil. Researchers were seduced by this simple and effective methodology, used it to develop more efficient models which integrate current knowledge in the field of pedology, microbiology, chemistry etc. (see Manzoni et al [8])
Improving models is then a continuous and important process. Some authors incorporate physiological mechanisms such assimilation process (Allison et al [70]) or priming effect (Fontaine et al [26] and Perveen et al [27]). Others based their improvement on soil complexity and heterogeneity and presented spatially distributed models (Goudjo et al 2011[17], Hammoudi et al 2015[69], Chenu et al 2014[71], Braakhekke et al 2013[18], Elzein and Balesdent2015 [16]). Others prefer to look in the heterogeneity inside the quality of soil organic matter.
In 1996, Agren and Bosatta presented the continuous-quality theory [15]. Those authors used only two interdependent compartments : a microbial compartment and a substrate compartment. To consider an infinite number of substrate qualities, they provided the time evolution equation for a fraction of quality q.
The theory by Agren and Bossata proposed thus to take account of the complete and complex biochemical spectrum of compounds in the SOM from labile to stable. Of course, to get the dynamic of all the substrate, they took the sum over all qualities. Their theory can deliver complicated mathematical object : partial differential equations, integro-differential equations or a mixture of these. Fortunately, in some particular cases, exact solutions can be derived or efficiently approximated ([72]).
Based on this theory, Nilsson et al 2005 [73] provides a more efficient way to detect changes in farming management. Using by the Agreen and Bossatta model, they simulate a more effective indicator : the microbial quotient, that is the ratio between microbial biomass carbon and soil organic carbon (See also Nilsson thesis [74]).
In this paper, we followed Agren and Bosatta's formalism to present a model of soil organic matter cycle based on MOMOS ([23]) and featured with : continuous-quality SOM and age effect . We did not use a physical measurable quality like particle size as in Bruun et al 2010 [33] but continued to use chemically computed degradation coefficients and we implement infinite compartments.
We also integrated a transport operator that will model age effect in order to represent the change of quality of SOM with years : SOM become in average more stable with time, thus microbial biomass will first decompose younger and more labile material.
The MOMOS model emphasized the role of microbial community. The mas-

ter ordinary differential equation governing microbial biomass is nonlinear. It will be difficult (if not impossible) to derive the exact solution. Fortunately computers are pretty faster, and approximated solution can be calculated quickly.
The master differential equation governing organic matter is a linear reaction-diffusion-advection equation. The main objective of modelling is to provide an accurate framework with less parameters that will link the formalism of continuous-quality and the MOMOS model. We first focused to validate mathematically this model, then calibrate it and validate it experimentally.

5.2 Methods.

5.2.1 The model and basic concepts.

The multi-compartments MOMOS model (Pansu et al 2010 [23]) is based on the following differential system :

$$\dot{u} = F(T,\theta) \begin{pmatrix} -k_{VL}u_1 + f_1(t) \\ -k_{VS}u_2 + f_2(t) \\ k_{VL}u_1 + k_{VS}u_2 - k_{MB}u_3 - qu_3^2 + k_{HL}u_4 + k_{HS}u_5 \\ -(k_{HLS} + k_{HL})\,u_4 + k_{MB}u_3 \\ -k_{HS}u_5 + k_{HLS}u_4 \end{pmatrix}, \quad (5.2.1)$$

where the different parameters k are stoichiometric positive constants derived from the experience and q is a parameter related to the soil characteristics (for more details see Pansu et al 2004 [22]). The function u_3 models the dynamics of microbial carbon and the other state variables u_i, $i = 1, 2, 4, 5$ model the dynamics of stable and labile compartments of vegetal and of humus. In this case, we work with finite number of SOM fractions.
A continuous quality of SOM implies that we have not a finite number of compartments of organic carbon (qualities) any more but infinite set of qualities $\{x, x \in \Omega\}$. We will take here $\Omega =]0, 1[$.
Each quality x has its decomposability rate $k_0(x)$. This function is decreasing on Ω, which means that the most degradable fraction is localized near $x = 0$, and the more stable one is localized near $x = 1$.
To adapt MOMOS in order to consider continuous quality carbon distribution, we consider a derived formulation of (5.2.1). The decomposability rate function $k_0(\cdot)$ will be corrected by moisture function and soil respiration function linked to real climatic data. Hence, substrate of quality x and at a time t will be decomposed at a rate $k(t, x) = F(T, \theta)k_0(x)$. Notice that time

dependence is in fact a dependence on climatic data.
The differential system (5.2.1) become :

$$\begin{cases} \dot{u} = -k_1(t)u - qu^2 + \int_\Omega k(t,x)v(t,x)dx \text{ for } t > 0, \\ v_t = \frac{\partial}{\partial x}(a\frac{\partial}{\partial x}v - \alpha(t,x)v) - k(t,x)v + k_1(t)ug(x) + f(t,x) \ in\ \Omega_T, \\ a\frac{\partial}{\partial x}v(t,0) - \alpha(t,0)v(t,0) = 0,\ t \in (0,T) \\ a\frac{\partial}{\partial x}v(t,1) - \alpha(t,1)v(t,1) = 0,\ t \in (0,T) \\ u(0) = u_0 \in \mathbb{R}^+, v(0,\cdot) = v_0 \in L^2_+(\Omega). \end{cases} \tag{5.2.2}$$

where $L^2_+(\Omega)$ is the set of positive function in $L^2_+(\Omega)$. Here u_t stands for the temporal evolution of microbial biomass while $v_t(.,x)$ stands for the temporal evolution of the fraction x of SOM including humus (HL,HS) and vegetal carbon(VL,VS).
The quantity $\int_\Omega k(t,x)v(t,x)dx$ corresponds to the organic carbon mass obtained by degradation over all qualities. The microbial biomass loses matter by mineralization $-q(t)u^2$ and by mortality $-k_1(t)u$.
The dead microbial biomass is reinjected in the substrate compartment following a Gaussian distribution function g centered on some quality x_0 , x_0 is fixed by the orginal MOMOS model, such that $k_0(x_0) = k_{HL}$. That is :

$$x_0 = 1 - \sqrt[n]{(k_{HL} - k_{VS})/k_{VL}} \ and \ \int_\Omega g(x)dx = 1.$$

The model input is represented by f(t,x).
Finally, the flux term $a\nabla v - \alpha(t,x)v$ represents the interactions between different qualities and can be interpreted as follow :
Age-effect : the term $-\alpha(t,x)v$ is the advective term and represents the effect of age on the chemo-biological processes of the organic substrate.
For example we know that for all t, $k(t,.)$ is a decreasing function in x and $\alpha(t,x)$ is positive, which means that the organic carbon will become more and more stable in the system.
Randomness : the term $a\nabla v$ represents the randomness of the transformation of the organic carbon from a quality x at a time t, to a quality $x + dx$, with small dx at a time $t + dt$, with dt small.
This type of flux describes the transformations along the x axis (the quality axis) was used by Bruun et al [33].

5.2.2 Parameterization.

The different parameters and functions incorporated are deduced in some way from the original MOMOS model as one can see below.

Function or parameter	Expression
$F(T,\theta)$	$F(\theta)F(T)$: Climat data correction function.
$F(T)$	$Q_{10}^{((T-T_{op})/10)}$: The soil respiration function
$F(\theta)$	$\text{Min}(\theta/WHC, 1)$
$k_1(t)$	$F(T,\theta)k_{MB}$
$q(t)$	$F(T,\theta)q$
$k(t,x)$	$F(T,\theta)k(x)$
$k_0(x)$	$(k_{VL}(1-x)^n + k_{HS})$: the decomposition function
a	10^{-5} Small positive constant fixed empirically.
$\alpha(t,x)$	$F(T,\theta)K_{HLS}(10^{-4} + e^{((x-x_0)^2)})$
$g(x)$	Gaussian function centered on x_0

5.3 Results.

5.3.1 Mathematical validation.

With specific conditions on the initial condition the system (5.2.2) has a unique positive solution.

Theorem 5.1. *Let $(u_0, v_0(\cdot))$ be a positive initial condition in $\mathbb{R} \times L^2(\Omega)$. If $f \in L^2(0,T,L^2(\Omega))$, $q(\cdot), k_1(\cdot) \in L^\infty(0,T)$ and $k \in L^\infty(\Omega_T)$ be all positive then there exists a unique positive weak solution to* (5.2.2).

Its worthy to notice that conditions on data are less restrictive. Indeed, data sets are incomplete and climate functions are not so smooth. All we need to apply the theorem is to have bounded data functions $F(T,\theta)$,$f(x,t)$ and initial distribution $v(x,0)$ in some natural functional space.
This result remain valid if we choose to adapt RothC, Century or any other linear SOM model. If the model is nonlinear, the result can probably be extended with appropriate assumptions.(see section 5.6.1)
We can also modify the system of equations to take into account for example priming effect and the previous result stay valid.
The numerical results were obtained by coupling Matlab R 2014 and Comsol5.0.(see section 5.6.2)

5.3.2 Calibration.

For the sake of efficiency we have drown on the experience gained on the original MOMOS model in order to have the smallest number of parameters

to be calibrated.
In the calibration step we look for the the optimal values of 5 parameters ($Q_{10}, n, q, k_{HLS}, k_{MB}$) instead of 7 in the original momos model.
We used data sets collected by Pansu ([22],[23]) to calibrate and validate the original MOMOS model (5.2.1). Pansu collected data from experiences carried out in six contrasting ecosystems (see [22] for more technical details on sites).
We randomly picked up three sites to use their correspondent data to calibration (Gavidia, Bahrina, Banco). We used the data of the remaining three other sites for validation (Tovar, Rosa, El Vigia).

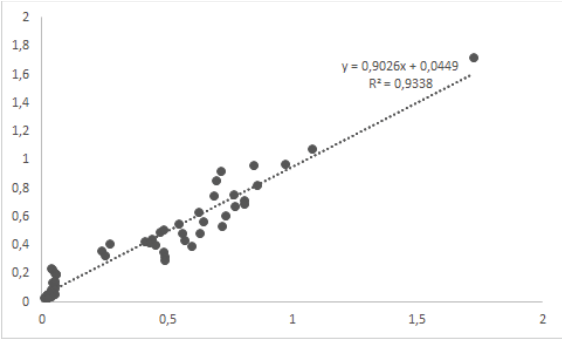

Figure 5.1: Relation between predicted values and measured values of total carbon and microbial carbon for three sites : Gavidia, Bahrina and Banco

We get these values

Q_{10}	3.261
n	4.214
q	1.991
k_{HLS}	0.00039
k_{MB}	0.45
$RMSE$	0.555
R^2	93.3%

5.3.3 Validation.

In this step, all the parameters are fixed at the calibration values except those which depend on the site's characteristics : Q_{10}, n, q, k_{MB}.

Rosa :

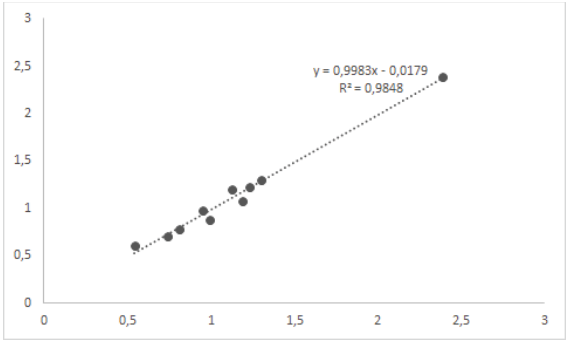

Figure 5.2: Relation between predicted values and measured values of total carbon for Rosa site

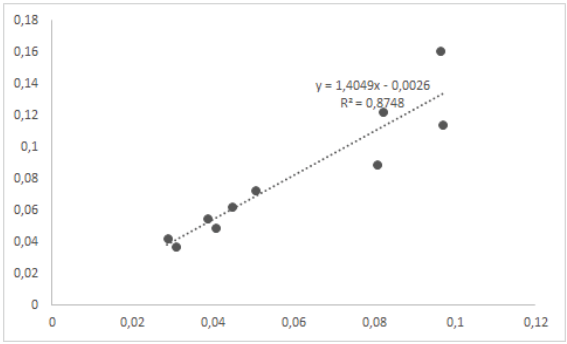

Figure 5.3: Relation between predicted values and measured values of microbial carbon for Rosa site

Q_{10}	2.833
n	4.785
q	0.966
k_{HLS}	0.00039
k_{MB}	0.45
$RMSE$	0.053
Error	5.02%

Tovar :

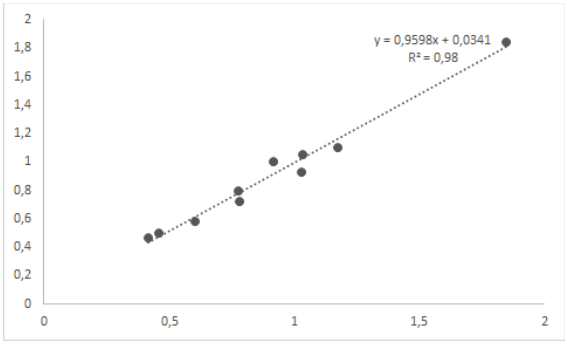

Figure 5.4: Relation between predicted values and measured values of total carbon for Tovar site

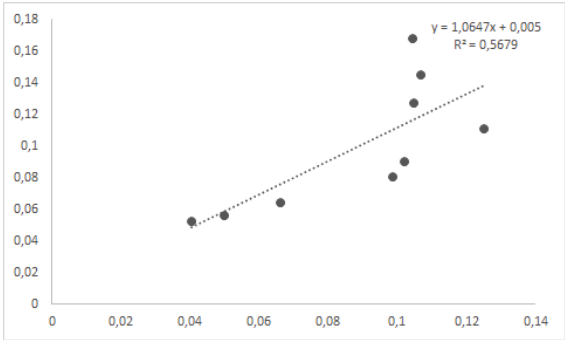

Figure 5.5: Relation between predicted values and measured values of microbial carbon for Tovar site

Q_{10}	2.464
n	4.166
q	0.780
k_{HLS}	0.00039
k_{MB}	0.45
$RMSE$	0.043
Error	4.52%

El Vigia :

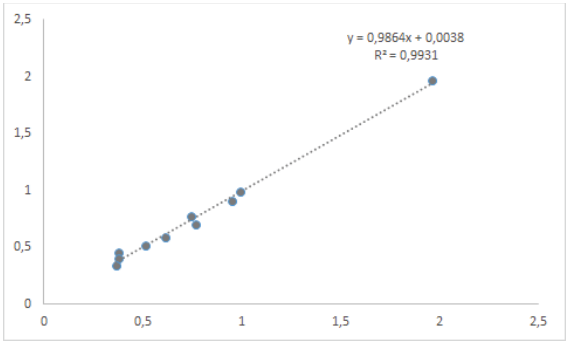

Figure 5.6: Relation between predicted values and measured values of total carbon for Vigia site

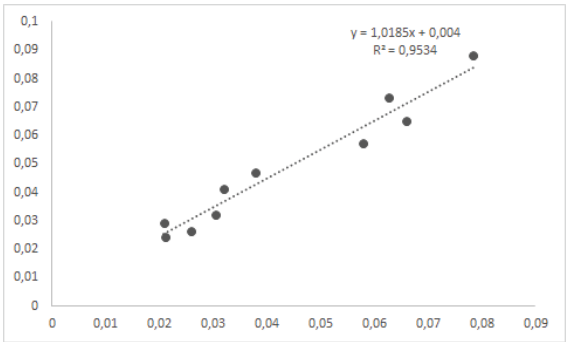

Figure 5.7: Relation between predicted values and measured values of microbial carbon for Vigia site

Q_{10}	3.09
n	4.785
q	0.951
k_{HLS}	0.00039
k_{MB}	0.45
$RMSE$	0.030
Error	3.77 %

5.4 Discussion.

As expected, the numerical results of the model give good approximations of the in situ experiments figures, since considering an infinite number of compartments improves the results of the original model.
We need for this new model high values of Q_{10} which are still in an acceptable range. In fact, Raich and Schlesinger 1992 [75] collected Q_{10} values published for different in situ experiments and showed that there are ranged from 1.3 to 3.3. In Hashimoto 2005 [76], published Q_{10} values for soil respiration in Japanese forest are also ranged from 1.3 to 3.45. Moreover, in order to get the desired sensibility on climate data we observed the great importance of Q_{10} value during the sensibility tests. For this reason we included Q_{10} as a parameter to be calibrated instead of being fixed to 2 (its mean value) as in the original MOMOS model.
The second more important factor is the metabolic coefficient q, ranged in our simulations from 0.78 to 1.991. This is the factor, as in the original MOMOS, controls the mass losses and consequently the total carbon remaining in soil. It is linked to soil properties (texture, pH etc) and is ranged from 1.3 to 3.8 in the original MOMOS model.
The quality function exponent "n" varies from 4.166 to 4.785. Changing the value of this parameter does not change the quality range (always $[k_{VS}, k_{VL}]$ but can give more weight to labile fractions (if n is big).
The estimated values of microbial biomass are "good" with a statistical correlation factor R^2 of 87.4% for Rosa site and 95.3% for El Vigia site. Only estimations of Tovar site had an R^2 factor of 56.7%. For the soil total soil carbon we get better prediction. The statistical correlation factor R^2 for both Rosa and Tovar sites is 98%. The best R^2 is obtained for El Vigia site with 99%.
In this model we had to calibrate 5 parameters and only 3 of them changed during the validation step.

5.5 Conclusion.

In the global effort to obtain better models of soil organic carbon dynamics, the theory of Agreen and Bosatta offers a wide application area to enhance ordinary compartmental models using techniques they presented. Indeed, considering a continuous quality of SOM is a natural idea to improve SOM common models.
In this paper, we successfully integrate their ideas to an existent SOM model

and we get a robust and well-posed mathematical system that corresponds better to reality. This prototype is very promising and can be modulated to meet researchers and land-manager's needs.
Providing simple and, in the same time, efficient models is important in order to get to essential conclusions. This model considers the complexity of the SOM while remaining easy to use and to manipulate. Furthermore, for this data set, it gives better predictions of the experiments figures comparing to the original MOMOS model. Besides it has less parameter to be calibrated.
Additionally, as we resolve the system of equation in a one dimensional domain, this prototype can even be used in global predictive models or in crop models without any significant computational costs.

5.6 Supplementary material

5.6.1 Mathematical validation of the model

We use here the Faedo Galerkin method, the Ascoli theorem and compacity arguments to prove the existence of a global solution.
Let us first recall the system equations

$$\begin{cases} \dot{u} = -k_1(t)u - qu^2 + \int_\Omega k(t,x)v(t,x)dx \text{ for } t > 0, \\ v_t = \frac{\partial}{\partial x}(a\frac{\partial}{\partial x}v - \alpha(t,x)v) - k(t,x)v + k_1(t)ug(x) + f(t,x) \ in\ \Omega_T, \\ a\frac{\partial}{\partial x}v(t,0) - \alpha(t,0)v(t,0) = 0,\ t \in (0,T) \\ a\frac{\partial}{\partial x}v(t,1) - \alpha(t,1)v(t,1) = 0,\ t \in (0,T) \\ u(0) = u_0 \in \mathbb{R}^+, v(0,\cdot) = v_0 \in L^2_+(\Omega). \end{cases} \tag{5.6.1}$$

with the no-flux boundary condition

$$\begin{cases} a\frac{\partial}{\partial x}v(t,0) - \alpha(t,0)v(t,0) = 0,\ t \in (0,T) \\ a\frac{\partial}{\partial x}v(t,1) - \alpha(t,1)v(t,1) = 0,\ t \in (0,T) \end{cases} \tag{5.6.2}$$

Here $\Omega = (0,1)$ and $\Omega_T = (0,T) \times \Omega$.
First let define $(\cdot,\cdot)$ to be the usual scalar product in $L^2(\Omega)$:

$$(p,q) = \int_\Omega p(x)q(x)dx. \tag{5.6.3}$$

Definition : We say that (u,v) is a weak solution of (5.6.1) and (5.6.2) if

$u \in W^{1,3/2} \cap L^3([0,T])$
$v \in L^\infty(0,t;L^2(\Omega)) \cap L^2(0,t;H^1(\Omega)), v_t \in L^2(0,t;(H^1(\Omega))')$

such that

$$\dot{u} = -k_1(t)u - q|u|u + \int_\Omega k(t,x)v(t,x)dx$$

and

$$\int_{\Omega_T} \frac{\partial v}{\partial t}\phi = \int_{\Omega_T} (a\nabla v\nabla\phi - \alpha(t,x)v\nabla\phi) + \int_{\Omega_T} (-k(t,x)v + k_1(t)ug(x) + f(t,x))\phi$$

for all $\phi \in L^2(0,T;H^1(\Omega))$.
We prove the following theorem

Theorem. *Let $(u_0, v_0(\cdot))$ be a positive initial condition in $\mathbb{R} \times L^2(\Omega)$. Let $f \in L^2(0,T,L^2(\Omega))$, $q(\cdot), k_1(\cdot) \in L^\infty(0,T)$ and $k \in L^\infty(\Omega_T)$ be all positive functions, then there exists a unique positive weak solution to* (5.6.1) *and* (5.6.2).

Proof. We proceede in several steps.
First Step : Construction of an approximate solution
Since the space H^1 is a separable Hilbert space, it contains a countable dense subset $\{w_1, \ldots, w_n, \ldots\} \subset X$ of linearly independent elements. We assume that they are orthonormal in $L^2(\Omega)$.
We look for a function $v_m(\cdot, x)$ such that

$$v_m(t,x) = \sum_{i=1}^{m} g_{i,m}(t)w_i$$

where the functions $g_{i,m}(\cdot)$ and $u_m(\cdot)$ verify the ordinary differential system

$$\begin{cases} \dot{u}_m = -k_1(t)u - q|u_m|u_m + \sum_{i=1}^{m} (\int_\Omega w_i k(t,x)dx) g_{i,m}(t) \\ \dot{g}_{i,m}(t) = -\sum_{i=1}^{m} g_{i,m}(\nabla w_i, \nabla w_j) - \sum_{i=1}^{m} g_{i,m}(\alpha(t,x)w_i, \nabla w_j) \\ -\sum_{i=1}^{m} g_{i,m}(k(t,x)w_i, w_j) + (f(t,x), w_j), \end{cases} \tag{5.6.4}$$

coupled with the initial condition

$$\begin{cases} u_m(0) = u_0 \\ g_{i,m}(0) = (v_{0,m}, w_i), \end{cases}$$

where

$$v_{0,m} = \sum_{i=1}^{m} \beta_{i,m} w_i \to v_0 \text{ in } L^2(\Omega) \text{ when } m \to \infty.$$

From classical results on ordinary differential systems (see for example Coddington [62]) we have the existence of a local solution on the time interval $[0, \rho^m)$.
To prove global existence we need some estimates that we collect in the sequel.

Second step : A priori estimates
We multiply the first equation of (5.6.4) by u_m and we integrate over $[0, t)$ with $t < \rho^m$ then we multiply the second by v_m and we integrate over $[0, t) \times \Omega$ to get

$$u_m^2 + \int_0^t k_1(s)u^2 + \int_0^t q(s)|u_m|u_m^2 \leq u_m^2(0) + \int_0^t \left(\int_\Omega (k(s,x)v_m(s,x)dx)u_m(s) \right) ds \quad (5.6.5)$$

and

$$\|v_m(t,\cdot)\|^2_{L^2(\Omega)} + a\|\nabla v_m\|^2_{L^2(0,t;\Omega)} \leq \varepsilon\|\nabla v_m\|^2_{L^2(0,t;\Omega)} + C_\varepsilon\|v_m(t,\cdot)\|^2_{L^2(0,t;\Omega)} + C_1\|u_m\|^2_{L^2(0,t)} + C_2. \quad (5.6.6)$$

Hence by Young inequality we have

$$u_m^2 \leq C + C\left(\|u_m\|^2_{L^2(0,t)} + \|v_m(t,\cdot)\|^2_{L^2(0,t;\Omega)} \right). \quad (5.6.7)$$

Taking the sum of (5.6.7) and (5.6.6) in which we set $\varepsilon = \frac{a}{2}$ leads to

$$u_m^2 + \|v_m(t,\cdot)\|^2_{L^2(\Omega)} \leq C + C\left(\|u_m\|^2_{L^2(0,t)} + \|v_m(t,\cdot)\|^2_{L^2(0,t;\Omega)} \right). \quad (5.6.8)$$

From Gronwall lemma we obtain the existence of a positive constant C independent of m such that

$$u_m^2 + \|v_m(t,\cdot)\|^2_{L^2(\Omega)} \leq C \quad (5.6.9)$$

and from (5.6.5) we have for all $m \in \mathbb{N}$

$$\|u_m\|^3_{L^3(0,t)} \leq C \quad (5.6.10)$$

for some positive C.
Moreover, from (5.6.6) we conclude that the sequence $(v_m)_{m\in\mathbb{N}}$ is uniformly bounded in $L^\infty(0,t;L^2(\Omega)) \cap L^2(0,t;H^1(\Omega))$. The local solution can then be

extended and $\rho^m = T$.

Step 3. Convergence of the sequences
Convergence of u_m : From (5.6.7) we know that $(u_m)_{m\in\mathbb{N}}$ is uniformly bounded. We prove that this sequence is equicontinuous in order to apply Ascoli theorem.
For all $t_0, t_1 \in [0,T]$ we have from the first equation of (5.6.4)

$$|\int_{t_0}^{t_1} \dot{u}_m dt| \leq |\int_{t_0}^{t_1} k_1(t)u_m dt| + |\int_{t_0}^{t_1} q(t)u_m^2(t)dt| + |\int_{t_0}^{t_1} \left(\int_\Omega k(t,x)v_m(t,x)dx\right) dt|.$$

From the a priori estimates (5.6.8) and conditions on the model functions k_1, q and k we have a postive constant C such that :

$$|\int_{t_0}^{t_1} \dot{u}_m dt| \leq C|t_1 - t_0|,$$

that is for all $t_0, t_1 \in [0,T]$ we have

$$|u_m(t_1) - u_m(t_2)| \leq C|t_1 - t_0|.$$

The sequence $(u_m)_{m\in\mathbb{N}}$ is uniformly bounded and equicontinuous family of continuous functions then by Ascoli theorem, it exists a subsequence that we denote (u_{m_k}) that converge uniformly on $[0,T]$ to a continuous function u. If the solution of the problem (5.6.4) is unique then all the sequence converges not only a subsequence.
Convergence of v_m : We all ready showed that the sequence $(v_m)_{m\in\mathbb{N}}$ is uniformly bounded in $L^\infty(0,t;L^2(\Omega)) \cap L^2(0,t;H^1(\Omega))$.
We resolve again the following system verified by the subsequence (u_{m_k}, v_{m_k})

$$\begin{cases} \dot{u}_{m_k} = -k_1(t)u_{m_k} - q|u_{m_k}|u_{m_k} + \int_\Omega k(t,x)v_{m_k}(t,x)dx \\ \frac{\partial v_{m_k}}{\partial t} = \frac{\partial}{\partial x}(a\frac{\partial}{\partial x}v_{m_k} - \alpha(t,x)v_{m_k}) - k(t,x)v_{m_k} + k_1(t)u_{m_k}g(x) \\ +f(t,x) \end{cases} \quad (5.6.11)$$

coupled with the initial condition

$$u_{m_k} = u_0$$
$$v_{m_k}(0,x) = v_{0,m}$$

and the no-flux boundary condition

$$a\frac{\partial}{\partial x}v_{m_k}(t,x) - \alpha(t,x)v_{m_k} = 0 \text{ when } x = 0,1 \text{ and } t > 0.$$

If we let $k \to \infty$ in (5.6.11) then thanks to the dominated convergence theorem and the convergence of $u_{m_k} \to u$ and we get limit functions

$$u \in W^{1,3/2}([0,T]) \cap L^3([0,T]) \tag{5.6.12}$$

and

$$v \in L^\infty(0,T;L^2(\Omega)) \cap L^2(0,T;H^1(\Omega)), \tag{5.6.13}$$

such that

$$\begin{cases} \dot{u} = -k_1(t)u - q|u|u + \int_\Omega k(t,x)v(t,x)dx \\ \frac{\partial v}{\partial t} = \frac{\partial}{\partial x}(a\frac{\partial}{\partial x}v - \alpha(t,x)v) - k(t,x)v + k_1(t)ug(x) + f(t,x) \end{cases}$$

The second equation of (5.6.11) is linear, we get then the convergence of all of its terms.

Step4. Uniqueness of the solution
Suppose that there exist two solution (u_1, v_1) and (u_2, v_2), then $U = u_1 - u_2$ and $V = v_1 - v_2$ verify

$$\begin{cases} \dot{U} = -k_1(t)U - q(|u_1|u_2 - |u_2||u_2|) + \int_\Omega k(t,x)V(t,x)dx \\ \frac{\partial V}{\partial t} = \frac{\partial}{\partial x}(a\frac{\partial}{\partial x}V - \alpha(t,x)V) - k(t,x)V + k_1(t)Ug(x) \\ +f(t,x) \end{cases} \tag{5.6.14}$$

coupled with the initial condition $U(0) = 0$ and $V(0,x) = 0$ in $L^2(\Omega)$ and the boundary condition

$$a\frac{\partial}{\partial x}V(t,x) - \alpha(t,x)V(t,x) = 0 \text{ if } x = 0,1 \text{ and } t > 0.$$

We multiply the first equation of (5.6.14) by U and the second by V then we use the fact that for all $u_1, u_2 \in \mathbb{R}$

$$(|u_1|u_2 - |u_2||u_2|)(u_1 - u_2) \geq 0$$

to deduce that

$$U^2(t) + \|v(t,\cdot)\|_{L^2(\Omega)} \leq C \int_0^t \left(U^2(s) + \|v(t,\cdot)\|_{L^2(\Omega)}\right) ds.$$

Since $U(0) = 0$ and $V(0,x) = 0$ in $L^2(\Omega)$ then

$$U^2(t) + \|v(t,\cdot)\|_{L^2(\Omega)} = 0.$$

The uniqueness of the solution is proved.

Step5. The positivity of the solution
To prove the positivity of the solution we use the idea of Efendiev [63]. We consider the follwing system

$$\begin{cases} \dot{u} = -k_1(t)u - q|u|u + \int_\Omega k(t,x)|v(t,x)|dx \\ \frac{\partial v}{\partial t} = \frac{\partial}{\partial x}(a\frac{\partial}{\partial x}v - \alpha(t,x)v) - k(t,x)v + k_1(t)ug(x) + f(t,x) \end{cases} \tag{5.6.15}$$

with the same initial condition and boundary-condition as before.
Like previous we find that this new system has a unique solution. Further more, if we multiply the first equation by $-u^-$ and the second by $-v^-$ we prove that the solution is positive. Hence the solution of (5.6.15) is the unique solution of (5.2.2) which finish the proof. □

5.6.2 Comsol-Matlab Application Code

In this section, we list the essential code for the Comsol-Matlab application. For the calibration and the validation steps, we used the same Comsol m-file that we modify to consider the right climate data and initial conditions. We give here the example of El Vigia site.
We list also the code for the Matlab User Interface Application used in the calibration and validation steps.

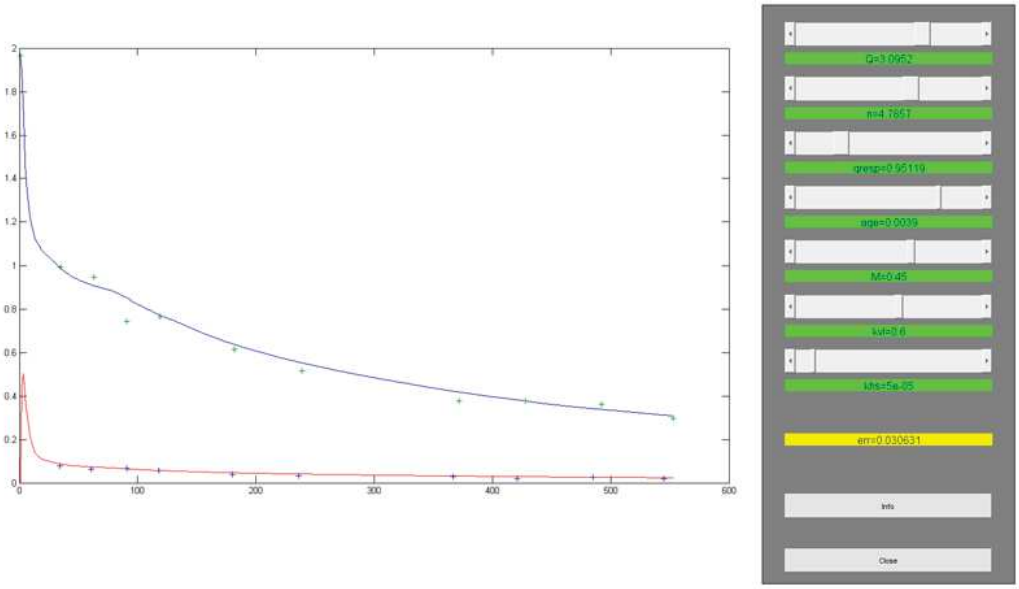

Figure 5.8: User Interface of the application for the validation procedure - El Vigia

Comsol-Matalb Script

```
function [MB, C] = momosvig(Q,n, qresp,age,M,kvl,khs)

import com.comsol.model.*
import com.comsol.model.util.*

model = ModelUtil.create('Model');

model.modelPath('C:\Users\Alaa\Documents'); % to change
```

```
model.label('momosqc.mph');
%================================
%Parameters settings
%================================
model.param.set('kvl', kvl);
model.param.set('khs', khs);
model.param.set('n', n);
model.param.set('d', '0.00001');
model.param.set('kmb', M);
model.param.set('qresp', qresp);
model.param.set('Q', Q);
model.param.set('khls', '0.00003');
model.param.set('fs', '0.107');
model.param.set('kvs', '0.003');
model.param.set('khl', '0.05');
model.param.set('age', '0.00001');
x_0=1-((khl-khs)/kvl)^(1/n);
kvs=0.003;
x_1=1-((khl-khs)/kvs)^(1/n);

model.modelNode.create('comp1');
%================================
%Functions setting and climate data
%================================
model.func.create('an1', 'Analytic');
model.func.create('int1', 'Interpolation');
model.func.create('int2', 'Interpolation');
model.func.create('gp1', 'GaussianPulse');
model.func.create('gp2', 'GaussianPulse');
model.func.create('gp3', 'GaussianPulse');
model.func.create('rect1', 'Rectangle');
kx=strcat(kvl,'*(1-x)^',n,'+',khs);
model.func('an1').set('expr', kx);
model.func('an1').set('dermethod', 'manual');
model.func('an1').set('funcname', 'k');

model.func('int1').set('table', ); %  Temperature data here.
model.func('int1').set('funcname', 'T'); % Temperature function.
```

```
model.func('int2').set('table', ); % Moisture data here.
model.func('int2').set('funcname', 'w'); % Moisture function.

model.func('gp1').set('sigma', '0.04');
model.func('gp1').set('funcname', 'inivl');
model.func('gp2').set('location', x_1);
model.func('gp2').set('sigma', '0.04');
model.func('gp2').set('funcname', 'inivs');
model.func('gp3').set('location', x_0);
model.func('gp3').set('sigma', '0.04');
model.func('gp3').set('funcname', 'g');
model.func('rect1').set('lower', '0.2');
model.func('rect1').set('upper', '0.46');
model.func('rect1').set('funcname', 'v');

%=================================
%Mesh and solver settings
%=================================
model.geom.create('geom1', 1);

model.mesh.create('mesh1', 'geom1');

model.geom('geom1').create('i1', 'Interval');
model.geom('geom1').run;

model.cpl.create('intop1', 'Integration', 'geom1');
model.cpl('intop1').selection.set([1]);

model.physics.create('c', 'CoefficientFormPDE', 'geom1');
model.physics('c').field('dimensionless').component({'u1' 'u2'});

model.mesh('mesh1').create('edg1', 'Edge');

model.result.table.create('tbl1', 'Table');
model.result.table.create('tbl2', 'Table');

model.view('view1').axis.set('xmax', '1.0499999523162842');
model.view('view1').axis.set('xmin', '-0.04999998211860657');

model.cpl('intop1').set('opname', 'intop');
```

```
model.physics('c').feature('cfeq1').set('c', {'0'; '0'; '0'; 'd'});
model.physics('c').feature('cfeq1').set('a',...
{'Q^((T(t)-20)/10)*w(t)*(kmb+qresp*abs(u1))';...
 '-kmb*Q^((T(t)-20)/10)*w(t)*g(x)/intop(g(x))'; ...
 '0'; 'Q^((T(t)-20)/10)*w(t)*k(x)'});
model.physics('c').feature('cfeq1').set('f',...
{'Q^((T(t)-20)/10)*w(t)*intop(u2*k(x))'; '0'});
fstring= strcat('-Q^((T(t)-20)/10)*w(t)*(v(x)+0.0001)*',age,'');
model.physics('c').feature('cfeq1').set('al', {'0'; '0'; '0'; fstring });
model.physics('c').feature('init1').set('u2',...
'1.963*(fs*inivs(x)/intop(inivs(x))+(1-fs)*inivl(x)/intop(inivl(x)))');


model.result.table('tbl1').comments('Moyenne sur ligne 1 (u1)');
model.result.table('tbl2').comments('Moyenne sur ligne 1 (u2)');

model.study.create('std1');
model.study('std1').create('time', 'Transient');

model.sol.create('sol1');
model.sol('sol1').study('std1');
model.sol('sol1').attach('std1');
model.sol('sol1').create('st1', 'StudyStep');
model.sol('sol1').create('v1', 'Variables');
model.sol('sol1').create('t1', 'Time');
model.sol('sol1').feature('t1').create('fc1', 'FullyCoupled');
model.sol('sol1').feature('t1').feature.remove('fcDef');

model.study('std1').feature('time').set('initstudyhide', 'on');
model.study('std1').feature('time').set('initsolhide', 'on');
model.study('std1').feature('time').set('solnumhide', 'on');
model.study('std1').feature('time').set('notstudyhide', 'on');
model.study('std1').feature('time').set('notsolhide', 'on');
model.study('std1').feature('time').set('notsolnumhide', 'on');

model.result.dataset.create('an1_ds1', 'Function1D');
model.result.dataset.create('an1_ds2', 'Function1D');
model.result.dataset.create('an1_ds3', 'Function1D');
model.result.numerical.create('int1', 'IntLine');
```

```
model.result.numerical('int1').selection.all;
model.result.numerical('int1').set('probetag', 'none');

model.study('std1').feature('time').set('tlist', 'range(0,1,552)');

model.sol('sol1').attach('std1');
model.sol('sol1').feature('t1').set('tlist', 'range(0,1,552)');
model.sol('sol1').runAll;
model.result.numerical.create('intt', 'IntLine');
model.result.numerical('intt').selection.all;
model.result.numerical('intt').set('expr', 'u1');
model.result.table.create('tbt', 'Table');
model.result.numerical('intt').set('table', 'tbt');
model.result.numerical('intt').setResult;
%================================
% Get results in MB and C vectors
%================================
MB1 = model.result.numerical('intt').getReal();
MB=MB1';
model.result.numerical('intt').selection.all;
model.result.numerical('intt').set('expr', 'u2+u1');
model.result.table.create('tbt2', 'Table');
model.result.numerical('intt').set('table', 'tbt2');
model.result.numerical('intt').setResult;
C1= model.result.numerical('intt').getReal();
C=C1';

end
```

Matlab script fot the user interface for the calibration procedure :

```
function model_calibrate(action)
%global var to extract
global MBmall MBsall Ctotmall Ctotsim TM TC


%read measured data from file
    data=xlsread('donneesMB-CTOT');
    data(:,1)=data(:,1)-ones(1147,1);%%decalage en temps
```

```
    for j=2:13
    tmp=isnan(data(:,j));
    k=0;
    for i=1:length(tmp)
    if tmp(i,1)==false
        k=k+1;
        T(k,j)=data(i,1);
        indice(k,j)=i;
    end
    end
    end
    TMB=T(1:10,2:7);
    TCtot=T(1:11,8:13);
    indiceMB=indice(1:10,2:7);
    indiceCtot=indice(1:11,8:13);

persistent sig figNumber hndlList;

if nargin<1,
    action='initialize';
    sig = [];
elseif nargin==1
  if ~ischar(action)
       x = action;
       sig = x;
       action = 'initialize';
   end
end


if strcmp(action,'initialize'),
   %===================================
   % Information for all buttons
    labelColor=[0.9 0.9 0.9];
    yInitPos=0.90;
    menutop=0.95;
    top=0.4;
    left=0.785;
    btnWid=0.175;
    btnHt=0.04;
```

```
textHeight = 0.05;
textWidth = 0.08;

% Spacing between the button and the next command's label
spacing=0.05;


%====================================
% generate  figure
figNumber=figure( ...
    'Name','Calibration', ...
    'NumberTitle','off', ...
    'Backingstore','off', ...
    'Visible','off');

%====================================
% Set up the axes
axHndl1=axes( ...
    'Units','normalized', ...
    'Position',[0.10 0.70 0.60 0.22], ... /// [x y width height])
    'Drawmode','fast', ...
    'Visible','on');
axHndl2=axes( ...
    'Units','normalized', ...
    'Position',[0.10 0.4 0.60 0.22], ...
    'Drawmode','fast', ...
    'Visible','on');
axHndl3=axes( ...
    'Units','normalized', ...
    'Position',[0.10 0.1 0.60 0.22], ...
    'Drawmode','fast', ...
    'Visible','on');

%====================================
% The console
frmBorder=0.019; frmBottom=0.04;
frmHeight = 0.92; frmWidth = btnWid;
yPos=frmBottom-frmBorder;
frmPos=[left-frmBorder yPos frmWidth+2*frmBorder frmHeight+2*frmBorder];
```

```
uicontrol( ...
    'Style','frame', ...
    'Units','normalized', ...
    'Position',frmPos, ...
    'BackgroundColor',[0.5 0.5 0.5]);

%===================================
% 1st Bouton
menuNumber=1;
yPos=menutop-(menuNumber-1)*(btnHt+spacing);

labelStr='Nom Bouton 1';
callbackStr='GUI_model(''actionbouton1'');';
btnPos=[left yPos-btnHt btnWid btnHt];

btn1Hndl=uicontrol( ...
      'units'   , 'normalized',...
     'Style','Slider',...
     'Min',1,'Max',4,'Value',3.261,...
     'SliderStep', [0.1 0.1], ...
     'Position',btnPos, ...
     'String',labelStr, ...
     'Callback',callbackStr);
Qtext = uicontrol('style','text',...
     'units'   , 'normalized',...
     'position',[left 0.88-(menuNumber-1)*spacing btnWid 0.02 ],...
     'string','Q= 3.261',...
     'backgroundcolor','g',...
     'fontsize',12);

%===================================
% 2nd Bouton
menuNumber=2;
yPos=menutop-(menuNumber-1)*(btnHt+spacing);

  btnPos=[left yPos-btnHt btnWid btnHt];
  labelStr='Nom Bouton 2';
  callbackStr='GUI_model(''actionbouton1'');';

  btn2Hndl=uicontrol( ...
```

```
      'units'   , 'normalized',...
      'Style','Slider',...
      'Min',1,'Max',7,'Value',4.214,...
      'SliderStep', [0.1 0.1], ...
      'Position',btnPos, ...
      'String',labelStr, ...
      'Callback',callbackStr);
  Qtext2 = uicontrol('style','text',...
      'units'   , 'normalized',...
      'position',[left 0.88-(menuNumber-1)*(btnHt+spacing) btnWid 0.02 ],...
      'string','n= 4.214',...
      'backgroundcolor','g',...
      'fontsize',12);

%====================================
% 3rd Bouton
menuNumber=3;
yPos=menutop-(menuNumber-1)*(btnHt+spacing);

  btnPos=[left yPos-btnHt btnWid btnHt];
  labelStr='Nom Bouton 2';
  callbackStr='GUI_model(''actionbouton1'');';

  btn3Hndl=uicontrol( ...
      'units'   , 'normalized',...
      'Style','Slider',...
      'Min',0.1,'Max',4,'Value',1.991,...
      'SliderStep', [0.1 0.1], ...
      'Position',btnPos, ...
      'String',labelStr, ...
      'Callback',callbackStr);
 Qtext3 = uicontrol('style','text',...
      'units'   , 'normalized',...
      'position',[left 0.88-(menuNumber-1)*(btnHt+spacing) btnWid 0.02 ],...
      'string','qresp= 1.991',...
      'backgroundcolor','g',...
      'fontsize',12);

%====================================
% 4th Bouton
```

```
menuNumber=4;
yPos=menutop-(menuNumber-1)*(btnHt+spacing);

  btnPos=[left yPos-btnHt btnWid btnHt];
  labelStr='Nom Bouton 2';
  callbackStr='GUI_model(''actionbouton1'');';

  btn4Hndl=uicontrol( ...
     'units'   , 'normalized',...
     'Style','Slider',...
     'Min',10^-4,'Max',5*10^-3,'Value',0.0039,...
     'SliderStep', [10^-4 10^-4], ...
     'Position',btnPos, ...
     'String',labelStr, ...
     'Callback',callbackStr);
 Qtext4 = uicontrol('style','text',...
     'units'   , 'normalized',...
     'position',[left 0.88-(menuNumber-1)*(btnHt+spacing) btnWid 0.02 ],...
     'string','age= 0.0039',...
     'backgroundcolor','g',...
     'fontsize',12);
 %===================================
 % 5th Bouton
 menuNumber=5;
 yPos=menutop-(menuNumber-1)*(btnHt+spacing);

  btnPos=[left yPos-btnHt btnWid btnHt];
  labelStr='Nom Bouton 2';
  callbackStr='GUI_model(''actionbouton1'');';

  btn5Hndl=uicontrol( ...
     'units'   , 'normalized',...
     'Style','Slider',...
     'Min',0.2,'Max',0.6,'Value',0.45,...
     'SliderStep', [0.05 0.05], ...
     'Position',btnPos, ...
     'String',labelStr, ...
     'Callback',callbackStr);
 Qtext5 = uicontrol('style','text',...
     'units'   , 'normalized',...
```

```
    'position',[left 0.88-(menuNumber-1)*(btnHt+spacing) btnWid 0.02 ],...
    'string','M= 0.45',...
    'backgroundcolor','g',...
    'fontsize',12);
%=====================================
% 6th Bouton
menuNumber=6;
yPos=menutop-(menuNumber-1)*(btnHt+spacing);

 btnPos=[left yPos-btnHt btnWid btnHt];
 labelStr='Nom Bouton 2';
 callbackStr='GUI_model(''actionbouton1'');';

 btn6Hndl=uicontrol( ...
    'units'   , 'normalized',...
    'Style','Slider',...
    'Min',0.1,'Max',1,'Value',0.6,...
    'SliderStep', [0.05 0.05], ...
    'Position',btnPos, ...
    'String',labelStr, ...
    'Callback',callbackStr);
 Qtext6 = uicontrol('style','text',...
    'units'   , 'normalized',...
    'position',[left 0.88-(menuNumber-1)*(btnHt+spacing) btnWid 0.02 ],...
    'string','kvl= 0.6',...
    'backgroundcolor','g',...
    'fontsize',12);
%=====================================
% 7e Bouton
 menuNumber=7;
 yPos=menutop-(menuNumber-1)*(btnHt+spacing);

 btnPos=[left yPos-btnHt btnWid btnHt];
 labelStr='Nom Bouton 2';
 callbackStr='GUI_model(''actionbouton1'');';

 btn7Hndl=uicontrol( ...
    'units'   , 'normalized',...
    'Style','Slider',...
    'Min',0.00001,'Max',0.0005,'Value',0.00005,...
```

```
    'SliderStep', [0.00001 0.00001], ...
    'Position',btnPos, ...
    'String',labelStr, ...
    'Callback',callbackStr);
 Qtext7 = uicontrol('style','text',...
    'units'   , 'normalized',...
    'position',[left 0.88-(menuNumber-1)*(btnHt+spacing) btnWid 0.02 ],...
    'string','khs= 0.00005',...
    'backgroundcolor','g',...
    'fontsize',12);
%====================================
%rmse text ui
Qtext8 = uicontrol('style','text',...
    'units'   , 'normalized',...
    'position',[left 0.88-(menuNumber)*(btnHt+spacing) btnWid 0.02 ],...
    'string','err= --',...
    'backgroundcolor','yellow',...
    'fontsize',12);


%==================================
% The INFO button
labelStr='Info';
callbackStr='GUI_model(''info'')';
helpHndl=uicontrol( ...
    'Style','pushbutton', ...
    'Units','normalized', ...
     'BackgroundColor',labelColor, ...
    'Position',[left frmBottom+btnHt+spacing btnWid btnHt], ...
    'String',labelStr, ...
    'Callback',callbackStr);

%==================================
% The CLOSE button
labelStr='Close';
callbackStr='close(gcf)';
closeHndl=uicontrol( ...
    'Style','pushbutton', ...
    'Units','normalized', ...
     'BackgroundColor',labelColor, ...
```

```
        'Position',[left frmBottom btnWid btnHt], ...
        'String',labelStr, ...
        'Callback',callbackStr);


    % 'UserData' set up
    hndlList=[ axHndl1 axHndl2 axHndl3  btn1Hndl Qtext btn2Hndl ...
     Qtext2 btn3Hndl Qtext3 btn4Hndl Qtext4 btn5Hndl Qtext5 Qtext8 ...
      btn6Hndl Qtext6 btn7Hndl Qtext7];

    set(figNumber, ...
        'Visible','on', ...
        'UserData',hndlList);


        %=========================

elseif strcmp(action,'actionbouton1'),

   hndlList = get(figNumber,'UserData');
   Qnum =num2str(get(hndlList(4),'Value'));
   n =num2str(get(hndlList(6),'Value'));
   qresp =num2str(get(hndlList(8),'Value'));
   age =num2str(get(hndlList(10),'Value'));
   M=num2str(get(hndlList(12),'Value'));
   kvl=num2str(get(hndlList(15),'Value'));
   khs=num2str(get(hndlList(17),'Value'));

   %=========================
   %update value on console
   set(hndlList(5),'String', strcat('Q= ', Qnum));
   set(hndlList(7),'String', strcat('n= ', n));
   set(hndlList(9),'String', strcat('qresp= ', qresp));
   set(hndlList(11),'String', strcat('age= ', age));
   set(hndlList(13),'String', strcat('M= ', M));
   set(hndlList(16),'String', strcat('kvl= ', kvl));
   set(hndlList(18),'String', strcat('khs= ',khs));

   hndlList = get(figNumber,'UserData');
   err=0;
```

```
axes(hndlList(1));
%=========================
%Barinas
%=========================
   %run the simulation and get result vor barinas
   [MB, C] = momosbar(Qnum,n,qresp,age,M,kvl,khs);
   % plot it !
   %get mesured data
   MBm1= data(indiceMB(:,2),3);
   Ctotm1=data(indiceCtot(:,2),9);
   %get the coreespondant simulated data to calculate the error
   MBs1=MB(indiceMB(:,2));
   Ctots1=C(indiceCtot(:,2));
   MB1=MB(indiceMB(:,2));
   C1=C(indiceCtot(:,2));
   err=err+(MBm1-MB1)'*(MBm1-MB1)+(Ctotm1-C1)'*(Ctotm1-C1);
   cla
   plot(MB,'r')

   hold on
   plot(C)
   hold on
   plot(indiceMB(:,2),MBm1,'+',indiceCtot(:,2),Ctotm1,'+');

%=========================
%site Banco: same procedure
%=========================
axes(hndlList(2));
   [MB, C] = momosbanc(Qnum,n,qresp,age,M,kvl,khs);
   MBm2= data(indiceMB(:,6),7);
   Ctotm2=data(indiceCtot(:,6),13);
   MBs2=MB(indiceMB(:,6));
   Ctots2=C(indiceCtot(:,6));
   cla
   plot(MB,'r')


   hold on
   plot(C)
   hold on
```

```
   plot(indiceMB(:,6),MBm2,'+',indiceCtot(:,6),Ctotm2,'+');
   MB1=MB(indiceMB(:,6));
   C1=C(indiceCtot(:,6));
   err=err+(MBm2-MB1)'*(MBm2-MB1)+(Ctotm2-C1)'*(Ctotm2-C1);
%=========================
%site Gavidia: same procedure
%=========================
axes(hndlList(3));
   [MB, C] = momosgav(Qnum,n,qresp,age,M,kvl,khs);
   MBm3= data(indiceMB(:,5),6);
   Ctotm3=data(indiceCtot(:,5),12);
   MBs3=MB(indiceMB(:,5));
   Ctots3=C(indiceCtot(:,5));

   cla
   plot(MB,'r')


   hold on
   plot(C)
   hold on
   plot(indiceMB(:,5),MBm3,'+',indiceCtot(:,5),Ctotm3,'+');
   MB1=MB(indiceMB(:,5));
   C1=C(indiceCtot(:,5));



   err=err+(MBm3-MB1)'*(MBm3-MB1)+(Ctotm3-C1)'*(Ctotm3-C1);
 set(hndlList(14),'String', strcat('err= ', num2str(err)));

 MBsall=[MBs1 MBs2 MBs3];
 Ctotsim=[Ctots1 Ctots2 Ctots3];
   MBmall=[MBm1 MBm2 MBm3];
   Ctotmall=[Ctotm1 Ctotm2 Ctotm3];
   TM=indiceMB;
   TC=indiceCtot;
 %====================================

 %====================================
 % Help
```

```
    elseif strcmp(action,'info'),
     h0=msgbox({'Need Help? contact' 'alaaeddine.hammoudi@univ-montp2.fr'});


    return

end
```

Matlab script fot the user interface for the calibration procedure :

```
function model_validate(action);

global validmbm validmbs validctotm validctots Tbm Tcm MB C
%read measured data from file
    data=xlsread('donneesMB-CTOT');
    data(:,1)=data(:,1)-ones(1147,1);%%decalage en temps
    for j=2:13
    tmp=isnan(data(:,j));
    k=0;
    for i=1:length(tmp)
    if tmp(i,1)==false
        k=k+1;
        T(k,j)=data(i,1);
        indice(k,j)=i;
    end
    end
    end
    TMB=T(1:10,2:7);
    TCtot=T(1:11,8:13);
    indiceMB=indice(1:10,2:7);
    indiceCtot=indice(1:11,8:13);
% Modèle classique de GUI

persistent sig figNumber hndlList;

if nargin<1,
    action='initialize';
    sig = [];
elseif nargin==1
```

```
  if ~ischar(action)
       x = action;
       sig = x;
       action = 'initialize';
   end
end



if strcmp(action,'initialize'),
   %====================================
   % Information for all buttons
    labelColor=[0.9 0.9 0.9];
    yInitPos=0.90;
    menutop=0.95;
    top=0.4;
    left=0.785;
    btnWid=0.175;
    btnHt=0.04;
    textHeight = 0.05;
    textWidth = 0.08;

    % Spacing between the button and the next command's label
    spacing=0.05;


    %==================================
    % Generate figure
    figNumber=figure( ...
        'Name','titre de la figure', ...
        'NumberTitle','off', ...
        'Backingstore','off', ...
        'Visible','off');




    %==================================
    % Set up the axes
    axHndl1=axes( ...
```

```
    'Units','normalized', ...
    'Position',[0.10 0.20 0.60 0.72], ... /// [x y width height])
    'Drawmode','fast', ...
    'Visible','on');


%==================================
% The console
frmBorder=0.019; frmBottom=0.04;
frmHeight = 0.92; frmWidth = btnWid;
yPos=frmBottom-frmBorder;
frmPos=[left-frmBorder yPos frmWidth+2*frmBorder frmHeight+2*frmBorder];

uicontrol( ...
    'Style','frame', ...
    'Units','normalized', ...
    'Position',frmPos, ...
    'BackgroundColor',[0.5 0.5 0.5]);


%==================================
% 1st slider
menuNumber=1;
yPos=menutop-(menuNumber-1)*(btnHt+spacing);

  labelStr='Nom Bouton 1';
  callbackStr='GUI_model_valid(''actionbouton1'');';
  btnPos=[left yPos-btnHt btnWid btnHt];

  btn1Hndl=uicontrol( ...
      'units'   , 'normalized',...
     'Style','Slider',...
     'Min',1,'Max',4,'Value',2.4643,...
     'SliderStep', [0.1 0.1], ...
     'Position',btnPos, ...
     'String',labelStr, ...
     'Callback',callbackStr);
 Qtext = uicontrol('style','text',...
     'units'   , 'normalized',...
     'position',[left 0.88-(menuNumber-1)*spacing btnWid 0.02 ],...
```

```
     'string','Q= 2.4643',...
     'backgroundcolor','g',...
     'fontsize',12);

%====================================
% 2nd slider
menuNumber=2;
yPos=menutop-(menuNumber-1)*(btnHt+spacing);

  btnPos=[left yPos-btnHt btnWid btnHt];
  labelStr='Nom Bouton 2';
  callbackStr='GUI_model_valid(''actionbouton1'');';

  btn2Hndl=uicontrol( ...
     'units'   , 'normalized',...
     'Style','Slider',...
     'Min',1,'Max',7,'Value',4.14,...
     'SliderStep', [0.1 0.1], ...
     'Position',btnPos, ...
     'String',labelStr, ...
     'Callback',callbackStr);
Qtext2 = uicontrol('style','text',...
     'units'   , 'normalized',...
     'position',[left 0.88-(menuNumber-1)*(btnHt+spacing) btnWid 0.02 ],...
     'string','n= 4.14',...
     'backgroundcolor','g',...
     'fontsize',12);

   %====================================
% 3rd slider
menuNumber=3;
yPos=menutop-(menuNumber-1)*(btnHt+spacing);

  btnPos=[left yPos-btnHt btnWid btnHt];
  labelStr='Nom Bouton 2';
  callbackStr='GUI_model_valid(''actionbouton1'');';

  btn3Hndl=uicontrol( ...
     'units'   , 'normalized',...
     'Style','Slider',...
```

```
     'Min',0.1,'Max',4,'Value',0.7809,...
     'SliderStep', [0.1 0.1], ...
     'Position',btnPos, ...
     'String',labelStr, ...
     'Callback',callbackStr);
Qtext3 = uicontrol('style','text',...
     'units'   , 'normalized',...
     'position',[left 0.88-(menuNumber-1)*(btnHt+spacing) btnWid 0.02 ],...
     'string','qresp= 0.7809',...
     'backgroundcolor','g',...
     'fontsize',12);

%===================================
% 4th slider
menuNumber=4;
yPos=menutop-(menuNumber-1)*(btnHt+spacing);

  btnPos=[left yPos-btnHt btnWid btnHt];
  labelStr='Nom Bouton 2';
  callbackStr='GUI_model_valid(''actionbouton1'');';

  btn4Hndl=uicontrol( ...
     'units'   , 'normalized',...
     'Style','Slider',...
     'Min',10^-4,'Max',5*10^-3,'Value',0.0039,...
     'SliderStep', [10^-4 10^-4], ...
     'Position',btnPos, ...
     'String',labelStr, ...
     'Callback',callbackStr);
Qtext4 = uicontrol('style','text',...
     'units'   , 'normalized',...
     'position',[left 0.88-(menuNumber-1)*(btnHt+spacing) btnWid 0.02 ],...
     'string','age= 4*10^-4',...
     'backgroundcolor','g',...
     'fontsize',12);
%===================================
% 5th slider
menuNumber=5;
yPos=menutop-(menuNumber-1)*(btnHt+spacing);
```

```
  btnPos=[left yPos-btnHt btnWid btnHt];
  labelStr='Nom Bouton 2';
  callbackStr='GUI_model_valid(''actionbouton1'');';

  btn5Hndl=uicontrol( ...
     'units'   , 'normalized',...
     'Style','Slider',...
     'Min',0.2,'Max',0.6,'Value',0.45,...
     'SliderStep', [0.05 0.05], ...
     'Position',btnPos, ...
     'String',labelStr, ...
     'Callback',callbackStr);
Qtext5 = uicontrol('style','text',...
     'units'   , 'normalized',...
     'position',[left 0.88-(menuNumber-1)*(btnHt+spacing) btnWid 0.02 ],...
     'string','M= 0.45',...
     'backgroundcolor','g',...
     'fontsize',12);
    %===================================
% 6th slider
menuNumber=6;
yPos=menutop-(menuNumber-1)*(btnHt+spacing);


  btnPos=[left yPos-btnHt btnWid btnHt];
  labelStr='Nom Bouton 2';
  callbackStr='GUI_model_valid(''actionbouton1'');';

  btn6Hndl=uicontrol( ...
     'units'   , 'normalized',...
     'Style','Slider',...
     'Min',0.1,'Max',1,'Value',0.6,...
     'SliderStep', [0.05 0.05], ...
     'Position',btnPos, ...
     'String',labelStr, ...
     'Callback',callbackStr);
Qtext6 = uicontrol('style','text',...
     'units'   , 'normalized',...
     'position',[left 0.88-(menuNumber-1)*(btnHt+spacing) btnWid 0.02 ],...
     'string','kvl= 0.6',...
```

```
     'backgroundcolor','g',...
     'fontsize',12);
 %==================================
 % 7th slider
menuNumber=7;
yPos=menutop-(menuNumber-1)*(btnHt+spacing);

  btnPos=[left yPos-btnHt btnWid btnHt];
  labelStr='Nom Bouton 2';
  callbackStr='GUI_model_valid(''actionbouton1'');';

  btn7Hndl=uicontrol( ...
     'units'   , 'normalized',...
     'Style','Slider',...
     'Min',0.00001,'Max',0.0005,'Value',0.00005,...
     'SliderStep', [0.00001 0.00001], ...
     'Position',btnPos, ...
     'String',labelStr, ...
     'Callback',callbackStr);
Qtext7 = uicontrol('style','text',...
     'units'   , 'normalized',...
     'position',[left 0.88-(menuNumber-1)*(btnHt+spacing) btnWid 0.02 ],...
     'string','khs= 0.00005',...
     'backgroundcolor','g',...
     'fontsize',12);
%==================================
%rmse error ui
Qtext8 = uicontrol('style','text',...
     'units'   , 'normalized',...
     'position',[left 0.88-(menuNumber)*(btnHt+spacing) btnWid 0.02 ],...
     'string','err= --',...
     'backgroundcolor','yellow',...
     'fontsize',12);


%==================================
% Help button
labelStr='Info';
callbackStr='GUI_model_valid(''info'')';
helpHndl=uicontrol( ...
```

```
        'Style','pushbutton', ...
        'Units','normalized', ...
         'BackgroundColor',labelColor, ...
        'Position',[left frmBottom+btnHt+spacing btnWid btnHt], ...
        'String',labelStr, ...
        'Callback',callbackStr);

    %====================================
    % The close  button
    labelStr='Close';
    callbackStr='close(gcf)';
    closeHndl=uicontrol( ...
        'Style','pushbutton', ...
        'Units','normalized', ...
         'BackgroundColor',labelColor, ...
        'Position',[left frmBottom btnWid btnHt], ...
        'String',labelStr, ...
        'Callback',callbackStr);

   %====================================
    % 'UserData'
    hndlList=[ axHndl1   btn1Hndl Qtext btn2Hndl Qtext2 btn3Hndl ...
    Qtext3 btn4Hndl Qtext4 btn5Hndl Qtext5 Qtext8 btn6Hndl Qtext6 btn7Hndl Qtext7];

    set(figNumber, ...
        'Visible','on', ...
        'UserData',hndlList);


    %====================================

elseif strcmp(action,'actionbouton1'),
   %get data (parameter value for simulation) from UserData
   hndlList = get(figNumber,'UserData');
   Qnum =num2str(get(hndlList(2),'Value'));
   n =num2str(get(hndlList(4),'Value'));
   qresp =num2str(get(hndlList(6),'Value'));
   age =num2str(get(hndlList(8),'Value'));
   M=num2str(get(hndlList(10),'Value'));
   kvl=num2str(get(hndlList(13),'Value'));
```

```
   khs=num2str(get(hndlList(15),'Value'));

   %===================================
   %update displayed values on console
   set(hndlList(3),'String', strcat('Q= ', Qnum));
   set(hndlList(5),'String', strcat('n= ', n));
   set(hndlList(7),'String', strcat('qresp= ', qresp));
   set(hndlList(9),'String', strcat('age= ', age));
   set(hndlList(11),'String', strcat('M= ', M));
   set(hndlList(14),'String', strcat('kvl= ', kvl));
   set(hndlList(16),'String', strcat('khs= ',khs));

   hndlList = get(figNumber,'UserData');
   err=0;
   axes(hndlList(1));
   %===================================
   % Rosa
   %===================================
%       [MB, C] = momosrosa(Qnum,n,qresp,age,M,kvl,khs);
%
%       MBm= data(indiceMB(:,4),5);
%       Ctotm=data(indiceCtot(:,4),11);
%       cla
%       plot(MB,'r')
%
%
%       hold on
%       plot(C)
%       hold on
%       Tbm=indiceMB(:,4);
%       Tcm=indiceCtot(:,4);
%       plot(Tbm,MBm,'+',Tcm,Ctotm,'+');
%       MB1=MB(indiceMB(:,4))
%       C1=C(indiceCtot(:,4))
%       err=err+(MBm-MB1)'*(MBm-MB1)+(Ctotm-C1)'*(Ctotm-C1);
   %===================================
   % Tovar:
   %===================================
%         [MB, C] = momostov(Qnum,n,qresp,age,M,kvl,khs);
%
```

```
%       MBm= data(indiceMB(1:9,3),4);
%       Ctotm=data(indiceCtot(:,3),10);
%       cla
%       plot(MB,'r')
%       ebm=std(MBm)*ones(size(MBm));
%
%       hold on
%       plot(C)
%       hold on
%
%       Tbm=indiceMB(1:9,3);
%       Tcm=indiceCtot(:,3);
%       plot(Tbm,MBm,'x',Tcm,Ctotm,'+');
%       MB1=MB(indiceMB(1:9,3))
%       C1=C(indiceCtot(:,3))
%       err=err+(MBm-MB1)'*(MBm-MB1)+(Ctotm-C1)'*(Ctotm-C1);
    %====================================
    %El Vigia
    %====================================
    %
    %
    %
    %
   %run simulatation
   [MB, C] = momosvig(Qnum,n,qresp,age,M,kvl,khs);
   %get measured data
      MBm= data(indiceMB(1:10,1),2);
      Ctotm=data(indiceCtot(1:11,1),8);

      cla
      plot(MB,'r')


      hold on
      plot(C)
      hold on
      plot(indiceMB(1:10,1),MBm,'+',indiceCtot(1:11,1),Ctotm,'+');
      MB1=MB(indiceMB(1:10,1));
      C1=C(indiceCtot(1:11,2));
   %get the rmse
```

```
      err=err+(MBm-MB1)'*(MBm-MB1)+(Ctotm-C1)'*(Ctotm-C1);

   %export to global variable for further analysis.
      validmbm=MBm;
      validmbs=MB1;
      validctotm=Ctotm;
      validctots=C1;
    %get the rmse
      err=err+(MBm-MB1)'*(MBm-MB1)+(Ctotm-C1)'*(Ctotm-C1);
    %update error value on  screen
    set(hndlList(12),'String', strcat('err= ', num2str(err)));
        %====================================
    %====================================
    elseif strcmp(action,'info'),
     h0=msgbox({'Need Help? contact' 'alaaeddine.hammoudi@univ-montp2.fr'});


    return



end
```

Chapitre 6

A model with chemotaxis effect.

Abstract
We deal here with a new version of the MOMOS (Modelling Organic changes by Micro-Organisms of Soil) model, recently introduced by M. Pansu. We study reaction-diffusion featured with chemotaxis. We prove the existence of a unique positive solution for different chemotactic functions and with domain dimension $n \leq 3$.

6.1 Introduction.

Chemotaxis is the ability of some bacteria to direct their movement towards the gradient of chemicals contained in their environment. In soil, some bacteria micro-organisms that degrade organic carbon (SOC) are motile and chemotactic. The existence of the phenomena is observed in experiments [38] and on the field. Nevertheless at our best knowledge no model of terrestrial carbon cycle is considering it. Indeed, these models are essentially compartmental corresponding naturally to systems of ordinary differential equations (e.g Century, RothC, MOMOS) [8]. They are used globally to estimates for example soil CO_2 emissions and locally in land management and crop optimization.
Prototypes of spatial soil organic models were proposed but still rare.Some of them use system of partial differential equations : Balesdent et al [16] combined vertical directed transport of organic carbon with a degradation phenomena and diffusion. More recently, Goudjo et al [17] proposed a three dimensional model for dissolved organic matter using also a system of PDE.

Other authors opted for a finite sequence of interconnected systems of ordinary differential equations each localized in a soil layer (see [77]).
We previously studied the model MOMOS proposed by Pansu (see [22],[23]), which is a nonlinear ordinary differential system [61] on which we based a simple spatial prototype in order to test later, the effect of soil heterogeneity on the model results [69]. Later, we derived from MOMOS a simple two equations model that takes into account chemotaxis. We proved the existence of Turing pattern that may provide possible explanations of the formation of soil aggregations, of the bacterial and micro-organisms spatial organizations (hotspots in soil) or justify the formation of the microscopic patterns observed by Vogel et al [38].
Keller-Segel model was the earliest mathematical system with concerns to chemotaxis [45]. Many others models emerge specially in biology and ecology. Most of authors focused their efforts essentially on existence and on asymptotic behaviour of solutions in one or two dimensional domains in order to avoid blow-up of solutions (see [46], [44], [40] and [49] [48] and references therein.)

Our main concern is to prove the existence of a unique solution to the minimal MOMOS model featured with a chemotaxis effect. We consider the problem with two different form of the chemotactic function h. A first form that do not prevent overcrowding and a second that do prevent this phenomena.
The paper is then organized as follow. In the second Section we recall the system MOMOS and its equations. We also present some notations, results and tools that we use through the paper.
In Section 6.3, we focus on the classical case $h(u) = u$. We present sufficient conditions to get global solution, and prove the existence of an exponential attractor.
In Section 6.4, we consider the second form of the function $h = u(M - u)$, $M > 0$. This function was proposed by Wrzosek in order to prevent overcrowding. It turns off chemotaxis term when u achieves a threshold M. This feature will help, proving that local solutions are actually global.
Finally, in the last section we keep using the second form of h to get well-posedness result in three dimensional domain with minimal restrictions on initial conditions and on the forcing term.

6.2 Mathematical preliminary and notations.

The MOMOS system of ordinary differential equations can be written as :

$$\dot{\mathbf{y}} = \mathbf{g}(t, \mathbf{y})$$

where

$$\mathbf{y} = \begin{pmatrix} u \\ v \\ w \end{pmatrix}$$

and

$$\mathbf{G}(t, \mathbf{y}) = \begin{pmatrix} -k_1(t)u - q(t)u^2 + k_2(t)v + k_3(t)w + f(t) \\ k_1(t)u - (k_2(t) + k_4(t))v \\ k_4(t)v - k_3(t)w. \end{pmatrix}$$

In these equation u stands for the alive microbial biomass quantity, v and w model soil organic matter of different quality (different decomposition rates).
In reality, the functions k_i $i \in \{1, 2, 3, 4\}$, q and f depend not only on time due to their dependence on temperature and moisture but also on space because of the variability in soil clay content. The phenomena described by MOMOS can be also subjected to the influence of transport and sedimentation through transport and diffusion. In this paper we derive a simpler model which consist in two equations taking in account diffusion and chemotaxis.
We introduce then following reaction-diffusion-chemotaxis system (P_h)

$$\begin{cases} \partial_t u - a\Delta u = -\beta \mathrm{div}(h(u)\nabla v) - k_1 u - q|u|u + k_2 v, \quad (t, x) \in Q_T \\ \partial_t v - d\Delta v = -k_2 v + k_1 u + f, \quad (t, x) \in \Omega_T \\ \nabla u \cdot \nu = \nabla v \cdot \nu = 0, \quad (t, x) \in \Sigma_T \\ u(0) = u_0 \quad \text{in } \Omega \\ v(0) = v_0 \quad \text{in } \Omega \end{cases} \tag{P_h}$$

where $h(\cdot)$ is a continuous function that will modulate the chemotactic effect.
In the first equation of (P_h), we changed the term qu^2 by $q|u|u$ for more accuracy since qu corresponds to a kinetic coefficient that cannot be negative.

Unless it is explicitly indicated, Ω is a bounded region in $\mathbb{R}^2$ of C^3 class, the constants a, β, q, d, k_1 and k_2 are strictly positive, and f is in some admissible space to be fixed later.
We recall here some known results (see [39], [41] and references therein) that will help in the sequel.

Interpolation space :
For $0 \leq s_0 < s < s_1 < \infty$, $H^s(\Omega)$ *is the interpolation space* $[H^{s_0}(\Omega), H^{s_1}(\Omega)]_\theta$ *with* $s = (1-\theta)s_0 + \theta s_1$ *between* $H^{s_0}(\Omega)$ *and* $H^{s_1}(\Omega)$. *Furthermore, we have*

$$\|.\|_{H^s(\Omega)} \leq \|.\|^{1-\theta}_{H^{s_0}(\Omega)} \|.\|^{\theta}_{H^{s_1}(\Omega)}. \tag{6.2.1}$$

Embedding theorem :
When $0 < s < 1$, $H^{s_0}(\Omega) \subset L^p(\Omega)$ *for* $\frac{1}{p} = \frac{1-s}{2}$ *with the estimate*

$$\| \cdot \|_{L^p(\Omega)} \leq C_s \| \cdot \|_{H^s(\Omega)}$$

When $s = 1$, $H^1(\Omega) \subset L^q(\Omega)$ *for any* $1 \leq q < \infty$ *and*

$$\| \cdot \|_{L^q(\Omega)} \leq C_{q,p} \| \cdot \|^{1-p/q}_{H^1(\Omega)} \| \cdot \|^{p/q}_{L^p(\Omega)} \tag{6.2.2}$$

where $1 \leq p \leq q < \infty$.
When $s > 1$ $H^s(\Omega) \subset C(\overline{\Omega})$ *with continuous embedding.*

Fractional Power of the laplace operator :
Let $L = -\Delta + 1$ *be the Laplace operator acting in* $L^2(\Omega)$ *with the domain* $D(L) = \{u \in H^2(\Omega); \frac{\partial u}{\partial \nu} = 0 \text{ on } \partial\Omega\}$, *where* L *is a self-adjoint positive definite operator. Then for* $0 \leq \theta < \frac{3}{4}$,

$$D(L^\theta) = H^{2\theta}(\Omega) \text{ (with norm equivalence)} \tag{6.2.3}$$

and for $\frac{3}{4} < \theta < \frac{3}{2}$,

$$D(L^\theta) = H^{2\theta}_\nu(\Omega) \text{ (with norm equivalence)} \tag{6.2.4}$$

with $H^{2\theta}_\nu(\Omega) = \{u \in H^{2\theta}(\Omega); \frac{\partial u}{\partial \nu} = 0 \text{ on } \partial\Omega\}$ *(See theorems 16.7 and 16.9 [41]).*

Useful inequalities

Biler's lemma (see [78])
With some increasing function $p(.)$ we have for any $\eta > 0$

$$\|u\|^3_{L^3(\Omega)} \leq \eta \|u\|_{H^1(\Omega)} N^1_{log}(u) + p(\eta^{-1})\|u\|_{L^1(\Omega)}, u \in H^1_+(\Omega) \tag{6.2.5}$$

here $N^1_{log}(u) = \|(u+1)log(u+1)\|_{L^1(\Omega)}$.

For $u \in H^1(\Omega), v \in H^{2+\varepsilon}(\Omega)$ we have

$$\|\nabla(u\nabla v)\|_{L^2(\Omega)} \leq C_\varepsilon \|u\|_{H^1(\Omega)} \|v\|_{H^{2+\varepsilon}(\Omega)} \tag{6.2.6}$$

If $u \in H^{1+\varepsilon}(\Omega), v \in H^2(\Omega)$ we get

$$\|\nabla(u\nabla v)\|_{L^2(\Omega)} \leq C_\varepsilon \|u\|_{H^{1+\varepsilon}(\Omega)} \|v\|_{H^2(\Omega)} \tag{6.2.7}$$

If $u \in H^2(\Omega), v \in H^3(\Omega)$ we get

$$\|\nabla(u\nabla v)\|_{H^1(\Omega)} \leq C \|u\|_{H^2(\Omega)} \|v\|_{H^3(\Omega)} \tag{6.2.8}$$

Local Existence
We need first to prove the existence of local solution of P_h. For this purpose, we use the result obtained by Yagi and based on the Galerkin method(see [44] [41]).
Let V and H be seperable Hilbert spaces with dense and compact embedding $V \subset H$. Let V' be the dual space of V and identify H and H' to get :

$$V \subset H \subset V'$$

The duality product between V and V' is denoted by $< \cdot, \cdot >$. It coincides with the scalar product of H on $H \times H$, The scalar product on H is denoted by $(\cdot, \cdot)$. The norm of H, V and V' are denoted by $|\cdot|_H$, $\|\cdot\|$ and $\|\cdot\|_*$ respectively.
Consider the following Cauchy problem of a semilinear abstract differential equation,

$$\begin{aligned} &\frac{dY}{dt} + AY = G(Y) + F(t),\ 0 < t \leq T \\ &Y(0) = Y_0, \end{aligned} \tag{6.2.9}$$

in the space V'.
Here, A is the positive definite self-adjoint operator of H defined by a symmetric sesquilinear form $a(Y, \tilde{Y})$ on V, with $< AY, \tilde{Y} >= a(Y, \tilde{Y})$.

Assumptions on $a(\cdot,\cdot)$

(a.i) $a(Y,\tilde{Y})| \leq M\|Y\|\|\tilde{Y}\|, \qquad Y,\tilde{Y} \in V$
(a.ii) $|a(Y,Y)| \geq \delta\|Y\|^2, \qquad Y \in V$

with some δ and $M > 0$. A is also bounded from V to V'.

Assumptions on $G(\cdot)$
$G(.)$ is a given continuous function for V to V' satisfying :
(g.i) For each $\zeta > 0$, there exists an increasing continuous function ϕ_ζ : $[0,\infty) \to [0,\infty)$ such that :

$$\|G(Y)\|_* \leq \zeta\|Y\| + \phi_\zeta(|Y|_H), \qquad Y \in V$$

(g.ii) For each $\zeta > 0$, there exists an increasing continuous function ψ_ζ : $[0,\infty) \to [0,\infty)$ such that :

$$\|G(Y) - G(\tilde{Y})\|_* \leq \zeta\|Y - \tilde{Y}\| + \psi_\zeta(|Y|_H + |\tilde{Y}|_H) \times |Y - \tilde{Y}|_H(\|Y\| + \|\tilde{Y}\| + 1), \qquad Y,\tilde{Y} \in V$$

Finally $F(\cdot) \in L^2(0,T;V')$ is a given function and $Y_0 \in H$ is an initial value. then, the follwing result is verified [44]

Theorem 6.1. *Under (a.i), (a.ii), (g.i) and (g.ii), for every* $F(\cdot) \in L^2(0,T;V')$ *and* $Y_0 \in H$*, there exists a unique local solution* Y *of* (6.2.9) *such that*

$$Y \in H^1(0,T(Y_0,F);V') \cap C([0,T(Y_0,F)];H) \cap L^2(0,T(Y_0,F),V)$$

Here $T(Y_0,F)$ *is determined by the norm* $|Y_0|_H$ *and* $\|F\|_{L^2(0,T;V')}$

6.3 Case $h(u) = u$.

6.3.1 Local existence and positivity.

We prove the following result :

Proposition 6.1. *Let* $\varepsilon_0 > 0$*. Let* $u_0 \in L^2(\Omega)$, $v_0 \in H^{1+\varepsilon_0}(\Omega)$ *and* $f \in L^2(0,T;H^{\varepsilon_0}_+(\Omega))$ *be positive functions then* (P_h) *has a unique positive local solution on* $(0,T_0)$ *such that*

$$u \in H^1(0,T_0;L^2(\Omega)) \cap C([0,T_0];H^1(\Omega)) \cap L^2(0,T_0,H^2_\nu(\Omega)),$$
$$v \in H^1(0,T_0;H^1(\Omega)) \cap C([0,T_0];H^2_\nu(\Omega)) \cap L^2(0,T_0,H^3_\nu(\Omega)),$$

where T_0 *depends only on* $\|f\|_{L^2(0,T;H^{\varepsilon_0}(\Omega))}$, $\|u_0\|_{L^2(\Omega)}$ *and* $\|v_0\|_{H^{1+\varepsilon_0}(\Omega)}$.

Proof. First Step : Construction of a unique local solution
Let $A_1 = -a\Delta + k_1$ and $A_2 = -d\Delta + k_2$ be two operators with the same domain $H^2_\nu(\Omega)$.
A_1 and A_2 are two positive self-adjoint operators on $L^2(\Omega)$. We can then define their corresponding fractional power operators (see [41] and reference therein) with the same domain , as described in previous section.
Let $V = H^1(\Omega) \times H^{2+\varepsilon_0}(\Omega)$ and $H = L^2(\Omega) \times H^{1+\varepsilon_0}(\Omega)$, for some fixed $0 < \varepsilon_0 < 1/2$.
Identifying H with its dual space, we have :
$V \subset H = H' \subset V'$ and $V' = (H^1(\Omega))' \times H^{\varepsilon_0}(\Omega)$ with the duality product

$$< \tilde{U}, U >_{V' \times V} = < \tilde{u}, u >_{(H^1(\Omega))' \times H^1(\Omega)} + (A_2^{\varepsilon_0/2}\tilde{v}, A_2^{1+\varepsilon_0/2}v)_{L^2(\Omega)}$$

where $\tilde{U} = (\tilde{u}, \tilde{v})$ and $U = (u, v)$.
We define a symmetric sesquilinear form on $V \times V$,

$$a(U, \tilde{U}) = (A_1^{1/2}u, A_1^{1/2}\tilde{u})_{L^2(\Omega)} + (A_2^{1+\varepsilon_0/2}v, A_2^{1+\varepsilon_0/2}\tilde{v})_{L^2(\Omega)}$$

for $\tilde{U} \in V, U \in V$.
This form defines a linear isomorphism

$$A = \begin{pmatrix} A_1 & 0 \\ 0 & A_2 \end{pmatrix}$$

from V to V' and A is then a positive definite self-adjoint operator in H.
Finally let $f(\cdot) \in L^2(0, T, H^{\varepsilon_0}(\Omega))$ and let G be :

$$G(U) := \begin{pmatrix} \beta\nabla(u\nabla v) - q|u|u + k_2 v \\ k_1 u \end{pmatrix}$$

for all $U = (u, v) \in V$.
We get then the following semilinear equation

$$\begin{aligned} &\frac{dY}{dt} + AY = G(Y) + F(t),\ 0 < t \leq T \\ &Y(0) = Y_0, \end{aligned} \tag{6.3.1}$$

in the space V' with $F(t) = \begin{pmatrix} 0 \\ f(t) \end{pmatrix}$.
In order to apply the existence result of theorem 6.1 to problem (6.3.1), we verify the assumptions on $a(\cdot, \cdot)$ and $G(\cdot, \cdot)$.
The assumptions on $a(\cdot, \cdot)$ are satisfied (see [44]). We verify that conditions

on G are also satisfied.
Verification of $g.i$:
For $U = (u, v) \in V$ we have $\frac{\partial v}{\partial n} = 0$ on $\partial\Omega$ and

$$\begin{aligned}\|\nabla \cdot (u\nabla v)\|_{(H^1(\Omega))'} &\leq C\|u\|_{L^4(\Omega)}\|\nabla v\|_{L^4(\Omega)} \\ &\leq \|u\|^{1/2}_{L^2(\Omega)}\|u\|^{1/2}_{H^1(\Omega)}\|v\|^{1/2}_{H^1(\Omega)}\|v\|^{1/2}_{H^2(\Omega)} \\ &\leq \|u\|^{1/2}_{L^2(\Omega)}\|u\|^{1/2}_{H^1(\Omega)}\|v\|^{(1+\varepsilon_0)/2}_{H^{1+\varepsilon_0}(\Omega)}\|v\|^{(1-\varepsilon_0)/2}_{H^{2+\varepsilon_0}(\Omega)} \\ &\leq C|U|^{1+\varepsilon_0/2}_H\|U\|^{1-\varepsilon_0/2}\end{aligned}$$

and

$$\|v\|_{(H^1(\Omega))'} \leq C|U|_H.$$

Moreover,

$$\|u\|_{H^{\varepsilon_0}(\Omega)} \leq C|U|^{1-\varepsilon_0}_H\|U\|^{\varepsilon_0}.$$

Hence the condition (g.i) is verified.
From the embedding theorem

$$\begin{aligned}|\int_\Omega (\tilde{u} - u)\nabla v \cdot \nabla\rho| &\leq C\|\tilde{u} - u\|_{L^2(\Omega)}\|\tilde{v}\|_{H^{2+\varepsilon_0}(\Omega)}\|\rho\|_{H^1(\Omega)} \\ |\int_\Omega \nabla(\tilde{v} - v)u \cdot \nabla\rho| &\leq C\|u\|_{H^1(\Omega)}\|\tilde{v} - v\|_{H^{1+\varepsilon_0}(\Omega)}\|\rho\|_{H^1(\Omega)}\end{aligned}$$

and finally using the interpolation theorem and Young inequality we obtain

$$\begin{aligned}\|u - \tilde{u}\|_{H^{\varepsilon_0}} &\leq C\|\tilde{U} - U\|^{\varepsilon_0}|\tilde{U} - U|^{1-\varepsilon_0}_H \\ &\leq \zeta\|\tilde{U} - U\| + C_\zeta|\tilde{U} - U|_H\end{aligned}$$

where $\zeta > 0$ is arbitrary. Then $G(\cdot)$ fulfills (g.ii) too.
Second Step : Positivity of the solution
Let us take the following semilinear system

$$\begin{aligned}\tfrac{dY}{dt} + AY &= \tilde{G}(Y) + F(t),\ 0 < t \leq T \\ Y(0) &= Y_0,\end{aligned}$$

where A, F and Y_0 are defined as previously, and where $\tilde{G}$ is defined by :

$$\tilde{G}(U) := \begin{pmatrix} \beta\nabla(u\nabla v) - q|u|u + k_2|v| \\ k_1 u \end{pmatrix}.$$

By theorem 1, we have the existence of local solution (u, v) on $[0, T_0']$, where $T_0' = T_0(U_0, F)$.
Let us define $u^+ = max(u, 0)$ and $u^- = max(-u, 0)$.
Multiply the first equation by $-u^-$ and integrate on space to get :

$$\frac{1}{2}\frac{d}{dt}\|u^-\|^2_{L^2(\Omega)} + a\|\nabla u^-\|^2_{L^2(\Omega)} + k_1\|u^-\|^2_{L^2(\Omega)} \leq \int_\Omega \beta u^- \nabla v \nabla u^- \\ \leq \|\nabla v\|_{L^\infty(\Omega)} \int_\Omega u^- \nabla u^-$$

for $0 < t \leq T_0'$.
Using Young inequality we get

$$\frac{1}{2}\frac{d}{dt}\|u^-\|^2_{L^2} + a\|\nabla u^-\|^2_{L^2} + \leq C_\varepsilon \|\nabla v\|^2_{L^\infty}\|u^-\|^2_{L^2} + \varepsilon\|\nabla u^-\|^2_{L^2}$$

with $\varepsilon > 0$ as small as we need and $C_\varepsilon > 0$.
Taking $\varepsilon = \frac{a}{2}$ we get

$$\frac{d}{dt}\|u^-\|^2_{L^2(\Omega)} \leq C_a\|\nabla v\|^2_{L^\infty(\Omega)}\|u^-\|^2_{L^2(\Omega)} \\ \leq C_a\|v\|^2_{H^{2+\varepsilon_0}(\Omega)}\|u^-\|^2_{L^2(\Omega)}$$

for some positive constant C_a.
Since $v \in L^2(0, T_0; H^{2+\varepsilon_0}(\Omega))$ and $\|u_0^-\|^2_{L^2} = 0$ then by Gronwall lemma u remains positive on $[0, T_0]$. By classical results of linear parabolic equations v is positive too on $[0, T_0]$, which finish the proof.

□

6.3.2 Global existence.

This section is devoted to prove the following result :

Theorem 6.2. *Let $\varepsilon_0 > 0$. Let $u_0 \in L^2(\Omega), v_0 \in H^{1+\varepsilon_0}(\Omega)$ and $f \in L^2(0, T, H^1_+(\Omega)) \cap L^\infty(\Omega_T)$ be positive functions, then there exists a unique global and positive solution (u, v) for the system (P_h) such that*

$$u \in H^1(0, T; (H^1(\Omega))') \cap C([0, T]; L^2(\Omega)) \cap L^2(0, T; H^1(\Omega))$$
$$v \in H^1(0, T; H^{\varepsilon_0}(\Omega)) \cap C([0, T]; H^{1+\varepsilon_0}(\Omega)) \cap L^2(0, T; H^{2+\varepsilon_0}_\nu(\Omega))$$

Proof. We proceed in several steps but first let us define the following functions :

$$\phi_c(t) = (\|u\|_{L^1(\Omega)} + (1+c)\|v\|_{L^1(\Omega)}), c \geq 0.$$

First Step
Let $f_{max} \geq 0$ such that $f(t,x) \leq f_{max}$ in Ω_T.
For each $\alpha > 0$ there exists $C_\alpha > 0$ and $C'_\alpha > 0$ such that

$$\phi_\alpha(t) \leq e^{-C_\alpha t}\phi_\alpha(0) + C'_\alpha \tag{6.3.2}$$

with $C'_\alpha = |\Omega|\frac{(1+\alpha)f_{max}+\alpha^2(k_1+\frac{k_2}{1+\alpha})^2\frac{1}{4q}}{C_\alpha}$
For this, we sum the first equation of (P_h) with the second equation multiplied by $(1+\alpha)$ and integrate on space. We obtain

$$\frac{d}{dt}\phi_\alpha(t) = -\alpha k_2\int_\Omega v + \alpha k_1\int_\Omega u + (1+\alpha)\|f\|_{L^1(\Omega)} - q\int_\Omega u^2$$

that is

$$\frac{d}{dt}\phi_\alpha(t) = -\alpha k_2\int_\Omega v - \frac{\alpha k_2}{1+\alpha}\int_\Omega u + (1+\alpha)\|f\|_{L^1(\Omega)} + \int_\Omega(-qu^2 + \alpha k_1 u + \frac{\alpha k_2}{1+\alpha}u)$$

since u and v are positive we get

$$\frac{d}{dt}\phi_\alpha(t) \leq \frac{-\alpha k_2}{1+\alpha}\phi_\alpha(t) + (1+\alpha)\|f\|_{L^1(\Omega)} + \int_\Omega \alpha^2(k_1 + \frac{k_2}{1+\alpha})^2\frac{1}{4q}.$$

Solving the differential inequality we obtain that

$$\frac{d}{dt}\phi_\alpha(t) \leq e^{-C_\alpha t}\phi_\alpha(0) + C'_\alpha(1 - e^{-C_\alpha t}).$$

Second Step
We bound $\|v\|_{H^1(\Omega)}$ and $N^1_{log}(u) = \|(u+1)log(u+1)\|_{L^1(\Omega)}$ in order to use Biler's lemma (6.2.5) and to bound high order term in the third step.
Multiply the first equation of (P_h) by $log(u+1)$ and integrate in space we have

$$\begin{aligned}\frac{d}{dt}\int_\Omega\{(u+1)log(u+1) - u\} + 4a\int_\Omega \|\sqrt{u+1}\|^2 dx \\ = \beta\int_\Omega \frac{u}{u+1}\nabla u\nabla v d + \int_\Omega(-k_1 u - qu^2 + k_2 v)log(u+1)dx.\end{aligned}$$

By Stokes theorem we have

$$\int_\Omega \frac{u}{u+1}\nabla u\nabla v dx = \int_\Omega (log(u+1)-u)\Delta v dx \leq \frac{\varepsilon'}{2}\|\Delta v\|^2_{L^2(\Omega)} + \frac{1}{2\varepsilon'}\|u\|^2_{L^2(\Omega)}$$

and

$$(k_1 u + qu^2)log(u+1) \geq C((u+1)log(u+1) - u)$$

with $C \leq k_1$.
Hence if we denote $\Psi(t) = \|(u+1)log(u+1) - u\|_{L^1(\Omega)}$, we have

$$\frac{d}{dt}\Psi(t) + k_1\Psi(t) \leq \frac{\varepsilon'}{2}\|\Delta v\|^2_{L^2(\Omega)} + (\frac{k_2^2}{2\varepsilon} + \frac{\beta^2}{2\varepsilon'})\|u\|^2_{L^2(\Omega)} + \frac{\varepsilon}{2}\|v\|^2_{L^2(\Omega)}. \tag{6.3.3}$$

Multiplying the second equation respectively by v and Δv we obtain that

$$\frac{1}{2}\frac{d}{dt}\int_\Omega v^2 + d\int_\Omega |\nabla v|^2 dx + k_2\int_\Omega v^2 dx = k_1\int_\Omega uv dx + \int_\Omega vf dx$$

and

$$\frac{1}{2}\frac{d}{dt}\int_\Omega |\nabla v|^2 + d\int_\Omega |\Delta v|^2 dx + k_2\int_\Omega |\nabla v|^2 dx = k_1\int_\Omega u\Delta v dx + \int_\Omega f\Delta v dx.$$

It follows that

$$\begin{aligned}\frac{d}{dt}\|v\|^2_{H^1(\Omega)} + d\|\Delta v\|^2_{L^2(\Omega)} + k_2\|v\|^2_{H^1(\Omega)} \\ \leq k_1^2(\frac{1}{k_2} + \frac{1}{d})\|u\|^2_{L^2(\Omega)} + (\frac{1}{k_2} + \frac{1}{d})\|f\|^2_{L^2(\Omega)}.\end{aligned} \tag{6.3.4}$$

Notice that

$$\frac{d}{dt}\phi_0 + q\|u\|^2_{L^2(\Omega)} = \|f\|_{L^1(\Omega)} \tag{6.3.5}$$

where $\phi_0(t) = \|u\|_{L^1(\Omega)} + \|v\|_{L^1(\Omega)}$.
Then summing (6.3.3), (6.3.4) and (6.3.5) multiplied by γ and taking $\varepsilon = \frac{k_2}{2}$, $\varepsilon' = \frac{d}{2}$ we obtain for $t \geq t_0$

$$\begin{aligned}\frac{d}{dt}g(t) + \sigma g(t) &\leq C\|f\|^2_{L^2(\Omega)} + \gamma(\|f\|_{L^1(\Omega)} + \phi_\alpha(t)) \\ &\leq C_p\end{aligned} \tag{6.3.6}$$

where $g(t) = \gamma\phi_0(t) + \Psi(t) + \|v\|^2_{H^1(\Omega)}$ and C_p is some positive constant depending on $f_{max}, a, d, q, k_1, k_2, |\Omega|$ and β.
We choose t_0 big enough to have $\phi_\alpha(t) \leq 2C'_\alpha$, for $t \geq t_0$ (see inequality (6.3.2)).
Taking into account that ϕ_α is bounded, we get

$$g(t) \leq e^{-\sigma(t-t_0)}g(t_0) + C, \text{ for } t \geq t_0. \tag{6.3.7}$$

Third Step.
We bound $\|u\|_{H^1(\Omega)}$ and $\|v\|_{H^3(\Omega)}$ in order to get global existence.
Take $t_1 < T_0$ such that $v(t_1) \in H^{2+\varepsilon_0}_\nu(\Omega)$ and $u(t_1) \in H^1(\Omega)$. Since $F(\cdot)$ is in $L^2(t_1, T, H^1(\Omega))$, we can reuse theorem 6.1 and prove that

$$u \in H^1(t_1, T_0; L^2(\Omega)) \cap C([t_1, T_0]; H^1(\Omega)) \cap L^2(t_1, T_0, H^2_\nu(\Omega))$$
$$v \in H^1(t_1, T_0; H^1(\Omega)) \cap C([t_1, T_0]; H^2_\nu(\Omega)) \cap L^2(t_1, T_0, H^3_\nu(\Omega))$$

then multiplying the first equation by u and integrate in space we get

$$\frac{1}{2}\frac{d}{dt}\|u\|^2_{L^2(\Omega)} + a\|\nabla u\|^2_{L^2(\Omega)} + k_1\|u\|^2_{L^2(\Omega)} + q\|u\|^3_{L^3(\Omega)} = \int_\Omega uv dx + \frac{\beta}{2}\int_\Omega u^2\Delta v$$

Using Young inequality we deduce

$$\int_\Omega u^2\Delta v \leq \eta\|\Delta v\|^3_{L^3(\Omega)} + \eta^{1/2}\|u\|^3_{L^3(\Omega)}$$

and using interpolation inequality we get

$$\|\Delta v\|_{L^3(\Omega)} \leq C\|v\|_{H^3(\Omega)}\|v\|_{H^2(\Omega)} \leq C\|v\|^{2/3}_{H^3(\Omega)}\|v\|^{1/3}_{H^1(\Omega)}.$$

Then using the Biler's lemma (6.2.5) we obtain

$$\begin{aligned}&\frac{1}{2}\frac{d}{dt}\|u\|^2_{L^2(\Omega)} + a\|\nabla u\|^2_{L^2(\Omega)} + k_1\|u\|^2_{L^2(\Omega)} + q\|u\|^3_{L^3(\Omega)} \\ &\leq \eta(\|v\|^2_{H^3(\Omega)} + \|u\|^2_{H^1(\Omega)}) \\ &\qquad + p(N^1_{log}(u) + \|u\|_{L^1(\Omega)} + \|v\|_{H^1(\Omega)} + 1/\eta). \end{aligned}\tag{6.3.8}$$

More, for $t_1 \leq t \leq T_0$, v is the solution of

$$\frac{d}{dt}v + A_2 v = k_1 u + f$$
$$v(t_1) \in H^1(\Omega)$$

in the space $H^1(\Omega)$.
As $D(A^{\frac{3}{2}}) = H^3_\nu(\Omega) \subset H^3(\Omega)$, we get

$$\frac{d}{dt}\|A_2 v\|^2_{L^2(\Omega)} + \delta\|v\|^2_{H^3(\Omega)} \leq C(\|u\|^2_{H^1(\Omega)} + \|f\|^2_{H^1(\Omega)}). \tag{6.3.9}$$

Hence, if $c_0 = min(a, k_1)$, by summing two inequalities (6.3.8) and (6.3.9) we have

$$\begin{aligned}
&\frac{d}{dt}(\|u\|^2_{L^2(\Omega)} + \alpha'\|A_2 v\|^2_{L^2(\Omega)}) + 2c_0\|u\|^2_{H^1(\Omega)} + \alpha'\delta\|v\|^2_{H^3(\Omega)} \\
&\leq \{2\eta + \alpha' C\}\|u\|^2_{H^1(\Omega)} + 2\eta\|v\|^2_{H^3(\Omega)} \\
&\qquad + p(f_{max} + N^1_{log}(u) + \|u\|_{L^1(\Omega)} + \|v\|_{H^1(\Omega)} + 1/\eta).
\end{aligned}$$

Taking $\eta = \frac{\alpha'\delta}{4}$ with α' sufficiently small we obtain :

$$\begin{aligned}
&\frac{d}{dt}(\|u\|^2_{L^2(\Omega)} + \alpha'\|A_2 v\|^2_{L^2(\Omega)}) + c_0\|u\|^2_{H^1(\Omega)} + \alpha'\frac{\delta}{2}\|v\|^2_{H^3(\Omega)} \\
&\qquad \leq p(f + N^1_{log}(u) + \|u\|_{L^1(\Omega)} + \|v\|_{H^1(\Omega)} + 1/\eta),
\end{aligned}$$

which means that there exists $\sigma' > 0$ such that

$$\begin{aligned}
&\frac{d}{dt}(\|u\|^2_{L^2(\Omega)} + \alpha'\|A_2 v\|^2_{L^2(\Omega)}) + \sigma'(\|u\|^2_{H^1(\Omega)} + \alpha'\|v\|^2_{H^3(\Omega)}) \\
&\qquad \leq p(f + N^1_{log}(u) + \|u\|_{L^1(\Omega)} + \|v\|_{H^1(\Omega)} + 1/\eta). \quad (6.3.10)
\end{aligned}$$

Integrating this in time and using (6.3.7), we get for all $t \geq t_1$

$$\|v\|^2_{H^2(\Omega)} + \|u\|^2_{L^2(\Omega)} \leq Ce^{-\sigma(t-t_1)}(\|v(t_1)\|^2_{H^2(\Omega)} + \|u(t_1)\|^2_{L^2(\Omega)}) + C. \tag{6.3.11}$$

Hence from (6.3.10) and (6.3.11)

$$\int_{t_1}^{t}(\|v\|^2_{H^3(\Omega)} + \|u\|^2_{H^1(\Omega)}) \leq C((t - t_1) + \|u(t_1)\|^2_{L^2(\Omega)} + \|v(t_1)\|^2_{H^2(\Omega)}).$$

This proves that the local solution can be extended to a global solution. □

6.3.3 Exponential attractor.

Let us suppose that f is a fixed positive constant.
With minor changes due to our different problem (P_h),we prove like in [44] the following theorems.

Theorem 6.3. *If $U_0 = (u_0, v_0) \in H^1(\Omega) \times H^2_\nu(\Omega)$ then there exists a unique local solution to* (6.3.1) *on* $[0, T_0]$ *with*

$$u \in H^1(0, T_0; L^2(\Omega)) \cap C([0, T_0]; H^1(\Omega)) \cap L^2(0, T_0, H^2_\nu(\Omega))$$
$$v \in H^1(0, T_0; H^1(\Omega)) \cap C([0, T_0]; H^2_\nu(\Omega)) \cap L^2(0, T_0, H^3_\nu(\Omega))$$

Theorem 6.4. *If $U_0 = (u_0, v_0) \in H^2_\nu(\Omega) \times H^3_\nu(\Omega)$ then there exists a unique local solution to* (6.3.1) *on* $[0, T_0]$ *with*

$$u \in H^1(0, T(U_0); H^1(\Omega)) \cap C([0, T(U_0)]; H^2_\nu(\Omega)) \cap L^2(0, T(U_0), H^3_\nu(\Omega)),$$
$$v \in H^1(0, T(U_0); H^2_\nu(\Omega)) \cap C([0, T(U_0)]; H^3_\nu(\Omega)) \cap L^2(0, T(U_0), D(A_2^2)(\Omega)).$$

In the sequel we prove the following

Proposition 6.2. *If $u_0 \in H^2_\nu(\Omega)$ and $v_0 \in H^3_\nu(\Omega)$ are positive then*

$$\|u(t)\|_{H^2(\Omega)} + \|v(t)\|_{H^3(\Omega)} \leq p(\|u_0\|_{H^2(\Omega)} + \|v_0\|_{H^3(\Omega)} + f)$$

for $0 < t < \infty$.

Proof. Let $u_0 \in H^2_\nu(\Omega)$ and $v_0 \in H^3_\nu(\Omega)$ be positive functions.
Using (6.3.11) we have

$$\begin{aligned}(\|u\|^2_{L^2(\Omega)} + \|v\|^2_{H^2(\Omega)}) \leq e^{-\sigma t}(\|u_0\|^2_{L^2(\Omega)} + \|v_0\|^2_{H^2(\Omega)}) \\ + p(f + N^1_{log}(u_0) + \|v_0\|_{H^1(\Omega)}) \quad (6.3.12)\end{aligned}$$

Multiplying the first equation of (P_h) by Δu and integrating over Ω, gives as in [44]

$$\begin{aligned}\frac{1}{2}\frac{d}{dt}\|\nabla u\|^2_{L^2(\Omega)} + a\|\Delta u\|^2_{L^2(\Omega)} + k_1\|\nabla u\|^2_{L^2(\Omega)} \leq \beta(\varepsilon\|\Delta u\|^2_{L^2(\Omega)} \quad (6.3.13)\\ + \frac{1}{2\varepsilon}\int_\Omega |\nabla u|^2|\nabla v|^2 + \frac{1}{2\varepsilon}\int_\Omega |u|^2|\Delta v|^2)\\ + \varepsilon'\|\nabla u\|^2_{L^2(\Omega)} + C_{\varepsilon'}\|\nabla v\|^2_{L^2(\Omega)},\end{aligned}$$

where $\varepsilon, \varepsilon'$ and $C_{\varepsilon'}$ are positive constants derived from Young inequality.
We obtain then

$$\begin{aligned}&\frac{1}{2}\frac{d}{dt}\|\nabla u\|^2_{L^2(\Omega)} + (a - \beta\varepsilon)\|\Delta u\|^2_{L^2(\Omega)} + k_1\|\nabla u\|^2_{L^2(\Omega)}\\ &\leq \frac{\beta}{2\varepsilon}(\int_\Omega |\nabla u|^2|\nabla v|^2 + \int_\Omega |u|^2|\Delta v|^2) + \varepsilon'\|\nabla u\|^2_{L^2(\Omega)} + C_{\varepsilon'}\|\nabla v\|^2_{L^2(\Omega)}\\ &\leq \frac{\beta}{2\varepsilon}(\eta\|\Delta u\|^2_{L^2(\Omega)} + p(\|u\|_{L^2(\Omega)} + \|v\|_{H^2(\Omega)} + \eta^{-1})) + \varepsilon'\|\nabla u\|^2_{L^2(\Omega)} + C_{\varepsilon'}\|\nabla v\|^2_{L^2(\Omega)}.\end{aligned}$$

Taking $\eta = \varepsilon^2, \varepsilon = \frac{a}{3\beta}$ leads to

$$\frac{d}{dt}\|\nabla u\|^2_{L^2(\Omega)} + a\|\Delta u\|^2_{L^2(\Omega)} + 2(k_1 - \varepsilon')\|\nabla u\|^2_{L^2(\Omega)} \leq \frac{\beta^2}{a} p(\|u\|_{L^2(\Omega)} + \|v\|_{H^2(\Omega)}) + C_{\varepsilon'}\|\nabla v\|^2_{L^2(\Omega)}. \quad (6.3.14)$$

Taking the second equation of (P_h) operated by Δ and choosing $\Delta^2 v$ as a test function and integrating, we have as in [44]

$$\frac{d}{dt}\|\nabla \Delta v\|^2_{L^2(\Omega)} + d\|\Delta^2 v\|^2_{L^2(\Omega)} + 2k_2\|\nabla \Delta v\|^2_{L^2(\Omega)} \leq \frac{k_1^2}{d}\|\Delta u\|^2_{L^2(\Omega)}. \quad (6.3.15)$$

We sum (6.3.15) multiplied by γ and (6.3.14). So,

$$\frac{d}{dt}(\|\nabla u\|^2_{L^2(\Omega)} + \gamma\|\nabla \Delta v\|^2_{L^2(\Omega)}) + \gamma d\|\Delta^2 v\|^2_{L^2(\Omega)} + (a - \frac{\gamma k_1^2}{d})\|\Delta u\|^2_{L^2(\Omega)}$$
$$+2(k_1 - \varepsilon')(\|\nabla u\|^2_{L^2(\Omega)} + \frac{k_2\gamma}{k_1 - \varepsilon'}\|\nabla \Delta v\|^2_{L^2}(\Omega)) \leq p(\|u\|_{L^2(\Omega)} + \|v\|_{H^2(\Omega)}).$$

Then for γ and ε'' small enough, there exists a positive constant σ' such that

$$\frac{d}{dt}(\|\nabla u\|^2_{L^2(\Omega)} + \gamma\|\nabla \Delta v\|^2_{L^2(\Omega)}) + \sigma''(\|\nabla u\|^2_{L^2(\Omega)} + \gamma\|\nabla \Delta v\|^2_{L^2(\Omega)}) \leq p(\|u\|_{L^2(\Omega)} + \|v\|_{H^2(\Omega)}). \quad (6.3.16)$$

So, we can find $\chi > 0$ such as (6.3.12) is valid when $\sigma = \chi$ and

$$(\|u\|^2_{H^1(\Omega)} + \|v\|^2_{H^3(\Omega)}) \leq e^{-\chi t}(\|u_0\|^2_{H^1(\Omega)} + \|v_0\|^2_{H^3(\Omega)}) + p(f + \|u_0\|_{L^2(\Omega)} + \|v_0\|_{H^2(\Omega)}) \quad (6.3.17)$$

and

$$\int_s^t (\|\Delta^2 v(s)\|^2_{L^2(\Omega)} + \|u(s)\|^2_{H^2(\Omega)})ds \leq C(\|v(s)\|^2_{H^3(\Omega)} + \|u(s)\|^2_{H^1(\Omega)}) + (t - s)p(f + \|u_0\|_{L^2(\Omega)} + \|v_0\|_{H^2(\Omega)}).$$

Finally, taking the first equation of (P_h) operated by ∇ and multiplied by $\nabla \Delta u$, gives like in [44]

$$\frac{1}{2}\frac{d}{dt}\|\Delta u\|^2_{L^2(\Omega)} + a\|\nabla \Delta u\|^2_{L^2(\Omega)} = \int_\Omega \nabla(\nabla . u \nabla v)\nabla \Delta u + k_1 \int_\Omega \nabla u . \nabla \Delta u + 2q \int_\Omega u \nabla u . \nabla \Delta u - k_2 \int_\Omega \nabla v . \nabla \Delta u, \quad (6.3.18)$$

that is

$$\frac{1}{2}\frac{d}{dt}\|\Delta u\|^2_{L^2(\Omega)} + a\|\nabla\Delta u\|^2_{L^2(\Omega)} \leq \frac{a}{2}\|\nabla\Delta u\|^2_{L^2(\Omega)} + C\int_\Omega |\nabla(\nabla.(u\nabla v)|^2 + C\int_\Omega |u\nabla u|^2 + \|\nabla v\|^2_{L^2(\Omega)}). \quad (6.3.19)$$

The terms $\int_\Omega |\nabla(\nabla.(u\nabla v)|^2 dx$ and $\int_\Omega |u\nabla u|^2$ of (6.3.19) can be bounded as in [40] (see the proof of proposition 4.1, step 5.),

$$\frac{1}{2}\frac{d}{dt}\|\Delta u\|^2_{L^2(\Omega)} + \frac{a}{2}\|\nabla\Delta u\|^2_{L^2(\Omega)} + \zeta\|\Delta u\|^2_{L^2(\Omega)} \leq \eta\|\nabla\Delta u\|^2_{L^2(\Omega)} + p(\|u\|_{H^1(\Omega)} + \|v\|_{H^3(\Omega)}). \quad (6.3.20)$$

Hence we can find a $\chi > 0$ such that (6.3.17) is valid and

$$\|u\|^2_{H^2(\Omega)} \leq e^{-\chi t}\|u_0\|^2_{H^2(\Omega)} + p(f + \|u_0\|_{H^1(\Omega)} + \|v_0\|_{H^3(\Omega)}). \quad (6.3.21)$$

and

$$\int_0^t \|u(s)\|^2_{H^3(\Omega)} ds \leq C(\|u_0\|^2_{H^2(\Omega)} + tp(f + \|u_0\|_{H^1(\Omega)} + \|v_0\|_{H^3(\Omega)}) \quad (6.3.22)$$

□

To prove the existence of an exponential attractor, we will use the following result :

Proposition 6.3. *Let $u_0 \in L^2(\Omega), v_0 \in H^{1+\varepsilon_0}(\Omega)$ be positive functions. Then there exists a continuous increasing function $p(\cdot)$, independent of u_0 and v_0 such that*

$$\|u\|^2_{H^2(\Omega)} + \|v\|^2_{H^3(\Omega)} \leq p(f + N^1_{log}(u_0) + \|v_0\|_{H^1(\Omega)} + t^{-1})$$

Proof. The proof follows the same lines as the proof of theorem 4.6 in [40] □

We can now prove the existence of an exponential attractor : Let $H = L^2(\Omega) \times H^1(\Omega)$ and consider the initial value problem

$$\begin{aligned} &\frac{dU}{dt} + AU = G(U) \\ &U(0) = U_0 \end{aligned} \quad (E)$$

in H, with A as in section 6.3.1 and $D(A) = H_n^2(\Omega) \times H_n^3(\Omega)$ and

$$G(U) := \begin{pmatrix} \beta\nabla(u\nabla v) - q|u|u + k_2 v \\ k_1 u + f \end{pmatrix}$$

Let $K = \{(u, v) \in L_+^2(\Omega) \times H_+^{1+\varepsilon_0}(\Omega)\}$ be the space of initial values and $U_0 \in K$.
We proved already the existence of a unique global solution $U = (u, v)$ continuous with respect to the initial condition U_0. We define then a continuous semigroup $\{S(t)_{t\geq 0}\}$ on K by $S(t)U_0 = U(t)$.
For a fixed $t > 0$, $S(t)$ maps K into $K \cap D(A)$.
Let B_r denotes a bounded ball of K with radius $r > 0$. We prove the following proposition :

Proposition 6.4. *There exists a constant $C > 0$ such that, for each $r > 0$ there exists t_r such that*

$$\sup_{t\geq t_r} \sup_{U_0\in B_r} \|S(t)U_0\|_{H^2(\Omega)\times H^3(\Omega)} \leq C$$

Proof. Fix $0 < r < \infty$. By t_r and C_r we shall denote some time and positive constant which depend on r but are uniform for $U_0 \in B_r$, respectively. By the previous proposition 6.3, there exist a time t_r and a constant C_r such that for $t \geq t_r$

$$(\|u(t)\|_{H^2(\Omega)}^2 + \|v(t)\|_{H^3(\Omega)}^2) \leq C_r \tag{6.3.23}$$

As in the proof of theorem 2 the desired estimate will be established step by step.
First we apply the inequality (6.3.2) to ϕ_α for $t \geq t_r$. Then

$$(\|u(t)\|_{L^1(\Omega)} + \|v(t)\|_{L^1(\Omega)}) \leq C(C_r e^{-C_\alpha(t-t_r)} + 1)$$

this shows that there exists another time denoted t_r such that for all $t \geq t_r$

$$(\|u(t)\|_{L^1(\Omega)} + \|v(t)\|_{L^1(\Omega)}) \leq C$$

with some universal positive constant C.
From (6.3.7) We get that

$$g(t) \leq C_r e^{-\sigma(t-t_r)} + C \text{ for } t \geq t_r.$$

Then it exists another time t_r and another universal positive constant C such that

$$\|v(t)\|_{H^1(\Omega)} \leq C \text{ for } t \geq t_r.$$

From (6.3.10) and (6.3.23) we deduce that

$$\|v(t)\|_{H^2(\Omega)} + \|u(t)\|_{L^2(\Omega)} \leq C_r e^{-\sigma(t-t_r)} + C \text{ for } t \geq t_r.$$

and that there exist another time t_r and another constant $C > 0$, such that

$$\|v(t)\|_{H^2(\Omega)} + \|u(t)\|_{L^2(\Omega)} \leq C \text{ for } t \geq t_r.$$

Finally using (6.3.21), (6.3.17) and repeat the argument we finish the proof. □

Let $\mathscr{B} = \{(u,v) \in H^2_\nu(\Omega) \times H^3_\nu(\Omega) \,/\, \|u\|_{H^2(\Omega)} + \|v\|_{H^3(\Omega)} \leq C\} \cap K$ with C the constant appearing in proposition 6.4. We proved that $\mathscr{B}$ is a compact absorbing set for $(\{S(t)\}_{t\geq 0}, K)$.
Hence by Temam([43]), there exist a global attractor $\mathscr{A} \subset K$, where $\mathscr{A}$ is a compact and connected subset of K.
Let $\mathscr{H} = \overline{\bigcup_{t\geq t_{\mathscr{B}}} S(t)\mathscr{B}}$ where $t_{\mathscr{B}}$ is such that $S(t)\mathscr{B} \subset \mathscr{B}$.
$\mathscr{H}$ is a compact set of K with $\mathscr{A} \subset \mathscr{H} \subset K$. Since $\mathscr{H}$ is absorbing and positively invariant for $\{S(t)_{t\geq 0}\}$ we need to apply theorem 2.1 of [40] (for a proof see theorem 3.1 [42]) to the dynamical system $(\{S(t)\}_{t\geq 0}, \mathscr{H})$ to get the following theorem

Theorem 6.5. *There exists an exponential attractor $\mathscr{M}$ of the dynamical system $(\{S(t)\}_{t\geq 0}, \mathscr{H})$ in H*

Proof. Since the forcing term f is constant and the reaction coupling in the first equation of (E) is linear in $U : k_2 v$, we apply the theorem bellow and the proof is the same as provided in [40].

Theorem. *(see [44] and [42])*
Let $\Gamma(t, U_0) = S(t)U_0$ be a mapping from $[0,T] \times \mathscr{H}$ into $\mathscr{H}$.
If G satisfies

$$\|G(U) - G(V)\| \leq \|A^{\frac{1}{2}}(U - V)\|, U, V \in \mathscr{H} \qquad (C_1)$$

and Γ is such that

$$\|\Gamma(t,U_0) - \Gamma(s,V_0)\| \leq C_T(|t-s| + \|U_0 - V_0\|_H, t, s \in [0,T], U_0, V_0 \in \mathscr{H} \quad (C_2)$$

for each $T > 0$
then there is an exponential attractor $\mathscr{M}$ for $(\{S(t)\}, \mathscr{H})$.

□

6.4 Case $h(u) = u(M-u)$.

Let M be a positive constant and consider a continuous function $\tilde{h}$ of h such as

$$\begin{cases} \tilde{h}(u) = u(M-u) \text{ if } 0 \leq u \leq M, \\ \tilde{h}(u) = 0 \text{ otherwise.} \end{cases} \tag{6.4.1}$$

If $\varepsilon_0 > 0$ and $f \in L^2(0,T;H^{\varepsilon_0}(\Omega))$ positive function, we prove, as previous, that it exists a unique local and positive solution (u,v) of (P_h) with $h = \tilde{h}$. We have the following result :

Proposition 6.5. *Let $\varepsilon_0 > 0$ and $f \in L^2(0,T;H^1(\Omega)) \cap L^\infty(\Omega_T)$ a positive function. For each positive $(u_0,v_0) \in L^2(\Omega) \times H^{1+\varepsilon_0}(\Omega)$ there exists a unique positive solution for (P_h) with $h(\cdot) = \tilde{h}(\cdot)$ and*

$$u_{\tilde{h}} \in H^1(0,T_0;(H^1(\Omega))') \cap C([0,T_0];L^2(\Omega)) \cap L^2(0,T_0;H^1(\Omega))$$
$$v_{\tilde{h}} \in H^1(0,T_0;H^{\varepsilon_0}(\Omega)) \cap C([0,T_0];H^{1+\varepsilon_0}(\Omega)) \cap L^2(0,T_0;H^{2+\varepsilon_0}_\nu(\Omega))$$

Proof. The proof is essentially the same as in section 6.3.2. □

Moreover we can prove that it exists M_0 such that :

Lemma 6.1. *For any $M \geq M_0$, let $M' = \frac{qM^2+k_1M}{k_2}$. If for a.e $x \in \Omega$ we have*

$$0 \leq u_0(x) \leq M \qquad\qquad 0 \leq v_0(x) \leq M',$$

then

$$0 \leq u(t,x) \leq M \qquad\qquad 0 \leq v(t,x) \leq M'$$

for a.e $(t,x) \in \Omega_T$.

Proof. let $\tilde{u} = M - u$ and $\tilde{v} = M' - v$. We get :

$$\tilde{u}_t = a\Delta\tilde{u} - \beta div(\tilde{h}(\tilde{u})\nabla\tilde{v}) - (2qM + k_1)\tilde{u} + q\tilde{u}^2 + k_2\tilde{v} + qM^2 + k_1M - k_2M'$$
$$\tilde{v}_t = d\Delta\tilde{v} - k_2\tilde{v} + k_1\tilde{u} + k_2M' - k_1M - f$$

Let $M_0 = (\frac{\|f\|_{L^\infty(\Omega_T)}}{q})^{\frac{1}{2}}$, $M \geq M_0$ and $M' = \frac{qM^2+k_1M}{k_2}$ then we have

$$qM^2 + k_1M - k_2M' = 0$$

and

$$k_2M' - k_1M - f \geq 0.$$

Multiply the first equation by $-\tilde{u}^-$ and the second by $-\tilde{v}^-$ and integrate in space. Using Young inequality we have

$$\frac{d}{dt}\|\tilde{u}^-\|^2_{L^2(\Omega)} \leq C\left(\int_\Omega -\tilde{u}^2\tilde{u}^- + \|\tilde{u}^-\|^2_{L^2(\Omega)} + \int_\Omega(-\tilde{v}^+\tilde{u}^- + \tilde{v}^-\tilde{u}^-\right)$$

and

$$\frac{d}{dt}\|\tilde{v}^-\|^2_{L^2(\Omega)} \leq C\left(\|\tilde{v}^-\|^2_{L^2(\Omega)} + \int_\Omega(-\tilde{v}^-\tilde{u}^+ + \tilde{v}^-\tilde{u}^-)\right).$$

Taking the sum of the two previous inequalities and since $q\tilde{u}^2(-\tilde{u}^-) \leq 0$, $-\tilde{u}^-\tilde{v}^+ \leq 0$ and $-\tilde{v}^-\tilde{u}^+ \leq 0$ we deduce

$$\frac{d}{dt}(\|\tilde{u}^-\|^2_{L^2(\Omega)} + \|\tilde{v}^-\|^2_{L^2(\Omega)}) \leq C(\|\tilde{u}^-\|^2_{L^2(\Omega)} + \|\tilde{v}^-\|^2_{L^2(\Omega)})$$

for some positive constant C. By Gronwall lemma we get

$$\|\tilde{u}^-\|^2_{L^2(\Omega)} + \|\tilde{v}^-\|^2_{L^2(\Omega)} = 0.$$

□

Remark. *From proposition 6.5 and lemma 6.1, $(u_{\tilde{h}}, v_{\tilde{h}})$ is a solution of (P_h) with $h(u) = u(M-u)$. The uniqueness of the solution is obtained in the following theorem.*

Theorem 6.6. *Let $h(u) = u(M-u)$. Let $f \in L^\infty(\Omega_T) \cap L^2(0,T;H^1(\Omega))$ be a positive function. Let $M \geq (\frac{(\|f\|_{L^\infty(\Omega_T)})}{q})^{\frac{1}{2}}$. Let $(u_0, v_0) \in L^2(\Omega) \times H^{1+\varepsilon_0}(\Omega)$ such that $0 \leq u_0 \leq M$ and $0 \leq v_0 \leq M'$ with $M' = \frac{qM^2+k_1M}{k_2}$ then there exists a unique global solution for (P_h) which is positive and such that*

$$u \in L^\infty(\Omega_T) \cap H^1(0,T;(H^1(\Omega))') \cap C([0,T];L^2(\Omega)) \cap L^2(0,T;H^1(\Omega))$$
$$v \in H^1(0,T;H^{\varepsilon_0}(\Omega)) \cap C([0,T];H^{1+\varepsilon_0}(\Omega)) \cap L^2(0,T;H^{2+\varepsilon_0}(\Omega))$$

and

$$0 \leq u \leq M \qquad\qquad 0 \leq v \leq M'$$

Proof. Let $0 \leq u_0 \leq M$ and $0 \leq v_0 \leq M'$. Suppose that there exists another solution (u, v). Then $\bar{u} = u_{\tilde{h}} - u$ and $\bar{v} = v_{\tilde{h}} - v$ verify

$$\begin{cases} \bar{u}_t = a\Delta\bar{u} - \beta \mathrm{div}\left(\tilde{h}(u_{\tilde{h}})\nabla v_{\tilde{h}} - h(u)\nabla v\right) - k_1\bar{u} - q(u + u_{\tilde{h}})\bar{u} + k_2\bar{v}, \\ \bar{v}_t = d\Delta\bar{v} - k_2\bar{v} + k_1\bar{u} \ \textit{in}\ \Omega_T. \\ \bar{u}_0 = \bar{v}_0 = 0 \in \Omega, \\ \nabla\bar{u}\cdot\nu = \nabla\bar{v}\cdot\nu = 0 \ \textit{on}\ \Sigma_T. \end{cases}$$

Multiplying the first equation with $\bar{u}$ and integrating leads to

$$\frac{1}{2}\frac{d}{dt}\|\bar{u}\|^2_{L^2(\Omega)} + a\|\nabla\bar{u}\|^2_{L^2(\Omega)} \leq C\left(\|\bar{u}\|^2_{L^2(\Omega)} + \|\bar{v}\|^2_{L^2(\Omega)}\right) + \int_\Omega \left(\tilde{h}(u_{\tilde{h}})\nabla v_{\tilde{h}} - h(u)\nabla v\right)\nabla\bar{u}. \quad (6.4.2)$$

Or

$$\int_\Omega \left(\tilde{h}(u_{\tilde{h}})\nabla v_{\tilde{h}} - h(u)\nabla v\right)\nabla\bar{u} \leq \int_\Omega \left(\tilde{h}(u_{\tilde{h}})\nabla v_{\tilde{h}} - \tilde{h}(u_{\tilde{h}})\nabla v\right)\nabla\bar{u} + \int_\Omega \left(\tilde{h}(u_{\tilde{h}})\nabla v - h(u)\nabla v\right)\nabla\bar{u}.$$

Since u and $u_{\tilde{h}}$ are in $L^\infty(\Omega_T)$ then

$$\int_\Omega \left(\tilde{h}(u_{\tilde{h}})\nabla v_{\tilde{h}} - \tilde{h}(u_{\tilde{h}})\nabla v\right)\nabla\bar{u} = \int_\Omega \left(\tilde{h}(u_{\tilde{h}})\nabla\bar{v}\right)\nabla\bar{u} \leq \frac{\varepsilon}{2}\|\nabla\bar{u}\|^2_{L^2(\Omega)} + C_\varepsilon\|\nabla\bar{v}\|^2_{L^2(\Omega)}$$

and

$$\int_\Omega \left(\tilde{h}(u_{\tilde{h}})\nabla v - h(u)\nabla v\right)\nabla\bar{u} = \int_\Omega \left(\tilde{h}(u_{\tilde{h}}) - h(u)\right)\nabla v\nabla\bar{u}$$
$$\leq \|u + u_{\tilde{h}}\|_{L^\infty(\Omega)}\int_\Omega \nabla v\nabla\bar{u}\bar{u} \leq \frac{\varepsilon}{2}\|\nabla\bar{u}\|^2_{L^2(\Omega)} + C_\varepsilon\|\nabla v\|^2_{L^\infty(\Omega)}\|\bar{u}\|^2_{L^2(\Omega)}.$$

Hence, choosing $\varepsilon = \frac{a}{2}$ and inequality (6.4.2) becomes

$$\frac{1}{2}\frac{d}{dt}\|\bar{u}\|^2_{L^2(\Omega)} + (\frac{a}{2})\|\nabla\bar{u}\|^2_{L^2(\Omega)} \leq C(1 + \|\nabla v\|^2_{L^\infty(\Omega)})\|\bar{u}\|^2_{L^2(\Omega)} + C'\|\bar{v}\|^2_{H^1(\Omega)} \quad (6.4.3)$$

with C and C' striclty positive constant.
Multiplying the second equation by $\bar{v}$ we obtain

$$\frac{1}{2}\frac{d}{dt}\|\bar{v}\|^2_{L^2(\Omega)}+d\|\nabla\bar{v}\|^2_{L^2(\Omega)}+k_2\|\bar{v}\|^2_{L^2(\Omega)} \leq C\left(\|\bar{u}\|^2_{L^2(\Omega)}+\|\bar{v}\|^2_{L^2(\Omega)}\right). \quad (6.4.4)$$

Taking the sum of (6.4) and (6.4.3) multiplied by γ sufficiently small such that $min(a, k_2) > \gamma C'$ we obtain

$$\frac{1}{2}\frac{d}{dt}\left(\|\bar{v}\|^2_{L^2(\Omega)}+\gamma\|\bar{u}\|^2_{L^2(\Omega)}\right) \leq C_\gamma(1+\|\nabla v\|^2_{L^\infty(\Omega)})\left(\|\bar{v}\|^2_{L^2(\Omega)}+\gamma\|\bar{u}\|^2_{L^2(\Omega)}\right).$$

We apply Gronwall lemma to end the proof. □

6.5 Case $N = 3$.

In order to prove the global existence of a solution of system (P_h), we supposed in the previous sections that Ω has dimension 2 and the initial condition $(u_0, v_0) \in L^\infty(\Omega) \times H^{1+\varepsilon_0}(\Omega)$ positive verifying some bounds. These conditions are so restrictive for a model of soil organic carbon.
Here we prove that if $h = \tilde{h}$ defined by (6.4.1) then (P_h) has a global positive solution when $dim(\Omega) = 3$ and for less regularity for both, initial data $(u_0, v_0) \in (L^2(\Omega))^2$ and forcing term $f \in L^2(0, T; L^2(\Omega))$ positive functions. Furthermore, if $(u_0, v_0) \in (L^\infty(\Omega))^2$ and $f \in L^\infty(\Omega_T)$ all positive, then the solution is unique.
We use the following setting :

$$\begin{aligned} V &= H^1(\Omega) \times H^1(\Omega), \\ H &= L^2(\Omega) \times L^2(\Omega), \\ V' &= (H^1(\Omega))' \times (H^1(\Omega))'. \end{aligned}$$

We let $\tilde{h}$ be a continuous function defined by (6.4.1). Let us consider the following system :

$$\begin{cases} \partial_t u - a\Delta u = -\beta div(\tilde{h}(\bar{u})\nabla v) - k_1 u - q|u|u + k_2 v \quad (t,x) \in \Omega_T, \\ \partial_t v - d\Delta v = -k_2 v + k_1 u + f \quad (t,x) \in \Omega_T, \\ \nabla u \cdot \eta(x) = \nabla v \cdot \eta(x) = 0 \quad (t,x) \in \Sigma_T, \\ u(0,\cdot) = u_0, v(0,\cdot) = v_0 \quad \text{in}\Omega, \end{cases} \quad \text{(P-S)}$$

where $(u_0, v_0) \in (L^2(\Omega))^2$ are positive functions.
Let $\bar{u} \in X = L^2(\Omega_T)$. We will apply Schauder fixed point theorem but let

us first gather some more information.

First Step : Invariant Ball
The existence of a unique local solution (u, v) follows by a direct application of theorem 6.1. First we prove the following result :

Proposition 6.6. *1- For any $\bar{u} \in X$, for all $(u_0, v_0) \in (L^2(\Omega))^2$ and $f \in L^2(0,T;L^2(\Omega))$ positive functions, there exists a unique and positive global solution (u, v) of* (P-S) *such that*

$$u \in H^1(0,T;(H^1(\Omega))') \cap C([0,T];L^2(\Omega)) \cap L^2(0,T;H^1(\Omega)),$$
$$v \in H^1(0,T;(H^1(\Omega))') \cap C([0,T];L^2(\Omega)) \cap L^2(0,T;H^1(\Omega)).$$

2- There exists a positive constant R such that for all $\bar{u} \in X$ we have

$$\|u\|_{L^2(\Omega_T)} \leq R. \tag{6.5.1}$$

Proof. By theorem 1, we prove the existence of a unique solution. To prove that it is global in time, we multiply the first equation by u and the second by v and use Young inequality to get

$$\frac{1}{2}\frac{d}{dt}\|u\|^2_{L^2(\Omega)} + a\|\nabla u\|^2_{L^2(\Omega)} + \int_\Omega \{k_1|u|^2 + q|u|^3\} \leq k_2 \int_\Omega \{u^2 + \frac{1}{4}v^2\}dx + \frac{M^2}{4}(\frac{M^2}{8a}\|\nabla v\|^2_{L^2(\Omega)} + \frac{a}{2}\frac{4}{M^2}\|\nabla u\|^2_{L^2(\Omega)}),$$

and

$$\frac{1}{2}\frac{d}{dt}\|v\|^2_{L^2(\Omega)} + d\|\nabla v\|^2_{L^2(\Omega)} + k_2\|v\|^2_{L^2(\Omega)} \leq \frac{k_2}{2}\|v\|^2_{L^2(\Omega)} + \int_\Omega \{\frac{k_1^2}{2k_2}u^2\}dx + \frac{k_2}{4}\|v\|^2_{L^2(\Omega)} + \frac{1}{k_2}\|f\|^2_{L^2(\Omega)}.$$

That is for any $\rho > 0$ we have

$$\frac{1}{2}\frac{d}{dt}(\rho\|u\|^2_{L^2(\Omega)} + \|v\|^2_{L^2(\Omega)}) + \frac{\rho a}{2}\|\nabla u\|^2_{L^2(\Omega)} + d\|\nabla v\|^2_{L^2(\Omega)} + \int_\Omega \{\rho k_1|u|^2 + \rho q|u|^3\} \leq \rho\frac{M^4}{32a}\|\nabla v\|^2_{L^2(\Omega)} + C\int_\Omega |u|^2 + \frac{1}{k_2}\|f\|^2_{L^2(\Omega)},$$

where $C = \frac{k_1^2}{2k_2} + k_2$. Let $\rho = \frac{16ad}{M^4}$. Rearranging the right hand side of the previous inequality gives

$$\frac{1}{2}\frac{d}{dt}(\rho\|u\|^2_{L^2} + \|v\|^2_{L^2(\Omega)}) + \frac{\rho a}{2}\|\nabla u\|^2_{L^2(\Omega)} + \frac{d}{2}\|\nabla v\|^2_{L^2(\Omega)} + \int_\Omega \{(\rho k_1 - C)|u|^2 + \rho q|u|^3\} \leq \frac{1}{k_2}\|f\|^2_{L^2(\Omega)}. \tag{6.5.2}$$

If $(\rho k_1 - C) \geq 0$ we finished the proof. If $(\rho k_1 - C) < 0$, by simple real analysis arguments, we prove that for any strictly positive $\lambda_0 < \rho q$ there exists $K_0 = -\frac{4}{27}\frac{(\rho k_1 - C)^3}{(\rho q - \lambda_0)^2}$ such that for all u

$$(\rho k_1 - C)|u|^2 + \rho q|u|^3 \geq \lambda_0|u|^3 - K_0.$$

Hence the inequality (6.5.2) becomes

$$\frac{1}{2}\frac{d}{dt}(\rho\|u\|^2_{L^2(\Omega)} + \|v\|^2_{L^2(\Omega)}) + \frac{\rho a}{2}\|\nabla u\|^2_{L^2(\Omega)} + \frac{d}{2}\|\nabla v\|^2_{L^2(\Omega)} + \int_\Omega \{\lambda_0|u|^3 - K_0\} \leq \frac{1}{k_2}\|f\|^2_{L^2(\Omega)}.$$

Hence v and u are in $L^\infty(0,T;L^2(\Omega)) \cap L^2(0,T,H^1(\Omega))$ and u_t and v_t are in $L^2(0,T;(H^1(\Omega))')$. This prove the first statement of the proposition . Furthermore we conclude from the previous estimates that there exists R independent of $\bar{u}$ such that

$$\|u\|_{L^2(\Omega_T)} \leq R.$$

□

We can then define the mapping $\Pi : X \to X$ such that $u = \Pi(\bar{u})$ is the unique solution of (P-S). From (6.5.1) the ball $B_R \subset X$ is invariant by Π.

Second Step : Compact Closure
We already proved that $\Pi(B_R) \subset \{u \in W, \|u\|_W \leq C\}$ where

$$W = \{u \in L^2(0,T;H^1(\Omega)), u_t \in L^2(0,T;(H^1(\Omega))')\}.$$

By the Aubin-Lions lemma we know that the embedding of W into $L^2(0,T,L^2(\Omega))$ is compact which ends the proof.
Third Step : Continuous Mapping
Let $z_n \in B_R$ such that $z_n \to z$ in $L^2(\Omega_T)$ strong and $u_n = \Pi(z_n)$ then $U_n = (u_n, v_n)$ satisfies the equation

$$\begin{cases} \partial_t u_n - a\Delta u_n = -\beta div(\tilde{h}(\bar{u_n})\nabla v_n) - k_1 u_n - q|u_n|u_n + k_2 v_n, (t,x) \in \Omega_T, \\ \partial_t v_n - d\Delta v_n = -k_2 v_n + k_1 u_n + f, (t,x) \in \Omega_T, \\ \nabla u_n \cdot \nu = \nabla v_n \cdot \nu = 0, \ (t,x) \in \Sigma_T, \\ u_n(0,\cdot) = u_0, v_n(0,\cdot) = v_0 \text{ in } \Omega, \end{cases} \tag{6.5.3}$$

we can prove that
u_n, v_n are bounded in $H^1(0,T;(H^1(\Omega))')\cap C([0,T];L^2(\Omega))\cap L^2(0,T;H^1(\Omega))$.
There exist a subsequence such that

$$\begin{cases} u_{n_k} \to u \text{ strongly in } L^2(\Omega_T) \text{ and } L^p(\Omega_T) \text{ for } p \leq \frac{10}{3}. \\ u_{n_k} \to u \text{ weakly in } L^2(0,T;H^1(\Omega)). \\ \partial_t u_{n_k} \to \partial_t u \text{ weakly in } L^2(0,T;(H^1(\Omega))'). \\ \nabla u_{n_k} \to \nabla u \text{ weakly in } L^2(0,T;L^2(\Omega)). \end{cases}$$

and same convergence for v_{n_k}.
Moreover, we can prove that v_{n_k} strongly converges in $L^2(0,T;H^1(\Omega))$ to v solution of the following problem

$$\begin{cases} \partial_t v - d\Delta v = -k_2 v + k_1 u + f \quad (t,x) \in \Omega_T, \\ \nabla v \cdot \nu = 0 \quad (t,x) \in \Sigma_T, \\ v_n(0,\cdot) = v_0 \quad \text{in}\Omega. \end{cases}$$

We pass to the limit in the first equation of (6.5.3). We obtain
the function $\tilde{h}$ is continuous then it exists a subsequence still denoted n_k such that

$$z_{n_k} \to z \text{ a.e in } \Omega_T$$

It exists a subsequence still denoted n_k such that

$$\begin{cases} \nabla v_{n_k} \to \nabla v \text{ a.e in } \Omega_T, \\ \tilde{h}(z_{n_k})\nabla v_{n_k} \text{ is bounded in } L^2(\Omega_T), \\ \tilde{h}(z_{n_k})\nabla v_{n_k} \to \tilde{h}(z)\nabla v \text{ a.e in } \Omega_T. \end{cases}$$

Hence by the dominated convergence theorem we get

$$\tilde{h}(z_{n_k})\nabla v_{n_k} \to \tilde{h}(z)\nabla v \text{ strongly in } L^2(\Omega_T).$$

We can then pass to the limit in the first equation and we get

$$\begin{cases} \partial_t u - a\Delta u = -\beta div(\tilde{h}(z)\nabla v) - k_1 u - q|u|u + k_2 v \quad (t,x) \in \Omega_T, \\ \partial_t v - d\Delta v = -k_2 v + k_1 u + f \quad (t,x) \in \Omega_T, \\ \nabla u \cdot \nu = \nabla v \cdot \nu = 0 \quad (t,x) \in \Sigma_T, \\ u(0,\cdot) = u_0, v(0,\cdot) = v_0 \quad \text{in } \Omega. \end{cases} \tag{6.5.4}$$

We proved that $u = \Pi(z)$.
By the uniqueness of the solution (u,v) of (6.5.4), we deduce that all the

sequence converges.
We showed that if $z_n \to z$ in $L^2(\Omega_T)$ strongly then

$$u_n = \Pi(z_n) \to \Pi(z) = u \text{ in } L^2(\Omega_T) \text{ strongly.}$$

We deduce that Π is a continuous mapping.
We can now apply the Schauder fixed point theorem to prove the existence statement of the following result :

Proposition 6.7. *Let $f \in L^2(0,T;L^2(\Omega))$. For each couple of positive functions $(u_0, v_0) \in L^2(\Omega)$ there exists a positive solution for the problem (P_h).*

To prove the positivity of the solution, we proceed as in section 6.4 : we multiply the first equation by $-u^-$ and the second by $-v^-$ and integrate in space to get :

$$\frac{1}{2}\frac{d}{dt}\|u^-\|^2_{L^2(\Omega)} + a\|\nabla u^-\|^2_{L^2(\Omega)} \leq \beta \int_\Omega h(u)\nabla v \nabla u^- + C(\|u^-\|^2_{L^2(\Omega)} + \|v^-\|^2_{L^2(\Omega)}),$$

and

$$\frac{1}{2}\frac{d}{dt}\|v^-\|^2_{L^2(\Omega)} + d\|\nabla v^-\|^2_{L^2(\Omega)} \leq C(\|u^-\|^2_{L^2(\Omega)} + \|v^-\|^2_{L^2(\Omega)}).$$

We observe from (6.4.1) that $\beta \int_\Omega h(u)\nabla v \nabla \tilde{u}^+ = 0$. We finish the proof using Gronwall lemma.
In the sequel we prove the following theorem :

Theorem 6.7. *Let $(u_0, v_0) \in L^\infty(\Omega)$ be positive functions. Let v_M such that $v_0(x) \leq v_M$ a.e in Ω and $f \in L^\infty(\Omega_T)$ be positive, then there exists $\alpha > 0$ such that*

$$0 \leq u(t,x) \leq Me^{\alpha t} \qquad 0 \leq v(t,x) \leq v_M e^{\alpha t}, \tag{6.5.5}$$

and the solution is unique.

Proof. Let $\tilde{u} = u - Me^{\alpha t}$ and $\tilde{v} = v - v_M e^{\alpha t}$ then we have

$$\tilde{u}_t = a\Delta\tilde{u} - \beta\nabla(h(u)\nabla\tilde{v}) - k_1\tilde{u} - q\tilde{u}^2 + k_2\tilde{v} - (\alpha M + k_1 M + 2quM - k_2 v_M)e^{\alpha t} - qM^2 e^{2\alpha t},$$

and

$$\tilde{v}_t = a\Delta\tilde{v} + k_1\tilde{u} + \{f + e^{\alpha t}((-k_2 - \alpha)v_M + k_1 M)\}.$$

Taking α big enough to have :

$$f + e^{\alpha t}((-k_2 - \alpha)v_M + k_1 M) \leq 0,$$

and

$$\alpha M + k_1 M + 2quM - k_2 v_M \geq 0,$$

then by multiplying the first equation by $\tilde{u}^+$ and the second by $\tilde{v}^+$ and proceeding as in section 6.4 we obtain

$$\frac{1}{2}\frac{d}{dt}\|\tilde{u}^+\|^2_{L^2(\Omega)} + a\|\nabla\tilde{u}^+\|^2_{L^2(\Omega)} \leq \beta\int_\Omega h(u)\nabla v\nabla\tilde{u}^+ + C(\|\tilde{u}^+\|^2_{L^2(\Omega)} + \|\tilde{v}^+\|^2_{L^2(\Omega)})$$

and

$$\frac{1}{2}\frac{d}{dt}\|\tilde{v}^+\|^2_{L^2(\Omega)} + d\|\nabla\tilde{v}^+\|^2_{L^2(\Omega)} \leq C(\|\tilde{u}^+\|^2_{L^2(\Omega)} + \|\tilde{v}^+\|^2_{L^2(\Omega)}).$$

Thanks to (6.4.1), $\beta\int_\Omega h(u)\nabla v\nabla\tilde{u}^+ = 0$. We finish the proof of (6.5.5) using Gronwall lemma.
A consequence of (6.5.5) is that (see theorems 9.2.1 and 9.2.2 of [79] or section 3 of [80])

$$v \in L^p(0, T, W^{2,p}(\Omega)) \text{ for all } p > 1. \tag{6.5.6}$$

We will use (6.5.6) to prove uniqueness.
Suppose that there exists two solutions (u_1, v_1) and (u_2, v_2). Then $\bar{u} = u_1 - u_2$ and $\bar{v} = v_1 - v_2$ verify

$$\begin{aligned}
&\bar{u}_t = a\Delta\bar{u} - \beta\nabla(h(u_1)\nabla v_1 - (h(u_2)\nabla v_2) - k_1\bar{u} - q{u_1}^2 + qu_2^2 + k_2\bar{v},\\
&\bar{v}_t = d\Delta\bar{v} - k_2\bar{v} + k_1\bar{u},\\
&\bar{u}_0 = \bar{v}_0 = 0 \ a.e \text{ in } \Omega.
\end{aligned} \tag{6.5.7}$$

Multiplying the first equation by $\bar{u}$, the second by $\bar{v}$ and integrating over Ω lead to

$$\begin{aligned}
\frac{1}{2}\frac{d}{dt}\|\bar{u}\|^2_{L^2(\Omega)} + a\|\nabla\bar{u}\|^2_{L^2(\Omega)} \leq \beta\int_\Omega |(h(u_1)\nabla v_1 - h(u_2)\nabla v_2)\nabla\bar{u}| \\
+ C(\|\bar{u}\|^2_{L^2(\Omega)} + \|\bar{v}\|^2_{L^2(\Omega)})
\end{aligned}$$

and

$$\frac{1}{2}\frac{d}{dt}\|\bar{v}\|^2_{L^2(\Omega)} + a\|\nabla\bar{v}\|^2_{L^2(\Omega)} = k_1\int_\Omega \bar{u}\bar{v}.$$

That is

$$\frac{1}{2}\frac{d}{dt}\|\bar{u}\|^2_{L^2(\Omega)} + a\|\nabla\bar{u}\|^2_{L^2(\Omega)} \leq \beta\int_\Omega |\{(h(u_1)-h(u_2))\nabla v_1 - h(u_2)(\nabla v_2 - \nabla v_1)\}\nabla\bar{u}| + C(\|\bar{u}\|^2_{L^2(\Omega)} + \|\bar{v}\|^2_{L^2(\Omega)}) \quad (6.5.8)$$

and

$$\frac{1}{2}\frac{d}{dt}\|\bar{v}\|^2_{L^2(\Omega)} + d\|\nabla\bar{v}\|^2_{L^2(\Omega)} + k_2\|\bar{v}\|^2_{L^2(\Omega)} \leq C(\|\bar{u}\|^2_{L^2} + \|\bar{v}\|^2_{L^2(\Omega)}) \quad (6.5.9)$$

Using (6.5.6) and Sobolev embeddings we deduce that for $p > 3$, $\nabla v_1 \in L^p(0,T;L^\infty(\Omega))$. Hence

$$\int_\Omega (h(u_1)-h(u_2))\nabla v_1\nabla\bar{u} \leq \|\nabla v_1\|_{L^\infty(\Omega)}\|\bar{u}\|_{L^2(\Omega)}\|\nabla\bar{u}\|_{L^2(\Omega)} \leq \varepsilon\|\nabla\bar{u}\|^2_{L^2(\Omega)} + C_\varepsilon\|\nabla v_1\|^2_{L^\infty(\Omega)}\|\bar{u}\|^2_{L^2(\Omega)} \quad (6.5.10)$$

and

$$\int_\Omega h(u_2)(\nabla v_2 - \nabla v_1)\nabla\bar{u} \leq \frac{M}{2}\|\nabla\bar{v}\|_{L^2(\Omega)}\|\nabla\bar{u}\|_{L^2(\Omega)} \leq \varepsilon\|\nabla\bar{u}\|^2_{L^2(\Omega)} + C_\varepsilon\|\nabla\bar{v}\|^2_{L^2(\Omega)} \quad (6.5.11)$$

Summing up (6.5.8) multiplied by a positive constant σ and (6.5.9) and using (6.5.10) and (6.5.11) gives the existence of a strictly positive constants c' and C such that :

$$\frac{1}{2}\frac{d}{dt}(\sigma\|\bar{u}\|^2_{L^2(\Omega)} + \|\bar{v}\|^2_{L^2(\Omega)}) + c'(\|\nabla\bar{u}\|^2_{L^{2(\Omega)}} + \|\nabla\bar{v}\|^2_{L^2(\Omega)}) \leq C(\sigma\|\bar{u}\|^2_{L^2(\Omega)} + \|\bar{v}\|^2_{L^2(\Omega)})$$

By Gronwall lemma we get that $u_1 = u_2$, $v_1 = v_2$ in $L^2(\Omega)$ and a.e.
Consequently $(u_1, v_1) = (u_2, v_2)$ in $L^2(0,T,H^1(\Omega)) \cap L^\infty(0,T,L^2(\Omega))$.
This ensure the uniqueness of the solution.

□

Chapitre 7

Microbial-scale heterogeneity with MOMOS.

7.1 Introduction.

Terrestrial ecosystems play a major role in regulating atmospheric greenhouse gas (CO_2, CH_4 and N_2O) concentrations ([50]). As CO_2 plays the greatest role in global radiative forcing, it is essential to have a thorough understanding of the global carbon cycle. Soils are one of the largest organic carbon (OC) compartments, estimated to be in the range of 1500-2400 Pg C (Ciais et al., 2013 [50]). Topsoils (0-30 cm) alone contain more carbon than the total vegetation living biomass and as much as the atmosphere (Ciais et al., 2013 [50]). Soil organic carbon (SOC) pools and turnover play key roles in building and sustaining soil fertility, which is a major food security component (Feller et al., 2012 [53]). Furthermore, it is now generally recognised that soil carbon plays a key role in all four classes (supporting, regulating, provisioning and cultural) of soil ecosystem services (Banwart et al., 2014 [81]).
With the exception of fluxes from land use change (such as deforestation and regrowth of vegetation), fluxes between terrestrial ecosystems and the atmosphere at global scale are currently unbalanced, creating a net terrestrial sink. Since 1960, the decadal mean of the annual terrestrial sink has been in the range 1.6 to 2.7 Pg C (Le Quéré et al., 2013 [51]), Global photosynthesis accounts for an annual uptake of nearly 123 Pg C (Beer et al., 2010 [82]) corresponding to nearly one seventh of the present atmospheric CO_2 stock. Autotrophic and heterotrophic respiration together provide a similar annual source of CO_2 but slightly less than gross photosynthesis. Soil respiration

(SR) alone has been estimated to be in the range 50-75 Pg C $yr^{-}1$ (Raich and Schlesinger, 1992 [75] ; Schimel 1995 [83]), with more than half being produced by heterotrophic respiration (Bond-Lamberty al., 2004 [84]).
Over several decades, soil scientists have increased their efforts to build accurate models of the role played by soils in ecosystem dynamics, both at local and global scales, based on the main regulating functions of nutrients, water quality and GHG emissions. Considerable research has been undertaken to understand soil carbon mineralization and the associated heterotrophic respiration. A large number of models have already been proposed. For instance, a recent review (Manzoni and Porporato, 2009 [8]) listed 250 different biogeochemical models that had been developed over the past eighty years and reported that the number of models had been increasing a rate of 6% per year since 1930. However, although there are a large number of models, these are based on a limited number of different conceptual approaches. Most mathematical representations use similar structures and formulations based on a compartmental model using the ordinary differential equation (ODE) formalism introduced 70 years ago (Hénin and Dupuis, 1945 [12]).In this formalism, soil C is considered to be the result of the equilibrium between inputs into and outputs out of the soil system and is modelled as a discrete set of different compartments (in most models from 2 to 5) with associated first-order ODEs describing their mass balance. The different compartments are often assumed to correspond to different chemical characteristics with different degrees of degradability (Hénin and Dupuis, 1945 [12] ; Manzoni and Porporato, 2009 [8]). The decomposition rates, which are applied to each pool, are governed by kinetic and stoichiometric laws and are mainly controlled by environmental conditions (soil moisture level, aeration and soil temperature). This formalism was used, for example, to build the Century model and its recent derivative Daycent (Del Grosso et al., 2005 [4]) as well as RothC which used field data from the longest-running agronomic experiment in the United Kingdom (Jenkinson and Rayner, 1977 [20]).
Most of these models were developed at field, plot or similar scale, but they have also been incorporated into more complex models (e.g. Lardy et al., 2011 [85]) or even global scale models such as the Community Land Model (Lawrence et al., 2011 [86]). Accurate predictions of the future climate and carbon cycle feedbacks, therefore, depend directly on the ability of the models to represent soil C decomposition and its sensitivity to environmental parameters (Kirschbaum 2006 [87] ; Hamdi et al ;, 2011, 2013 [6] [7]) and, more specifically, soil microbe activity (Kirschbaum 2006 [87] ; Schimel 2013 [88]).
Improving these models is still recognised as being of prime importance

(Treseder et al., 2011 [89] ; Adewopo et al., 2014 [90]), aiming primarily at providing a better representation of the microbial pool and its associated processes. Over the past decade, a number of improvements have been proposed, explicitly incorporating microbial content (Wieder et al., 2013 [56]), physiological mechanisms such as assimilation processes (Allison et al., 2010 [70] ; Xu et al.,2014 [91]) and priming effect (Fontaine et al., 2004 [26] ; Perveen et al., 2014[27]). In general, these approaches have been based on nonlinear ODE systems (Manzoni and Porporato, 2009 [8] ; Pansu et al., 2010 [23]) resolved only by numerical simulation and very rarely by formal mathematical analysis (Wang et al., 2014 [92] ; Hammoudi et al., 2015 [61]). The second major challenge was the representation of the spatial heterogeneity of small scale processes. The soil matrix is a complex, spatially heterogeneous system whose physical organisation has been studied for more than three decades (Tisdall and Oades, 1982 [93]). Research has shown the importance of taking account of the distribution, within the soil matrix, of microbial hot spots at micron scale (Young and Crawford, 2004 [94]). The authors (Young and Crawford, 2004 [94]) showed that improving the integration and representation of micron and submicron scale organisation revealed essential features of the soil. Moreover, a recent paper (Vogel et al., 2014 [38]) demonstrated, for the first time, that organic matter sequestration in soil occurs essentially only on small mineral particles with rough surfaces in organo-mineral clusters. The representation of this heterogeneity in soil models must be improved as a matter of urgency as this is the basis for determining the representation of the processes and feedback loops for the carbon and nitrogen dynamics. Attempts have been made either using a basic multi-agent system modelling approach (Masse et al., 2007 [9]) which is only suitable for numerical simulations, or using 3D, fractal and complex dimension models of the soil coupled with simple mechanistic representation of small scale processes (Monga et al., 2014 [71]). However, both approaches have limitations, partly owing to the computational power that is needed to represent the very large number of interactions and voxels, but mainly owing to the inability of nonlinear ODE to provide an adequate representation of the microbial physiology. The challenge is still to develop a framework that is as simple as possible while incorporating microbial contributions to C mineralization with a representation of the submicron heterogeneity and still give robust results at macro scale without using a complex 3D representation of the soil matrix.

This paper describes a means of meeting this challenge to provide a conceptual model framework that can be applied from microbial hotspot to global scale. A mechanistic soil carbon dynamics model with a nonlinear ODE sys-

tem was selected. This model emphasised the role of the microbial biomass and was then used as a basis for testing the minimum changes required to give an adequate representation of the submicron scale variability in the soil matrix. The main objective was to propose, and validate mathematically, a new conceptual mechanistic model, that was homogeneous at macro scale while being able to reproduce experimental observed soil heterogeneity at submicron scale. The options most commonly adopted by soil scientists and microbiologists were considered : 1) the diffusion process in the soil organic carbon substrate, and 2) the diffusion process plus a chemotactic model of soil microorganism mobility.

7.2 Material and Methods.

7.2.1 Mathematical representation of the models considered.

Decomposition model.

The MOMOS model (Modelling Organic changes by Micro-Organisms of Soil, Pansu et al., 2010 [23]) was selected because it focuses on the role of soil microbial biomass and has been proved to be mathematically valid providing a unique solution (Hammoudi et al., 2015 [61]). Moreover, if the carbon inputs are periodic, there is a unique periodic solution which is also a global attractor for any other solution of this periodic model.
As a first approach, a simplified theoretical model derived from MOMOS (Pansu et al., 2010 [23]) was considered. Instead of the five differential equations in the original model, this simplified theoretical model comprised only two differential equations, where the microbial biomass was u and the organic matter was v.
An additional simplifying hypothesis was made. As a first step, soil temperature, soil moisture, soil texture and organic input were considered to be isotropic and constant with time. As in the original MOMOS system, only the microbial compartment (u) was nonlinear. Hence, the reduced model can be expressed as :

$$\begin{aligned} \dot{u} &= -k_1 u - q u^2 + k_2 v \\ \dot{v} &= -k_2 v + k_1 u + f \end{aligned} \tag{7.2.1}$$

with the initial conditions (u_0, v_0) , where k_1 is the microbial mortality rate, k_2 is the soil carbon degradation rate,q is the metabolic quotient and f is the soil organic carbon input. It can be proven that the unique positive steady state (u_0^*, v_0^*), is stable (Hammoudi et al., 2015 [61]).

Decomposition model with simple diffusion.

As a second approach, a diffusion operator was added to this model. Many spatial models use diffusion operators to model mixing effects (Elzein and Balesdent, 1995 [16]). Compartmental models, such as MOMOS, that are widely used for modelling soil carbon turnover are spatially lumped. To consider the spatial effect on the carbon dynamics, Ω was defined as a bounded regular domain. A diffusion operator was introduced into the system of equations (7.2.1) to give the following system of partial differential equations :

$$\begin{aligned} u_t &= d_1 \Delta u - k_1 u - q u^2 + k_2 v \\ v_t &= d_2 \Delta v - k_2 v + k_1 u + f \ \ in \ \Omega_T \end{aligned} \tag{7.2.2}$$

with the initial conditions (u_0, v_0) and the no-flux boundary conditions

$$\nabla u.\eta = \nabla v.\eta = 0 \ \ on \ \partial\Sigma_T \tag{7.2.3}$$

Here d_1 and d_2 are the diffusion coefficients of microbes and soil organic carbon respectively, η is the normal outer vector to the boundary $\partial\Omega$ of a smooth and bounded two dimensional domain Ω.

Decomposition model with diffusion and chemotaxis.

Some bacteria and cells are able to direct their movement towards or away from chemicals (Abu-Ashour et al., 1994 [95]). This phenomenon is called chemotaxis. The chemotactic movement of bacteria to root exudates is well known to play an important role in rhizosphere colonisation (Soby and Bergman, 1983 [96] ; Futamata et al., 1998 [97] ; Somers et al., 2004 [98]). Field studies with tracers and laboratory experiments using soil columns were both used to demonstrate the effect of chemotaxis on microbial movements (e.g. Abu-Ashour et al., 1994 [95]).
The system (7.2.2) was modified to take account of chemotaxis, following the conventional Keller-Segel approach (Keller and Segel, 1970 [45]) using an advection-diffusion system. This comprised two parabolic equations in a smooth domain with no-flux boundary conditions. The advection term was controlled by the gradient of the chemo-attractant. Applying the same principles leads to the following parabolic system :

$$\begin{aligned} u_t &= d_1 \Delta u - \beta \nabla.(h(u) \nabla v) - k_1 u - q u^2 + k_2 v \\ v_t &= d_2 \Delta v - k_2 v + k_1 u + f \ \ in \ \Omega_T \end{aligned} \tag{7.2.4}$$

with initial conditions and no-flux boundary conditions (7.2.3). The parameter β is the chemotaxis sensitivity. As bacteria can release exoenzymes to avoid overcrowding, the function h can be selected to modulate the chemotaxis and limit overcrowding, as required. This new model was, therefore, a new variation of the Keller-Segel approach (Keller and Segel, 1970 [45]) with the reaction part modified to fit the MOMOS model.

7.2.2 Mathematical validation used for spatial heterogeneity analysis.

Although spatial heterogeneity can be verified visually in a numerical simulation, formal mathematical analysis is required to confirm its emergence and to provide a mathematical proof of the necessary conditions. For this purpose, the pattern formation theory that was introduced by Turing (1952) in his pioneering work in an attempt to explain morphogenesis was used. Turing (1952) suggested that spatial patterns (mathematically "non-constant equilibrium solutions") can be produced in reaction-diffusion systems under certain conditions. This theory has received more attention in recent decades and has been extensively investigated in many studies (e.g. Grindrod 1996 [37] ; Murray 2002, 2003 [35][36]), most of which concerned predator-prey systems (Shi et al., 2011 [99]). The mathematical criteria are based on matrices derived from equations and analysed using conditions on the determinant, trace and eigenvalues.

7.2.3 Parameterisation for numerical simulations.

A set of validated parameters derived from studies published (Pansu et al., 2010) was used to run numerical simulations to compare the outputs of the various models., The data used came from an Andean Páramo site (an example of an alpine tundra ecosystem) near Gavidia, Venezuela. This site is located in a glacial valley at 3400 m, near the upper limit of agriculture. The mean temperature is $8.9C$ with large daily fluctuations. Numerical simulations were obtained setting k_1, k_2, q, d_1, and d_2 to 0.4 day^{-1}, 0.6 day^{-1}, 0.075 day^{-1}, 10^{-3} surface-unit.day^{-1} and 10^{-4} surface-unit day^{-1} respectively.
As pattern geometries depend on the shape of the spatial domain (Murray, 2002[35]), two different forms of spatial domain were tested. The parameter f was set to 10^{-3} (mass-unit surface-unit^{-1} day^{-1}). Two different scalar functions were also tested to simulate overcrowding. The function h was set either to $h_1(x) = x$ which did not prevent any overcrowding, or to

$h_2(x) = x(u_{max} - x)$ which prevents overcrowding. The coefficient β was optimised to produce spatial heterogeneity, using the criteria established by Turing [34]. In the first case, β was set to 0.0393 surface-unit day^{-1} for both spatial domains and in the second case it was set to 0.15 surface-unit day^{-1}. Numerical simulations were performed using COMSOL Multiphysics® 5.0 (COMSOLAB, 2014 www.comsol.com).

7.3 Results.

7.3.1 Existence and conditions for the emergence of submicron-scale heterogeneity.

Firstly, the case with the simple diffusion model, equation system (7.2.2), was considered. As in Lotka-Volterra systems (Murray, 2002 [35]), also known as the predator–prey equations, diffusion alone cannot disturb a constant equilibrium, and so spatial heterogeneity cannot emerge. The complete demonstration is given section 7.6.1. In outline, the system (7.2.2) was non-dimensionalised and the matrix eigenvalues after linearisation were tested using the standard criteria, see for example Murray (2003). This showed that taking account of diffusion on its own cannot cause instability and no pattern can be generated. Moreover, this result can be extrapolated to any n-pool model, for any soil decomposition model (see SI text, section S1).
However, for the decomposition model with both diffusion and chemotaxis, it can be proven that the equilibrium solutions of the equation system (7.2.4) can be rendered non-stable under certain conditions, and thus produce patterns and spatial heterogeneity (see section 7.6.2). Once again, this result can be generalised for n-pool models. The proof, however, depends strongly on the structure of the model under consideration.

7.3.2 Numerical simulation.

Figures below shows the numerical simulations of the soil microbial biomass compartment for the nearly rectangular and circular domains, using either $h_1(x) = x$ which does not prevent any overcrowding (Fig 7.1 and 7.2), or $h_2(x) = x(u_{max} - x)$ which prevents overcrowding (Fig 7.3 and 7.4). These figures show the spatial variability and patterns obtained for soil microbial biomass after 60 days and for the two spatial domain shapes. The soil microbial biomass pattern agrees with the distribution within the soil matrix of the microbial hot spots at micron scale.

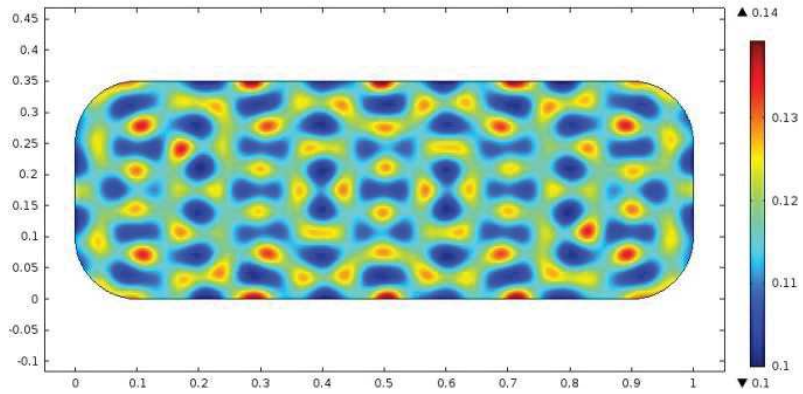

Figure 7.1: Spatial microbial biomass distribution when $h = h_1$ after 60 days.

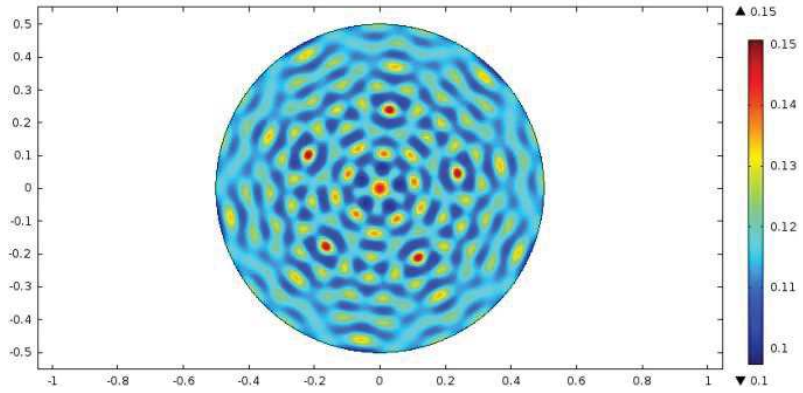

Figure 7.2: Spatial microbial biomass distribution when $h = h_1$ after 60 days.

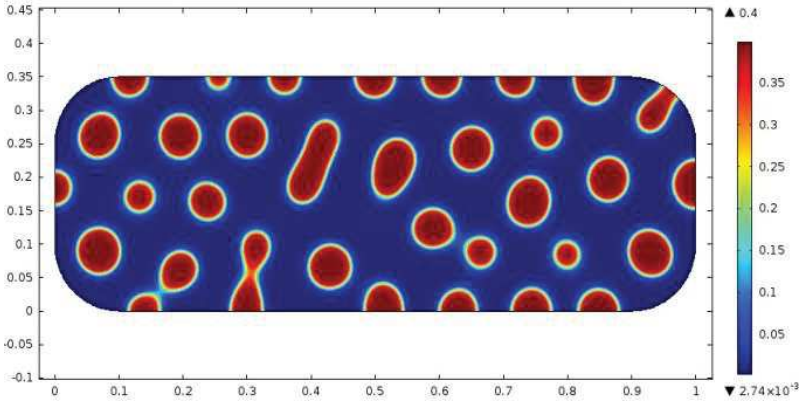

Figure 7.3: Spatial microbial biomass distribution when $h = h_2$ after 60 days.

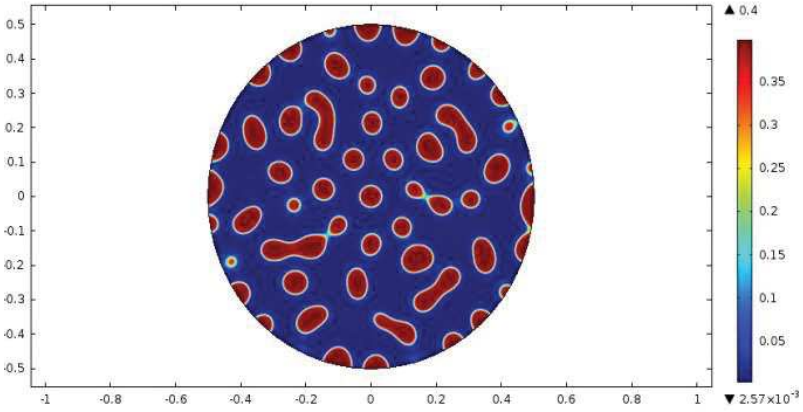

Figure 7.4: Spatial microbial biomass distribution when $h = h_2$ after 60 days.

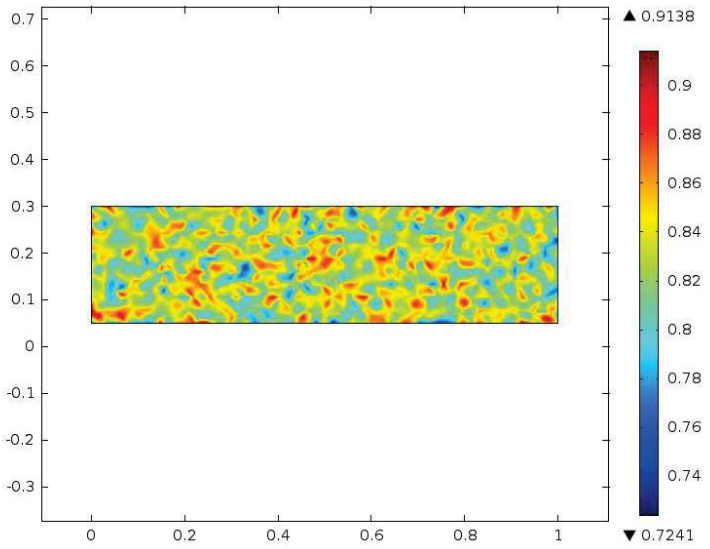

Figure 7.5: Distribution of the microbial biomass after 60 days.(Heterogeneity in the input distribution)

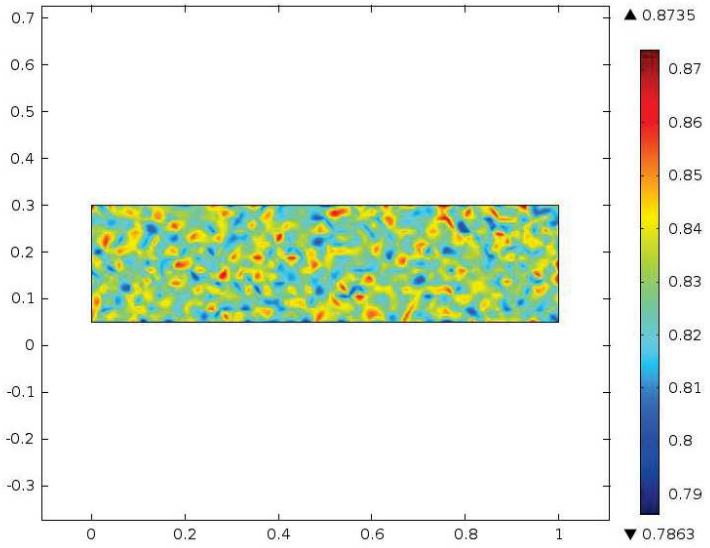

Figure 7.6: Distribution of the microbial biomass after 60 days. (Heterogeneity in the model's coefficients)

7.4 Discussion.

A theoretical framework was developed using a nonlinear mechanistic model of soil organic carbon decomposition that explicitly incorporated microbial biomass. So far as we are aware, this is the first time that a framework has been described and validated mathematically that can reconcile (i) research at field and plot level over the past seventy years (Manzoni and Poporato, 2009 [8]) and (ii) recent observations at submicron scale concerning the spatial heterogeneity of soil microbial biomass (Vogel et al., 2014 [38]). The theoretical framework proposed can represent the spatial heterogeneity of soil microbial biomass, but, more importantly, is still valid at global scale and will greatly improve future global soil carbon projections. However, it should be recognised that some similar results were found in other fields of biology or ecology using chemotactic systems applied to different types of cell (such as tumour cells) and macrofauna such as nematodes and insects. All these studies, however,focused on chemotaxis itself, modelling chemotaxis and the mathematical analysis of chemotaxis.
Chemotactic models are particular examples of more general cross-diffusion models. Crossdiffusion is the phenomenon in which a gradient in the concentration of one species/component induces a flux of another species/component. But, determining the existence of inhomogeneous steady states in cross-diffusion systems is complicated owing to strong nonlinear coupling and because the diffusion matrices may not be symmetric or positive definite (Jüngel, 2010 [100]). However, most research into cross-diffusion, such as the Lokta-Volterra models, concerned prey-predator systems and described the dynamics of biological systems in which two species interact, one as a predator and the other as prey. In these cases, cross-diffusion was used to model segregation and advection in the systems. For instance, some authors (e.g. Shi et al., 2011 [99]) studying the general instability analysis of cross-diffusion systems, reported that, in vegetation, a uniform steady state is stable in the absence of self-diffusion and cross-diffusion, still stable with self-diffusion only, but unstable with a strong cross-diffusion.
Another intuitive way of producing heterogeneity patterns, without the need for complex models, is to add heterogeneity either to the initial distribution of the inputs or to the various coefficients used in the equations of the models, as illustrated in Figures 7.5 and 7.6. However, this heterogeneity is purely stochastic and not mechanistic which clearly makes this approach less able to explain the complexity of the observations. Moreover, the calibration and validation steps would require complex data that is not easily accessible using conventional soil analysis approaches. This approach will

also be limited to a given scale and not be transferable to a global scale.

7.5 Conclusion.

Treseder et al. (2011)[89] made recommendations for integrating microbial ecology into ecosystem models. Following these recommendations, it was shown that it is possible to apply a mathematically simple approach to represent complex spatial variability at small scale using a model developed at field or plot scale that focused on the soil microbial biomass. There is no need to propose new models at field or global scale. This simple framework is a powerful means of reconciling a conventional modelling approach at field scale and recent observations at micron scale, while avoiding the pitfalls of increased complexity and reduced explanatory power (Low-Décarie et al., 2014 [101]). Moreover, this framework reconciles and does not conflict with the various approaches that focus on soil organic matter turnover, its protection and accessibility (Dungait et al., 2012 [102]), and even recently proposed theories such as the "trigger molecule hypothesis" (De Nobili et al., 2001 [103]).
We believe that this framework can help to improve the predictive capacity and accuracy of soil organic carbon behaviour in a context of global climate change.

7.6 Supplementary material

7.6.1 Non-emergence of spatial patterns in models with diffusion only

For the simplified equation systems (7.2.2) (with 2 pools), using the following notation :

$$\tilde{x} = \sqrt{\frac{k_1}{d_1}}x \quad \widetilde{t} = k_1 t \quad a = \frac{q}{k_1} \quad b = \frac{k_2}{k_1} \quad c = \frac{f}{k_1} \quad d = \frac{d_2}{d_1}$$

to give the following non-dimensional equations (we revoke the notation) :

$$\begin{cases} \partial_t u = \Delta u - u - au^2 + bv \\ \partial_t v = d\Delta v + u - bv + c \end{cases}, (x,t) \in \Omega \times (0;T) \tag{S1}$$

with the same initial conditions and boundary conditions as system (7.2.2). Without diffusion, the system (S1) has a unique positive steady state :

$$u^* = \sqrt{\frac{c}{a}} \qquad\qquad v^* = \frac{u^* + c}{b} \tag{S2}$$

To assess the steady state stability, the system is linearised around (u^*, v^*). Setting :

$$w_1 = u - u^* w_2 = v - v^*$$

gives the following linear system :

$$\begin{cases} \partial_t w_1 = \Delta w_1 - w_1 - 2au^* w_1 + bw_2 \\ \partial_t w_2 = d\Delta w_2 + w_1 - bw_2 \end{cases}, (x,t) \in \Omega \times (0;T), \tag{S3}$$

with no-flux boundary conditions (7.2.3).
As in Murray [35], we looked for a solution of the form :

$$\mathbf{w} = \begin{pmatrix} w_1 \\ w_2 \end{pmatrix} \propto e^{(i\mathbf{k}\cdot\mathbf{x} + \rho t)}. \tag{S4}$$

Taking $k = |\mathbf{k}|$ to be the Euclidean norm of the wave vector, the following eigenvalue problem must be solved :

$$\mathbf{A}\mathbf{w} = \rho\mathbf{w}, \tag{S5}$$

where $\mathbf{A}$ is the two by two matrix

$$\mathbf{A} = \begin{pmatrix} -1 - 2au^* - k^2 & b \\ 1 & -b - k^2 d \end{pmatrix}. \tag{S6}$$

The eigenvalue ρ depends on k.

Turing instability occurs (which means that spatial patterns appear) when $\rho\left(k^2\right) > 0$, for a given value of k.

In this problem the matrix $\mathbf{A}$ has a strictly negative trace and a strictly positive determinant, and so $\rho\left(k^2\right) < 0$ for all values of k.

Thus, according to those criteria (36), no patterns will emerge if only diffusion is considered.

Generalisation to n-pool model

This conclusion is also valid for n-pool models. The model can be written as :

$$\partial_t u_i - d_i \Delta u_i = f_i(\mathbf{u}), \tag{S7}$$

for all $i \in \{1, n\}$, where the second member satisfies *the cooperative condition* :

$$\frac{\partial f_i}{\partial u_j}(\mathbf{u}) \geq 0, \ \textit{for } i \neq j, \tag{S8}$$

for all $\mathbf{u} = (u_1, u_2, \ldots, u_n)$ in $\mathbb{R}^n_+$.

Let $\mathbf{u}^*$ be the steady state of

$$\partial_t u_i = f_i(u),$$

with $i \in \{1, n\}$ and let $\mathbf{A} = (a_{ij})_{1 \leq i,j \leq n}$ be the matrix of linearization around $\mathbf{u}^*$ i.e.

$$(a_{ij})_{1 \leq i,j \leq n} = \frac{\partial f_i}{\partial u_j}(\mathbf{u}^*). \tag{S9}$$

Generally, $\mathbf{A}$ satisfies the following conditions :

(a) the diagonal entries are all negative or zero,

(b) the off-diagonal entries are all positive or zero,

(c) the sum of entries of any column is negative or zero.

Any matrix satisfying these conditions is called a *compartmental matrix* (see Anderson, 1983). Hence, using the above properties and **Gerschgorin's theorem**, it can be proved that :

"The real part of any eigenvalue of a compartmental matrix is negative or zero. Moreover, the matrix has no purely imaginary eigenvalues." **(Anderson [104] Theorem 12.1)**

Diffusion can destabilize the steady state $\mathbf{u}^*$ if the real part of ρ is positive for the system :

$$\mathbf{B}\mathbf{w} = \rho\mathbf{w}, \tag{S10}$$

where $\mathbf{B} = \mathbf{A} - k^2\mathbf{D}$, $\mathbf{D}$ being the positive diagonal matrix of the diffusion coefficients d_i.

$\mathbf{B}$ clearly satisfies conditions (a), (b) (c) above, therefore by Anderson's theorem $Re\,(\rho) \leq 0$. Moreover, ρ cannot be zero because matrix $\mathbf{B}$ is strictly diagonally dominant. Thus the real part of ρ is strictly negative.

No pattern can emerge if only diffusion is considered.

7.6.2 Emergence of spatial patterns in models with diffusion and chemotaxis

As in the previous section, the system (7.2.4) was linearised around the steady state (u^*, v^*). This gives the following system ;

$$\begin{cases} \partial_t w_1 = \Delta w_1 - e\Delta w_2 - w_1 - 2au^* w_1 + bw_2 \\ \partial_t w_2 = d\Delta w_2 + w_1 - bw_2 \end{cases} , (x,t) \in \Omega \times (0;T), \quad \text{(S11)}$$

where

$$e = \gamma u^* g\left(u^*\right) \frac{k_1}{d_1}. \quad \text{(S12)}$$

Looking for solutions of the type (S4), the following eigenvalue problem must be solved :

$$\mathbf{B}\mathbf{w} = \rho \mathbf{w}, \quad \text{(S13)}$$

where $\mathbf{B}$ is the two by two matrix

$$\mathbf{B} = \begin{pmatrix} -1 - 2au^* - k^2 & b + ek^2 \\ 1 & -b - k^2 d \end{pmatrix}. \quad \text{(S14)}$$

In this case, the trace of matrix$\mathbf{B}$ is strictly negative while its determinant can be strictly negative for some values of k. Thus, taking chemotaxis into account in the system may lead to the emergence of spatial patterns.

Bibliographie

[1] Ritchie J. C. Sobecki T. M. Bloodworth H. Rawls W. J., Pachepsky Y. A. Effect of soil organic carbon on soil water retention. *Geoderma*, 116 (1) :61–76, 2003.

[2] Kwon K. C. Post W. M. Soil carbon sequestration and land-use change : processes and potential. *Global Change Biology*, 6 :317–328, 2000.

[3] Gifford R. M. Guo L. B. Soil carbon stocks and land use change : a meta analysis. *Global Change Biology*, 8(4) :345–360, 2002.

[4] Mosier A. R. Holland E. A. Pendall E. Schimel D. S. Ojima D. S. Del Grosso S. J., Parton W. J. Modeling soil co_2 emissions from ecosystems. *Biogeochem.*, 73 :71–91, 2005.

[5] Porporato A. Barry D. A. Batlle-Aguilar J., Brovelli A. Modelling soil carbon and nitrogen cycles during land use change. a review. *Agronomy for Sustainable Development*, 31(2) :251–274, 2011.

[6] Aïssa N. B. Hammouda M. B. Gallali T. Chotte J. L. Bernoux M. Hamdi S., Chevallier T. Short-term temperature dependence of heterotrophic soil respiration after one-month of pre-incubation at different temperatures. *Soil Biology and Biochemistry*, 43(9) :1752–1758, 2011.

[7] Sall S. Bernoux M. Chevallier T. Hamdi S., Moyano F. Synthesis analysis of the temperature sensitivity of soil respiration from laboratory studies in relation to incubation methods and soil conditions. *Soil Biology and Biochemistry*, 58 :115–126, 2013.

[8] Porporato A. Manzoni S. Soil carbon and nitrogen mineralization : Theory and models across scales. *Soil Biology and Biochemistry*, 41(7) :1355–1379, 2009.

[9] Brauman A. Sall S. Assigbetse K. Chotte J. L. Masse D., Cambier C. Mior : an individual-based model for simulating the spatial patterns of soil organic matter microbial decomposition. *European Journal of Soil Science*, 58(5) :1127–1135, 2007.

[10] N. Chotte J. L. Drogoul A. Perrier E. Cambier C. Blanchart E., Marilleau. Sworm : An agent-based model to simulate the effect of earthworms on soil structure. *European Journal of Soil Science*, 60(1) :13–21, 2009.

[11] Nikiforoff C. C. Some general aspects of the chernozem formation. *Soil Science Society of America Proceedings*, 1 :333–342, 1936.

[12] Dupuis M. Hénin S. Essai de bilan de la matière organique du sol. *Annales agronomiques*, 15(1) :17–29, 1945.

[13] Schlesinger W. H. Carbon balance in terrestrial detritus. *Annual Review of Ecology and Systematics*, 8 :51–81, 1977.

[14] Jacquez J. A. Compartmental analysis. biology and medicine. *Soil Biology and Biochemistry*, 16 :537, 1974.

[15] Bosatta E. Agren G. *Theoretical ecosystem ecology : understanding element cycles*. Cambridge University Press, 1996.

[16] Balesdent J. Elzein A. Mechanistic simulation of vertical distribution of carbon concentrations and residence times in soils. *Soil Science Society of America Journal*, 59(5) :1328–1335, 1995.

[17] Sy M. / Goudjo C., Lèye B. Weak solution to a parabolic nonlinear system arising in biological dynamic in the soil. *International Journal of Differential Equations*, 2011 :doi :10.1155/2011/831436, 2011.

[18] Beer C. Kattge J. Schrumpf M. Ahrens B Reichstein M. Braakhekke M. C., Wutzler T. Modeling the vertical soil organic matter profile using bayesian parameter estimation. *Biogeosciences*, 10 :399–420, 2013.

[19] Feller C. Herrmann P. Rémy J. C. Thuriès L., Pansu M. Kinetics of added organic matter decomposition in a mediterranean sandy soil. *Soil Biology and Biochemistry*, 33(7) :997–1010, 2001.

[20] Rayner J.H. Jenkinson D. S. The turnover of soil organic matter in some of the rothamsted classical experiments. *Soil science*, 123(5) :298–305, 1977.

[21] Cole C. V. Ojima D. S. Parton W. J., Schimel D. S. Analysis of factors controlling soil organic matter levels in great plains grasslands. *Soil Science Society of America Journal*, 51(5) :1173–1179, 1987.

[22] Sarmiento L. Metselaar K. Pansu M., Bottner P. Comparison of five soil organic matter decomposition models using data from a 14c and 15n labeling field experiment. *Global Biogeochemical Cycles*, 18(4), 2004.

[23] Rujano M. A. Ablan M. Acevedo D. Bottner P. Pansu M., Sarmiento L. Modeling organic transformations by microorganisms of soils in six contrasting ecosystems : validation of the momos model. *Global Biogeochemical Cycles*, 24, 2010.

[24] Bottner P. Sarmiento L. Pansu M., Machado D. Modelling microbial exchanges between forms of soil nitrogen in contrasting ecosystems. *Biogeoscience*, 11(4) :915–927, 2014.

[25] Brookes P. C. Powlson D. S., Hirsch P. R. The role of soil microorganisms in soil organic matter conservation in the tropics. *Nutrient Cycling in Agroecosystems*, 61(1-2) :41–51, 2001.

[26] Abbadie L. Mariotti A. Fontaine S., Bardoux G. Carbon input to soil may decrease soil carbon content. *Ecology letters*, 7(4) :314–320, 2004.

[27] Alvarez G. Klumpp K. Martin R. Rapaport A. Fontaine S. Perveen N., Barot S. Priming effect and microbial diversity in ecosystem functioning and response to global change : a modeling approach using the symphony model. *Global change biology*, 20(4) :1174–1190, 2014.

[28] Smith H.L. *Monotone Dynamical Systems, An introduction to the theory of competitive and cooperative systems.* American mathematical society, 1995.

[29] Balesdent J. Arrouays D. Martin M. P., Cordier S. Periodic solutions for soil carbon dynamics equilibriums with time-varying forcing variables. *Ecological Modelling*, 204(3) :523–530, 2007.

[30] Papanicolaou G. Bensoussan A., Lions J.L. *Asymptotic analysis for periodic structures.* 1978.

[31] Tartar L. Quelques remarques sur l'homogénéisation. *In Functional Analysis and Numerical Analysis, Proceedings of the Japan-France Seminar*, pages 468–482, 1976.

[32] Donato P. Cioranescu D. *An introduction to Homogenization.* New-York : Oxford University Press, 1999.

[33] Christensen B. T. Jensen L. S. Bruun S., Ågren G. I. Measuring and modeling continuous quality distributions of soil organic matter. *Biogeosciences*, 7(1) :27–41, 2010.

[34] Turing A.M. The chemical basis of morphogenesis. *Philosophical Transactions of the Royal Society of London*, 237(641) :37–72, 1952.

[35] Murray J.D. *Mathematical Biology I : An Introduction.* New-York : Springer,, 2002.

[36] Murray J.D. *Mathematical Biology II : Spatial Models and Biomedical Applications.* 2003.

[37] Grindrod P. *The theory and applications of reaction-diffusion equations : patterns and waves.* New-York : Oxford University Press, 1996.

[38] Höschen C. Buegger F. Heister K. Schulz S. Kögel-Knabner I. Vogel C., Mueller C. W. Submicron structures provide preferential spots for carbon and nitrogen sequestration in soils. *Nature communications*, 5, 2014.

[39] Lions J.L. *Quelques méthodes de résolution des problèmes aux limites non linéaires.* Paris : Dunod, 1969.

[40] Yagi A. Mimura M. Osaki K., Tsujikawa T. Exponential attractor for a chemotaxis-growth system of equations. *Nonlinear Analysis : Theory, Methods & Applications*, 51(1) :119–144, 2002.

[41] Yagi A. *Abstract Parabolic Evolution Equations and their Applications.* Heidelberg : Springer, 2010.

[42] Nicolaenko B. Teman R. Eden A., Foias C. *Exponential attractors for dissipative evolution equations, Research in Applied Mathematics.* Wiley New York, 1994.

[43] Temam R. *Navier-Stokes equations. Theory and numerical analysis.* Elsevier North-Holland, 1977.

[44] Yagi A. Ryu S. U. Optimal control of keller–segel equations. *Journal of Mathematical Analysis and Applications*, 256(1) :45 – 66, 2001.

[45] Segel L.A. Keller E. F. Initiation of slime mold aggregation viewed as an instability. *Journal of Theoretical Biology*, 26(3) :399 – 415, 1970.

[46] Bendahmane M. Mathematical analysis of reaction-diffusion system modeling predator-prey with prey-taxis. *Networks and Heterogeneous Media*, 3(4) :863–879, 2008.

[47] Morales-Rodrigo C. Cieślak T. Quasilinear non-uniformly parabolic–elliptic system modelling chemotaxis with volume filling effect. existence and uniqueness of global-in-time solutions. *Topol. Methods Nonlinear Anal*, 29(2) :361–381, 2007.

[48] Wrzosek D. Volume filling effect in modelling chemotaxis. *Mathematical Modelling of Natural Phenomena*, 5(1) :123–147, 2010.

[49] Painter K. Hillen T. Global existence for a parabolic chemotaxis model with prevention of overcrowding. *Advances in Applied Mathematics*, 26(4) :280–301, 2001.

[50] Bala G. Bopp L. Brovkin V. Canadell J. Thornton P. Ciais P., Sabine C. Carbon and other biogeochemical cycles. *Climate Change 2013 : The Physical Science Basis. Contribution of Working Group I to the Fifth Assessment Report of the Intergovernmental Panel on Climate Chang, . Cambridge University Press, Cambridge, United Kingdom and New York, NY, USA.*, pages 465–570, 2013.

[51] Boden T. Conway T. Houghton R.A. House J.I. Marland G. Peters G.P. van der Werf G.R. Ahlstrom A. Andrew R.M. Bopp L. Canadell J.G. Ciais P. Doney S.C. Enright C. Friedlingstein P. Huntingford C. Jain A.K. Jourdain C. Kato E. Keeling R.F. Klein Goldewijk K. Levis S. Levy P. Lomas M. Poulter B. Raupach M.R. Schwinger J. Sitch S. Stocker B.D. Viovy N. Zaehle S. Zeng N. Le Quéré C., Andres R.J. The global carbon budget 1959–2011. *Earth Syst. Sci. Data*, 2013.

[52] Lal R. Carbon sequestration. *Philosophical Transactions of the Royal Society B : Biological Sciences*, 2008.

[53] Bernoux M. Lal R. Manlay R. Feller C., Blanchart E. Soil fertility concepts over the past two centuries : The importance attributed to soil organic matter in developed and developing countries. *Archives of Agronomy and Soil Science*, 2012.

[54] Sandberg I. W. On the mathematical foundations of compartmental analysis in biology, medicine, and ecology. *IEEE Transactions on Circuits and Systems*, 25 :273–279, 1978.

[55] Paustian K. Killian K. Coleman K. Bernoux M. Falloon P. Powlson D.S. Batjes N.H. Milne E. Cerri C.C. Cerri C.E.P., Easter M. Simulating soc changes in 11 land use change chronosequences from the brazilian amazon with rothc and century models. *Agriculture Ecosystems and Environment*, 2007.

[56] Allison S.D. Wieder W.R., Bonan G.B. Global soil carbon projections are improved by modelling microbial processes. *Nature Climate Change*, 2013.

[57] Metselaar K. Herve D. Bottner P. Pansu M., Sarmiento L. Modelling the transformations and sequestration of soil organic matter in two contrasting ecosystems of the andes. *European Journal of Soil Science*, 2007.

[58] Wanner G. Hairer E., Norsett S. P. *Solving Ordinary Differential Equations I, Nonstiff Problems.* Springer, 2008.

[59] Teschl G. *Solving Ordinary Differential Equations I, Nonstiff Problems.* Springer, 2008.

[60] Ortega J. M. Numerical analysis : A second course. 1990.

[61] Bernoux M. Hammoudi A., Iosifescu O. Mathematical analysis of a nolinear model of soil carbon dynamics. *Differential Equations and Dynamical Systems*, 23(4), 2015.

[62] Levinson N. Coddington E.A. *Theory of Ordinay Differential Equations*. McGRAW-HILL PUBLISHING CO. LTD., 1987.

[63] Sonner S. Efendiev M. A. On verifying mathematical models with diffusion, transport and interaction. *Current advances in nonlinear analysis and related topics. GAKUTO Internat. Ser. Math. Sci. Appl.*, 32 :41–67, 2010.

[64] Trudinger N.S. Gilbarg D. *Elliptic Partial Differential Equations of Second Order*. 2nd Edition, Springer-Verlag, New York,, 1983.

[65] Ortega L.A. Leung A.W. Existence of monotone scheme for time-periodic nonquasimonotone reaction-diffusion systems : application to autocatalytic chemistry. *Journal of mathematical analysis and applications*, 221 :712–733, 1998.

[66] Pao C. V. Periodic solutions of parabolic systems with nonlinear boundary conditions. *Journal of Mathematical Analysis and Applications*, 234 :695–716, 1999.

[67] Pao C. V. Stabiliy and attractivity of periodic solutions of parabolic systems with time-delays. *Journal of Mathematical Analysis and Applications*, 304 :423–450, 2005.

[68] Meyer C. Matrix analysis and applied linear algebra. 2000.

[69] Bernoux M. Hammoudi A., Iosifescu O. Mathematical analysis of a spatially distributed soil carbon dynamics model. *accepted in Analysis and Applications*, 2015.

[70] Bradford M.A. Allison S.D., Wallenstein M.D. Soil-carbon response to warming dependent on microbial physiology. *Nature Geoscience*, 3 :336–340, 2010.

[71] Pot V. Coucheney E. Nunan N. Otten W. Chenu C. Monga O., Garnier P. Simulating microbial degradation of organic matter in a simple porous system using the 3-d diffusion-based model mosaic. *Biogeosciences*, 11 :2201–2209, 2014.

[72] Ågren G. I. Bosatta E. Exact solutions to the continuous-quality equation for soil organic matter turnover. *J. Theor. Biol.*, 224 :97–105, 2003.

[73] Ågren G. I. Nilsson K. S., Hyvönen R. Using the continuous-quality theory to predict microbial biomass and soil organic carbon following organic amendments. *European Journal of Soil Science*, 56 :397–405, 2005.

[74] Nilsson S.K. Modelling soil organic matter turnover. *Doctoral thesis : Swedish University of Agricultural Sciences, Uppsala,*, 2004.

[75] Schlesinger W. H. Raich J. W. The global carbon-dioxide flux in soil respiration and its relationship to vegetation and climate. *Tellus B*, 44 :81–99, 1992.

[76] Hashimoto S. $q_1 0$ values of soil respiration in japanese forests. *Journal of Forest Research*, 10(5) :409–413, 2005.

[77] Muys B. Kraigher H. Deckmyn G., Campioli M. Simulating c cycles in forest soils : Including the active role of micro-organisms in the anafore forest model. *Ecological Modelling*, 222 :1972–1985, 2011.

[78] Nadzieja T. Biler P., Hebisch W. The debye system : Existence and large time behavior of solutions. *Nonlinear Analysis : Theory, Methods & Applications*, 238 :1189 – 1209, 1994.

[79] Wang C. Wu Z., Yin J. *Elliptic & Parabolic Equations*. World Scientific publishing Co Ltd, 2006.

[80] Wrzosek D. Model of chemotaxis with threshold density and singular diffusion. *Nonlinear Analysis : Theory, Methods & Applications*, 73(2) :338–349, 2010.

[81] Cai Z. Gicheru P. Joosten H. Victoria R. Milne E. Noellemeyer E. Pascual U. Nziguheba G. Vargas R. Bationo A. Buschiazzo D. de-Brogniez D. Melillo J. Richter D. Termansen M. van Noordwijk M. Goverse T. Ballabio C. Bhattacharyya T. Goldhaber M. Nikolaidis N. Zhao Y. Funk R. Duffy C. Pan G. la Scala N. Gottschalk P. Batjes N. Six J. van Wesemael B. Stocking M. Bampa F. Bernoux M. Feller C. Lemanceau P. Montanarella L. Banwart S., Black H. Benefits of soil carbon : report on the outcomes of an international scientific committee on problems of the environment rapid assessment workshop. *Carbon Management*, 5(2) :185–192, 2014.

[82] Tomelleri E. Ciais P. Jung M. Carvalhais N. Rodenbeck C. Arain M.A. Baldocchi D. Bonan G.B. Bondeau A. Cescatti A. Lasslop G. Lindroth A. Lomas M. Luyssaert S. Margolis H. Oleson K.W. Roupsard O. Veenendaal E. Viovy N. Williams C. Woodward F.I. Papale D. Beer C., Reichstein M. Terrestrial gross carbon dioxide uptake : Global distribution and covariation with climate. *Science*, 329 :834–838, 2010.

[83] Schimel D.S. Terrestrial ecosystems and the carbon-cycle. *Global change biology*, 1 :77–91, 1995.

[84] Gower S.T. Bond-Lamberty B., Wang C.K. A global relationship between the heterotrophic and autotrophic components of soil respiration ? *Global Change Biology*, 10 :1756–1766, 2004.

[85] Soussana J.F. Lardy R., Bellocchi G. A new method to determine soil organic carbon equilibrium. *Environmental Modelling & Software*, 26 :1759–1763, 2011.

[86] Flanner M.G. Thornton P.E. Swenson S.C. Lawrence P.J. Zeng X. Yang Z.L. Levis S. Sakaguchi K. Bonan G.B. Slater A.G. Lawrence D.M., Oleson K.W. Parameterization improvements and functional and structural advances in version 4 of the community land model. *Journal of Advances in Modeling Earth Systems*, 3 :M03001, 2011.

[87] Kirschbaum M.U.F. The temperature dependence of organic-matter decomposition –still a topic of debate. *Soil Biology and Biochemistry*, 38 :2510–2518, 2006.

[88] Schimel J. Microbes and global carbon. *Nature Climate Change*, 3 :867–868, 2013.

[89] Bradford M.A. Brodie E.L. Dubinsky E.A. Eviner V.T. Hofmockel K.S. Lennon J.T. Levine U.Y. MacGregor B.J. Pett-Ridge J. Waldrop M.P. Treseder K.K., Balser T.C. Integrating microbial ecology into ecosystem models : challenges and priorities. *Biogeochemistry*, 109 :7–18, 2011.

[90] Bhomia R.K. Almaraz M. Bacon A.R. Eggleston E. Judy J.D. Lewis R.W. Lusk M. Miller B.-Moorberg C. Snyder E.H. Tiedeman M. Adewopo J.B., Van Zomeren C. Top-ranked priority research questions for soil science in the 21^{st} century. *Soil Science Society of America Journal*, 78 :337–347, 2014.

[91] Thornton P.E. Song X. Yuan F. Goswani S. Xu X., Schimel J.P. Substrate and environmental controls on microbial assimilation of soil organic carbon : a framework for earth system models. *Ecology letters*, 17 :547–555, 2014.

[92] Wieder W.R. Leite M. Medlyn B.E. Rasmussen M. Smith M.J. Agusto F.B. Hoffman F. Luo Y.Q. Wang Y.P., Chen B.C. Oscillatory behavior of two nonlinear microbial models of soil carbon decomposition. *Biogeosciences*, 11 :1817–1832, 2014.

[93] Oades J.M. Tisdall J.M. Organic matter and water-stable aggregates in soils. *Journal of soil science*, 33 :141–163, 1982.

[94] Crawford J.W. Young I.M. Interactions and self-organization in the soil-microbe complex. *Science*, 304 :1634–1637, 2004.

[95] Lee H. Whiteley H.R. Zelin S. Abu-Ashour J., Joy D.M. Transport of microorganism through soil. *Water, Air, and Soil Pollution*, 75 :141–158, 1994.

[96] Bergman K. Soby S. Motility and chemotaxis of rhizobium meliloti in soil. *Applied and environmental microbiology*, 46 :995–998, 1983.

[97] Ozawa H. Urashima Y. Sueguchi T. Matsuguchi T. Futamata H., Sakai M. Chemotactic response to amino acids of fluorescent pseudomonads isolated from spinach roots grown in soils with different salinity levels. *Soil science and plant nutrition*, 44(1) :1–7, 1998.

[98] Srinivasan M. Somers E., Vanderleyden J. Rhizosphere bacterial signalling : a love parade beneath our feet. *Critical reviews in microbiology*, 30 :205–235, 2004.

[99] Little K. Shi J., Xie Z. Cross-diffusion induced instability and stability in reaction-diffusion systems. *Journal of Applied Analysis and Computation*, 1 :95–119, 2011.

[100] Jüngel A. Diffusive and nondiffusive population models. *Mathematical Modeling of Collective Behavior in Socio-Economic and Life Sciences,*, eds Naldi G, Pareschi L, Toscani G, (Birkhäuser, Basel),, 2010.

[101] Granados M. Low-Décarie E., Chivers C. Rising complexity and falling explanatory power in ecology. *Frontiers in Ecology and the Environment*, 12 :412–418, 2014.

[102] Gregory A.S. Whitmore A.P. Dungait J.A., Hopkins D.W. Soil organic matter turnover is governed by accessibility not recalcitrance. *Global Change Biology*, 18 :1781–1796, 2012.

[103] Mondini C. Brookes P.C. De Nobili M., Contin M. Soil microbial biomass is triggered into activity by trace amounts of substrate. *Soil Biology and Biochemistry*, 33 :1163–1170, 2001.

[104] Anderson D.H. *Compartmental Modeling and Tracer Kinetics, Lecture Notes in Biomathematics*. Berlin : Springer-Verlag, 1983.

Modélisation et analyse mathématique de la dynamique du carbone organique dans le sol

La compréhension du cycle de la matière organique du sol (**MOS**) est un outil majeur dans la lutte contre le réchauffement climatique, la préservation de la biodiversité ainsi que dans la consolidation de la sécurité alimentaire. Dans ce contexte, cette thèse porte sur la modélisation et l'analyse mathématique de modèles de la dynamique du carbone organique dans le sol.

Dans le chapitre 2, nous avons étudié la robustesse et les propriétés mathématiques d'un modèle non linéaire (**MOMOS**). Nous avons montré que si les données sont périodiques nous obtenons l'existence d'une solution périodique attractive. Le chapitre 3 est consacré à la validation mathématique d'un modèle spatialisé basé sur les équations de **MOMOS**, auxquels nous avons ajouté des opérateurs de diffusion et de transport. L'effet de l'hétérogénéité spatiale sur ce modèle est étudié dans le chapitre 4 en utilisant des techniques d'homogénéisation. Suivant la méthodologie de Bosatta et Agren, nous dérivons un autre modèle à qualité continue, qui prend en compte l'effet de l'âge sur la décomposition de la **MOS**. Le chapitre 5 contient la validation mathématique et expérimentale du modèle. Enfin, nous considérons dans les chapitres 6 et 7, un modèle incluant l'effet de la chemotaxie. Nous montrons l'existence, la positivité et l'unicité des solutions dans des domaines suffisamment réguliers de dimension inférieure ou égale à 3.

Mots clés : Matière organique dans le sol – Advection-réaction-diffusion – Chemotaxie –modèle MOMOS – Solution périodique

Modelling and mathematical analysis of the dynamics of the organic carbon in soil

Understanding the soil organic matter (**SOM**) cycle is a major tool in the effort to reduce global warming, to preserve biodiversity and to improve food safety strategies. In this context, this thesis is about modelling and mathematical analysis of the dynamics of the organic carbon in soil.

In chapter 2, we validate mathematically a nonlinear soil organic carbon model (**MOMOS**) and we prove that, if data is periodic, then there is a unique attractive periodic solution. In chapter 3, we focus on the mathematical validation of a spatial model derived from **MOMOS** and where we used diffusion and transport operators. We prove also the existence of a periodic solution. In addition, the effect of soil heterogeneities on the model is studied in chapter 4 using homogenization techniques. Moreover, following the Bosatta and Agren methodology, we derive a continuous quality model taking in consideration the effect of age on the quality of **SOM**. We validate the model mathematically and experimentally in chapter 5. Finally, we consider in chapters 6 and 7 another model that takes into account the chemotaxis movement of soil microorganisms. We prove mainly the existence and uniqueness of a positive solution in a regular spatial domain of dimension less or equal to 3.

Key words : Soil organic matter – Advection-reaction-diffusion – Chemotaxis – MOMOS model – Periodic solution